University of Washington
Department of Civil and Environmental Engineering

DESIGN OF MONITORING SYSTEMS FOR DETECTION OF TRENDS IN STREAM QUALITY

D. P. Lettenmaier

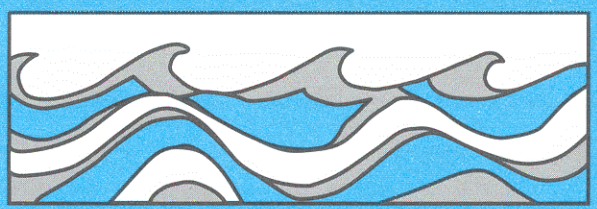

Water Resources Series
Technical Report No.39
August, 1975

Seattle, Washington
98195

Charles W. Harris Hydraulics Laboratory

Department of Civil Engineering

University of Washington

Seattle, Washington 98195

DESIGN OF MONITORING SYSTEMS FOR DETECTION OF TRENDS IN STREAM QUALITY

by

D. P. Lettenmaier

Technical Report No. 39

August 1975

Project Completion Report: "Optimal Water Quality Monitoring Procedures for Streams"
Project Period: July 1, 1974 through June 30, 1975
Principal Investigator: Stephen J. Burges, Assistant Professor of Civil Engineering, University of Washington

DOE Project Number W-19

Allocation Number: 145-02-13A-3998-2538
(State of Washington Water Research Center)

Abstract

This report addresses the important issue of developing a method for the design of stream quality monitoring networks for detecting trends. The problem solved involved determining spatial sample station locations and temporal sample frequencies given a fixed number of samples for a particular river basin.

Two principal issues important to monitoring were addressed. The first involved determining the statistical power of detecting a trend of given magnitude from temporally correlated samples. Two generalized power curves, one for Spearman's Rho test against a linear trend and one for Mann Whitney's test against a step trend, were developed. These two tools provide the necessary power test information for any correlated time series, for any standard deviation and any sample record length for the best available non parametric statistical tests for linear and step trends.

The second major activity involved the coupling of statistical methods and deterministic water quality models to determine the spatial location of sample stations such that the average trend detection would be a maximum. State estimation techniques were employed for this activity.

In the numbers of batch samples possible in current monitoring programs, this research showed that it is much more efficient to use a single station with a relatively high sample frequency than to use multiple stations with correspondingly lower frequencies.

Key words: Water Quality Monitoring; Trend Detection; Mathematical Models; Kalman Filters; Stream Sampling; Network Design; Time Series Analysis

TABLE OF CONTENTS

LIST OF TABLES

LIST OF FIGURES

Acknowledgements

The author is grateful for the assistance provided by Dr. T. D. Steele of the U. S. Geological Survey and Mr. Glenn Farris and Mr. James Stapleton of the Municipality of Metropolitan Seattle for making available the daily stream quality data used in Chapter 4. Mr. James Mahood of Kennedy Tudor Consulting Engineers and Mr. Roland Blanchette of the U. S. Army Corps of Engineers, Seattle District Office, provided the stream quality and effluent source data for the Spokane River used in Chapter 6, while similar data for the Snohomish County Planning Department. The assistance of these persons was extremely helpful. Mr. Richard Cunningham, State of Washington Department of Ecology, acted as that agency's project officer and provided useful input during the course of the investigation. The care and patience of Mrs. Yunja Yu and Mrs. Marian Schwarzenbach in typing the manuscript is gratefully acknowledged.

The report constitutes the author's thesis presented in partial fulfillment of the requirements for the degree of Doctor of Philosophy in Civil Engineering at the University of Washington. The thesis supervisor was Stephen J. Burges who was also principal investigator of this project.

The work upon which this report is based was supported in part by funds provided by the State of Washington Department of Ecology through the State of Washington Water Research Center.

CHAPTER 1

INTRODUCTION

I. Research Objectives

The objective of this research is to develop a methodology for the design of a stream quality monitoring network with the primary purpose of identification of the existence or absence of trends in a time series of measurements of water quality indicators. The time scale for trend identification is taken to be of the order of the permit renewal period for waste discharge permits, normally two to five years. The methodology is developed for the case of a free flowing stream; conditions in the estuarial segment of a river basin or in impoundments are not considered although suggestions for extension to these cases are made in Chapter 8. The constraints on the design methodology are taken to be summarized in a limit on the total number of samples which may be taken for any given river basin per unit time per water quality constituent.

The funding agency for this research, the Washington State Department of Ecology, expressed, prior to the initiation of the work, the desire that the proposed methodology allow a method for determining the improvement in system response for a given change in the constraint. Consequently, a requirement for the design methodology is that sensitivity to constraints be easily determined. This feature is essential to allow for cost-effectiveness considerations in funding of ambient water quality monitoring networks.

It was also desired that the methodology proposed in this research be demonstrated in the design of ambient water quality monitoring

systems for two streams of contrasting character in the State of Washington. The two streams chosen are the Snohomish River on the west slope of the Cascade Mountains, in a region with marine climate characteristic of the North Pacific Coast, and the Spokane River above Long Lake in the far eastern part of Washington State, in a region with climate and hydrologic conditions not atypical of much of the western interior of the United States.

II. Background

Public concern over environmental degradation in recent years has emphasized the need for environmental management in much the same way that full scale economic management began some 40 years ago. In the areas of both air and water quality, the approach has been to set standards which provide the objectives for environmental management in much the same way that prevailing interest rates, GNP, and other economic indices are used as economic objectives. The differences between the actual levels of these indices and the objectives or standard values provide criteria for control. If the actual values are in some sense better than the desired standard values, system response is deemed adequate and such action is taken as is necessary to maintain the existing levels. If the actual values are deemed inadequate, action is taken to improve future system response so that the objectives can be met. The action to be taken in either case is always subject to some constraints. These constraints almost always include components that are economic in nature, i.e., some cost is associated with management. This cost ideally should be more than balanced by the benefits to be derived from management. In addition to economic

constraints, physical, social and legal constraints may also be present.

A general environmental management system may be shown in schematic form as in Figure 1.1. The control loop is essentially of the type used in feedback control theory except that management, rather than physical components are associated with the elements of the loop.

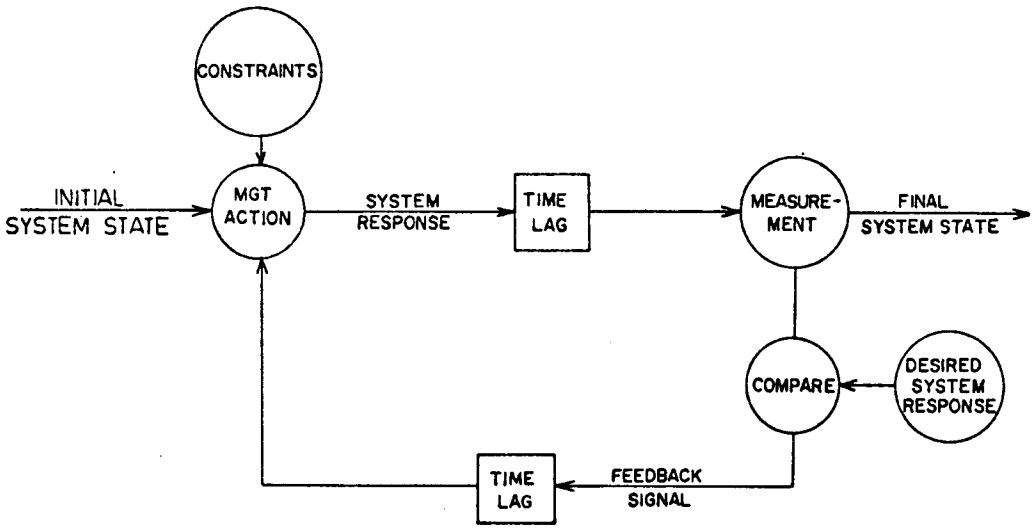

Figure 1.1. Stylized Environmental Management System

The critical nature of the feedback loop cannot be overemphasized. Without some form of a feedback system, response is essentially open ended. The point may be made that all systems have some form of feedback, that only the level of sophistication varies. Effective system response, however, requires special attention to feedback loop design as well as to the planning of the actual system management.

Environmental systems, and in particular water quality systems of the type investigated here, are well adapted to the type of management control outlined above. They have, in addition, a characteristic contributed by their physical nature: they are stochastic; the response of any given parameter is, in general, for fixed spatial coordinates a function of both time and a probability coordinate. Hence, knowledge of the time coordinate is insufficient to predict system response even given "perfect" management action because part of the system response can be attributed to chance. This may be expressed mathematically as $R(t) = D(t) + P(t)$, where $R(t)$ is the system response as a function of time, $D(t)$ is a deterministic component uniquely determined by the input and management action, and $P(t)$ is a probabilistic component at any time t. The probabilistic component $P(t)$ has two sources. First, errors in measurement of environmental parameters yield probabilistic outcomes, hence, it is unlikely that the actual values of the parameters of interest can be known. Second, the random nature of the physical driving forces themselves, particularly meteorological factors, yield an inherent probabilistic component present even if measurement errors could be eliminated.

It is essential that the stochastic nature of the system be recognized. For example, it is possible, especially where record lengths and sample sizes are small, to observe time series of parameters which appear to show a change with time when the apparent change is the result only of the random nature of the system response. This suggests that effective environmental management requires tools which are stochastic in nature, especially when $P(t)$ is of the same order of magnitude as $D(t)$. A stochastic approach has been found

necessary in design of hydrologic, or water quantity related systems (Fiering & Jackson, 1971). Because water quality is quantity-dependent, water quality management systems require stochastic methods as well.

The feedback loop of Figure 1.1 implies some kind of measurement. There is a definite cost associated with each measurement of water quality parameters; this cost generally is quite high on a per sample basis (Vanderholm, 1972). The high cost of data acquisition has resulted in a deficiency of water quality data; one rarely reads a report on water quality conditions without encountering some mention of data deficiency. This data deficiency and the high cost of data collection suggest that some effort in careful design of measurement systems might well be cost-beneficial. It is to this problem of measurement system design that the current work is addressed.

One must exercise caution in design of a water quality monitoring system as such systems have varying objectives. For instance, data may be collected for abatement purposes, i.e., to detect violation of water quality regulations. It may also be used to establish a base line of data for future references, especially where existing data are sparse. Data may be collected in an attempt to establish cause-effect relationships between parameters. And finally, data may be collected in an attempt to establish, over the long run, tendencies, or trends in the level and/or variability of water quality parameters. A trend detection objective was chosen after a review of the literature (presented in the following section) indicated an apparent lack of appreciation of the importance of designing sampling networks for trend detection. The sparseness of the trend detection literature was particularly noticeable when viewed in the framework of a feedback management control

system (Figure 1.1).

Guidelines for the design of sampling networks for objectives other than trend detection have been published in the literature. Abatement objectives have been shown, subject to the constraints normally encountered by most managing agencies, to be unrealistic objectives for monitoring system design (Vanderholm, 1972). This results from the spatial and temporal grid sizes required. Spatial sample spacing is required to be on the order of the distance between sources and temporal frequency must be on the order of $1/T_s$, where T_s is a typical spill duration. These requirements indicate that, even for an efficiency of around 50% in spill detection, a sampling effort much larger than that presently conducted by most states must be implemented (Ward, 1973). Monitoring for data base establishment and for building and calibration of cause-effect models requires sampling programs of the same general character, namely a relatively short time frame and a relatively extensive spatial grid. Surveys of this type lend themselves to traditional statistical analysis (Elliot, 1971; Slack, et al., 1973). A somewhat more sophisticated method is provided by Moore (1971) for handling the same problem. The results of the present research might be applied to the problem of design of area-intensive surveys (see Chapter 8), although this is not a principal objective of this work.

The importance of the design of monitoring systems for identification of trends in water quality parameters has a basic relationship with the overall management system schematized in Figure 1.1. It is the expressed objective of most water quality managing agencies and much of the applicable legislation (for instance, the Federal Water Pollution Control Act Amendments of 1972) that water quality indicators

be maintained at some given levels. To achieve this, various management actions are undertaken to either improve or maintain existing levels of water quality. Consequently, it is essential to estimate whether the system is responding as desired. This implies the identification of trends.

Operational considerations have often dictated the use of waste discharge permits. These permits are renewed periodically, and the managing agency must assess, based on ambient conditions, what discharge levels are acceptable. Hence, it is desirable to identify the existence or absence of trends over a time span on the order of the permit renewal time, usually two to five years. This is the time scale used throughout this work.

III. Literature Review

In the literature review conducted by the author, no work was found which proposed methods for the design of water quality monitoring systems for trend detection. The work reviewed fell into two classes, those which proposed methods for design of surveillance and monitoring systems, and those which attempted to identify trends in time series of water quality parameters. None of the work reviewed attempted to use the latter as an objective of the former.

A paper by Wolman (1971) was the only work reviewed which attempted to identify the coupling between the two areas. In this work a comprehensive survey was conducted to determine trends in the quality of U.S. rivers over the longest period for which data could be obtained. The most important conclusion of the study was that existing data were inadequate to identify trends in water quality. Specifically, the

paper concluded that existing data were insufficient in volume and that the parameters being measured were usually inadequate to identify trends in river quality. Wolman pointed to the establishment of the National Water Quality Network (Sayers, 1971) as being a step toward providing the necessary quantity of data, but stated that methods applicable to design of monitoring networks for determining trends were essentially nonexistent.

Because the literature is segmented in its approach, the review presented here is partitioned for clarity. Literature proposing or utilizing methods applicable to the design of monitoring systems is presented first, followed by work in trend identification. Literature specifically applicable to a particular portion of this research is reviewed in the text as it is introduced.

III.1. Monitoring and Surveillance System Design

Spectral analysis was proposed as a tool for stream quality analysis by Wastler (1963). The application suggested requires a large sample size, so is only applicable when continuous or near-continuous samples are taken over a short time horizon or when a very long record length is available. A further limitation is the requirement that grid spacing (spatial or temporal) be held constant. Gunnerson (1966) applied spectral analysis to a dissolved oxygen record derived from a continuous monitor on the Potomac estuary. By sequentially eliminating undesired observations and transforming the record to the frequency domain, he was able to determine the minimum number of observations required to preserve the essential properties of the spectrum. In the case investigated, the required observation period was about two hours. Recent

literature has reported few applications of spectral analysis to sample system design, possibly because of the rigid requirements on the observation intervals and the number of observations required to provide adequate sample estimates of the spectrum. The use of cross spectral analysis, proposed by Wastler but not pursued in detail, has also received little attention, perhaps for similar reasons.

Pomeroy and Orlob (1967) investigated several problems involved in the setting of water quality standards. Most of their discussion considers the problem of determining which water quality parameters should be included in the standards. Of particular interest, however, is their approach to the setting of guidelines for the establishment of a minimum surveillance system. A nomograph is presented which relates the number of stations required and the observation frequency per station to river basin characteristics. River basin characteristics are summarized in the total drainage area, the average slope along the watercourse, and the ratio of maximum to minimum flow in the stream. The basis for the nomograph was not presented. The relationships were apparently derived from empirical observations of the characteristics of river basins which were thought to be adequately sampled. The analysis is applicable primarily to the design of surveillance systems for establishing data bases suitable for identification of long term trends.

Kittrell (1969) prepared a handbook for the use of field personnel in designing of sampling surveys for water quality. The primary emphasis is on short term intensive surveys; the problem of permanent surveillance network design is not addressed.

A report prepared for the Federal Water Quality Administration (NUS Corp., 1970) investigated the design of water quality surveillance systems

from a systems analysis framework. The report considered data acquisition and handling problems, legal problems associated with site acquisitions, and admissibility in court of data obtained by various surveillance techniques. The technical aspects of site location and sampling frequency were not specifically addressed, however.

Arnold (1970) presented a sampling strategy which makes use of the theory of Markov chains. By the use of a model for stream quality and the assumption that quality parameters are distributed normally about the predicted value, acceptance levels for various deviations from the mean were defined. A time delay representing the time until the next sequential sample was associated with each acceptance level. Given the probability distribution of a measure of the state of the system (dissolved oxygen was used) the number of samples required was calculated assuming the system was "in control", meaning that no perturbations occured to make the actual dissolved oxygen levels lie outside designated confidence bounds about the modelled values. The application of this research is limited by its failure to include constraints often faced in the design of real sampling networks; specifically manpower constraints in field applications prevent the flexibility required to implement variable sampling strategies of the type proposed.

Sharp (1970; 1971) made use of the concept of stream order numbers to determine the approximate location of sampling stations in a stream network. The scheme employed was to determine the approximate centroid of a branch network based on making the equivalent stream order numbers at the outlet of each subnetwork approximately equal. A monitoring station would be located at the outlet of each subbasin, and the process iterated. The method has the advantage that the relative value of each

station is also an output. This procedure has been the basis for some more recent work (Sanders, 1974; Chamberlain, et al., 1974). It has the disadvantage that hydrologic conditions only are included explicitly; pollutant source information and system dynamics are not incorporated.

Some work in the related field of experimental design for model parameter estimation has been reported. The original work was by Box and Lucas (1959) and was extended to applications in water quality modelling by Atkinson and Hunter (1968) and Berthouex and Hunter (1971a,b). The basic method is to make an initial guess at the parameters, then use the theoretical development to determine spatial and temporal sample point locations. These values are then processed, and the location of the next sample point is calculated. The procedure is ideally suited to sampling for model calibration where a sequence of measurements can be taken and processed (possibly overnight) so as to determine the sample point locations for the next sequence. The methodology does not, however, appear to be applicable to the design of permanent monitoring systems.

Gupta (1973) proposed the use of the variance of the sample mean and the variance of the sample variance to determine the necessary temporal sampling interval to define essentially independent observations.

Two information measures, taken from earlier work by Bayley and Hammersley (1946) were used. These measures were defined as

$$I_1 = \frac{V(\bar{X})}{V_1(\bar{X})}$$

$$I_2 = \frac{V(S^2)}{V_1(S^2)}$$

where $\bar{X}$ is the sample mean, S^2 is the sample variance, and where V is a variance estimate based on an assumption of independence of the data and V_1 is a variance estimate based on a lag one Markov persistence model of the data. The lag was taken as the sample interval for purposes of specifying the lag one correlation coefficient. A predetermined information criterion was then specified, allowing the determination of a sampling interval. Unfortunately, the example used in the paper was based on streamflow data for which, at worst, daily measurements are available. The approach is data intensive, a feature which would make application to water quality data difficult. In fact, the approach used is not much different from that of Gunnerson (1966) except that computations are performed in the time, rather than frequency domain. The problem of obtaining a good estimate of the autocorrelation function based on a short time series is present as in the work of Gunnerson (1966).

Chamberlain, et al. (1974) proposed a method for determining both spatial and temporal sample station location based on a stochastic DO model developed by Stochastics, Inc. (1971). The model used incorporates the Streeter-Phelps equations in stochastic form. The variance and mean of the DO estimates were calculated using a first order approximation (Cornell, 1972). The river was then segmented and an ultimate segment priority based on the probability of violation of specified standards was computed. Sample station location were then based on the segment priorities. For a given sample station layout, effectiveness of the network was specified using a temporal priority measure. This temporal priority measure was defined as the ratio of the expected number of violations detected to the expected number of

violations for each station, and is a function of sample frequency. By constraining the sample frequency the network efficiency was evaluated as a function of the number of samples available. This is the only work reviewed thus far which addressed analytically the problem of both spatial and temporal sample location. One drawback of the method is that the design is based only on the assumed properties of the probability distribution of DO; the optimal design for DO sampling was assumed to be representative of the optimal sampling design for other water quality constituents. The method could probably be extended to include more parameters if the underlying stochastic DO model were generalized. The method is restricted, however, to use of the standards violation criterion. Consequently, while this method of monitoring system design is well-adapted to design of monitoring systems for abatement purposes, it is of little help in design for trend detection.

Sanders (1974) presented a design method for determining sample station locations and frequencies for the purposes of establishing base line water quality information and detecting trends. He utilized the method of Sharp (197_0; 197_1) to establish macroscopic station locations, and mixing length theory (Cleary and Adrian, 1973) to establish microscopic locations. Microscopic locations were set at the point where complete mixing below an outfall occurred or at the bottom of the reach if lateral mixing was incomplete. Analysis of variance (one or two way depending on whether vertical mixing was complete) was used to specify the number and location of stations needed in the cross-section. It was found that even when mixing was far from complete, high correlations existed between water quality parameter concentrations in the cross-section. The residual error in the yearly mean concentrations

at each station was used as a criterion for the number of stations required.

The work of Sanders is significant in that it represents the first attempt to relate sample location to turbulence characteristics of the stream. The sacrifice paid for including mixing characteristics in the design rather than using a one dimensional flow model was that assumptions of conservative constituent concentration dynamics and point source effluents with deterministic flow and concentrations were required. In addition, no method was presented for determining the tradeoff between sample station density and sample frequency. However, the results of the present work coupled with possible inclusion of mixing length phenomena discussed by Sanders could ultimately be included in extensions to both methods as discussed in Chapter 8.

Ward, in a series of papers based primarily on a Ph.D. dissertation by Vanderholm (1972) has investigated cost effectiveness of water quality surveillance systems (Ward, 1973; Vanderholm and Ward, 1973; Ward and Russell, 1973; Ward, Nichols, and Skogerboe, 1973; Ward and Vanderholm, 1973). The research addressed primarily the design of surveillance systems for abatement in contrast to much of the other work reviewed which is oriented more toward data base establishment and intensive surveys. The strategy used was to model a conservative pollutant by the convective diffusion equations. Instantaneous spills were "created" in the model at random time increments and at random spatial locations along the length of the stream modelled. Several strategies were investigated for the spatial location of stations. Various time frequencies of sampling were investigated, and for each an effectiveness measure, defined as the ratio of spills detected to total spills, was computed.

All samples were assumed to be instantaneous, grab samples. The results of this research allow a rough estimate of how extensive an abatement network needs to be. The assumption of a conservative pollutant makes the estimated effectiveness based on this study an upper bound on what might be expected in a real system. As such, it appears that under existing budget constraints (Cunningham, 1970; Ward and Vanderholm, 1973) the use of monitoring for abatement may not be a viable objective.

Moore (1971; 1973) made use of the linear Kalman filter, which had previously found application mostly in aerospace and marine navigation systems, for monitoring system design. The Kalman filter (see Chapter 3) utilizes both modelled and measured system response to arrive at a best estimate of the true state of a system. Moore's work incorporates the water quality model of Water Resources Engineers, Inc. with a linearized filter model to determine best estimates of four state variables for a reach of the Sacramento River. The four state variables were concentrations of phytoplankton, zooplankton, nitrate, and temperature. Since the Kalman filter algorithm estimates at each step a system state covariance matrix as well as the estimated system state vector, a variance criterion can be developed for the sample spacing. The strategy employed was to sample whenever the variance of any single state element exceeded a given amount, or alternatively when the sum of the estimated state variances exceeded some limit. Using this procedure the necessary sampling period was determined at a given station. The problem is much more complicated when spatial variation is introduced as well; the approach used was to define a state vector element for each constituent at each of a number of discrete locations. A trial and error approach was used to determine the "best" measurement matrix, i.e. which

variables were to be measured at each station. A variance constraint was then imposed, allowing determination of the optimal temporal sampling frequency.

Moore's work is significant in that it is the only work reviewed which can account for multiple quality measures varying in both space and time. It is also significant in being one of the few applications of filtering techniques to water quality data, an approach which is very attractive in that it incorporates both modeled and observed estimates of the system state in determining the best (minimum variance) estimate of the true system state. The work has several shortcomings, however. The constraining of the state variance estimates does not appear to be realistic; in management applications the cost is usually constrained. Also, the procedure used in determining spatial locations gives no guarantee of optimality, it can only determine which configuration among those tested is best. Finally, high computer costs forced the consideration of only four water quality indicators, and in fact, only one of these (temperature) is actually included in the water quality standards of Washington State.

Moore's work utilizes a dynamic stream quality model; hence, both spatial and temporal variations are included. Unfortunately, this constrains the optimization to be valid only for the given hydrograph. **A complete optimization will require optimizing over a probability distribution of hydrographs, and will be prohibitively expensive given existing computational speeds. Nevertheless, the filter method allows a convenient method of including the dynamics of parameter interactions as well as the dynamics of flow routing on the design methodology. The potential of this method merits further investigation.**

Perlis and Okunseinde (1974) utilized Kalman filter theory in design of a monitoring system for dissolved oxygen (DO) and biochemical oxygen demand (BOD) in a stream. This is the only other work known to the author which makes use of state estimation theory in monitoring system design. The method incorporates measurements of total organic carbon and DO, which are available with essentially no time delay, and BOD, which normally requires a five day laboratory analysis period. The specified monitoring network minimizes a cost function which includes a space integral of the estimation error and measurement costs. The model assumes steady state flow conditions; no temporal sampling strategy is included. Consequently, the network specified is applicable primarily to intensive surveys.

III.2. Trend Detection

Enviro Control (1972) prepared an analysis of nationwide trends in water quality for the Council on Environmental Quality. The analysis utilized stations in EPA's STORET system. Parameters examined included measures of oxygen depletion and demand (DO, BOD, TOC, COD), nutrients (NH_3 + organic N, NO_3 + NO_2, total P, soluble P), suspended solids and salinity. An attempt was made to establish flow dependence of each parameter at each station, although no attempt was made to normalize the raw data for this dependence. Stations were segregated into four classes according to population, agricultural development, and industrial development. Arbitrary limits were set for total variation of each parameter. If the total variation in a given parameter over the record length exceeded the limit, a trend was said to exist. It is unclear how the total variation was calculated; apparently the data

sequence was partitioned into two halves and the medians of the first and second sequence compared. The results, regardless of which method was used in calculation of total variation, are of questionable statistical validity as the confidence level was arbitrarily set for each parameter. Consequently, there is no common base for comparison of trends in different parameters since the effective confidence levels vary. The conclusions made as to general nationwide trends, namely an apparent increase in nutrient values and no change in other parameters over the record length (about eight years for most parameters at most stations) are of doubtful validity.

The Environmental Protection Agency (1974) prepared an inventory report of 22 U.S. waterways including an analysis of trends using data from EPA's STORET file. The 22 waterways were selected as belonging to one or more of three groups: the ten longest rivers, the ten rivers with the highest average annual flows, and the waters of the ten largest urban areas in the U.S. The available records were examined for trends in 28 parameters, although many of the 28 were essentially indicators of the same quantity and show similar results, for instance, NH_3, organic N, NO_2, $NO_3 + NO_2$, NO_3 (as NO_3), and NO_3 (as N) were all measured at one or more stations. The method used to determine trends was a comparison of the medians of the 1963-67 sequence with those of the 1968-72 sequence for each parameter. An upward trend was said to exist if the second median was larger than the first, a downward trend if the reverse was true. No statistical analyses were performed, hence no confidence limits are available which makes conclusions based on the results extremely dangerous. For instance, if a different method were used, e.g., confidence bounds placed on the difference between medians

of the two sequences and trends judged to exist only if the difference exceeded the value of the confidence bound, it is likely that few of the sequences would show trends because of the small sample sizes available and the natural variability of the time series. Alternatively, confidence bounds might be placed on the percentage values of increasing trends derived using the method of the report, although this is a difficult statistical problem. In the form presented, however, the results give little more than an educated guess as to what is really happening. The results presented suggest increasing levels of nutrients and decreasing levels of most other pollutants. This may be contrasted with the results of Enviro Control (1972) which showed few trends in most parameters with the exception of nutrient values, which both reports agree are increasing.

Steele, et al. (1974) conducted an analysis of historical water quality data from 88 stations of the United States Geological Survey (USGS) National Stream Quality Accounting Network (NASQUAN). The objective of the study was to determine areal and temporal variations in streamflow chemical quality and temperature. Only the latter objective is of interest here. Data limitations required consideration of specific conductance as the sole indicator of chemical quality. The method employed utilized Fourier decomposition of the record into yearly mean values and amplitude and phase coefficients corresponding to the annual cycle. New sequences were formed consisting of these yearly values, hence, each time series (of, for instance, daily values) yielded three time series of yearly values; a fourth was formed by adding yearly means to yearly amplitude coefficients. These time series were analyzed for trend using Kendall's tau and Mann-Whitney's tests (see Conover, 1971).

Fifteen of the 88 stations showed changes in one or more of the yearly temperature sequences, most of the changes in stream temperature were apparently attributable to increased regulation and were evidenced in decreases in the series of annual harmonic amplitude coefficients. Fifteen of the 88 stations showed significant (99% confidence levels were used throughout the study) changes in one or more of the annual chemical sequences, ten of these showed worsening conditions, five improving.

The results of the USGS (Steele, et al.) investigation are derived from methods with a sound statistical basis, hence, the results have considerably more meaning than those of the Enviro Systems or EPA studies. Principal limitations are sample station locations and parameters analyzed. Stations in the NASQUAN system usually are affiliated with USGS stream discharge stations and may not be in the best locations to allow conclusions on trends in water quality nationwide. The stations used are predominantly in rural areas where water quality is primarily affected by agricultural nonpoint sources, irrigation return flows, and impoundments; the Enviro Systems and EPA reports center more on urbanized areas where problems tend to be associated with urban runoff and point source discharges. In addition, the USGS report does not include nutrients, toxic substances, and oxygen demand measures, primarily because of lack of sufficient data. The incorporation of (classical) statistically valid methods in the USGS report results from the relative completeness of the records used, something not enjoyed by the other work. A comprehensive nationwide survey remains to be conducted, and will be a difficult undertaking because of gaps in data and so-called "wild points". The limitations of the existing work, however, point to

the necessity for such a study, as important long range decisions must be based on trends in nationwide water quality. Such a study might well profit from the nonlinear smoothing methods employed by Cleveland & Kleiner (1974) in their analysis of air pollution data.

CHAPTER 2

PROBLEM FORMULATION AND SOLUTION APPROACH

I. Analytical Formulation

The objective of the present research is to design a monitoring system for a state vector[a] of concentrations of water quality indicators $\bar{c}^*$. Here $\bar{c}^*$ is a time average concentration vector where the averaging time T_{av} is at least long enough to remove fluctuations due to turbulent flow structure; hence, the convective diffusion equation with source terms is (Ippen, 1966)

$$\frac{\partial \bar{c}^*}{\partial t} + \frac{\partial}{\partial x}(u^* \bar{c}^*) + \frac{\partial}{\partial y}(v^* \bar{c}^*) + \frac{\partial}{\partial z}(w^* \bar{c}^*) = \frac{\partial}{\partial x}\left(D_x \frac{\partial \bar{c}^*}{\partial x}\right)$$

$$+ \frac{\partial}{\partial y}\left(D_y \frac{\partial \bar{c}^*}{\partial y}\right) + \frac{\partial}{\partial z}\left(D_z \frac{\partial \bar{c}^*}{\partial z}\right) + \bar{r} \qquad (2.1)$$

where u^*, v^*, and w^* are longitudinal, transverse, and vertical velocity components averaged over the same time as $\bar{c}^*$, and $\bar{r}$ is a vector of source-sink terms.

Equation 2.1 is difficult to solve for $\bar{c}^*$, since the velocity field itself is rarely well known and because estimation of the diffision coefficients will require extensive data not usually available. Considerable simplification is possible, however, if the investigation is limited to the propagation of cross-sectional average concentrations

---

[a] Throughout this report, overbars (e.g. $\bar{a}$) indicate vectors, and underbars (e.g. $\underline{b}$) indicate matrices. Throughout this chapter the notation c* denotes "the average value of c".

and velocities. Under this condition the third and fourth terms on the left hand side of eq. 2.1 drop out, as no concentration flux is possible across the stream cross-section boundaries (supply and loss from benthal and atmospheric sources and sinks are included in $\bar{r}$).

An order of magnitude analysis may be performed on the remaining two terms on the left hand side of eq. 2.1. The maximum sampling frequency imposes a limit on the time scale of the fluctuations in $\bar{c}^*$ which can be tracked. Consequently, the averaging time for $\bar{c}^*$ must be on the order of the inter-sample time, thus, if the approximation $\frac{\partial \bar{c}^*}{\partial t} \simeq \frac{\bar{c}^*_{t+\Delta t} - c^*_t}{\Delta t}$ is made, and for clarity a state vector of dimension one is considered,

$$c^*_t \simeq \frac{1}{n}\left[\frac{c_o}{2} + \sum_{j=1}^{n-1} c_i + \frac{c_n}{2}\right] ,$$

$$c^*_{t+\Delta t} \simeq \frac{1}{n}\left[\frac{c_1}{2} + \sum_{j=2}^{n} c_i + \frac{c_{n+1}}{2}\right]$$

$$\text{and} \quad \frac{\partial c^*}{\partial t} \simeq \left[\frac{\frac{c_n+c_{n+1}}{2} - \frac{c_o+c_1}{2}}{n\Delta t}\right] , \tag{2.2}$$

$$\text{then} \quad \frac{\frac{\partial c^*}{\partial t}}{\frac{\partial}{\partial x}(u^* c^*)} \simeq \left[\frac{\frac{c_n+c_{n+1}}{2C} - \frac{c_o+c_1}{2C}}{n\Delta t}\right] \Bigg/ \left[u^* \frac{c_{x+\Delta x} - c_x}{C\Delta x}\right] \tag{2.3}$$

where u^* is assumed constant in space,

C is an arbitrary normalizing concentration value,

$t_{n+1} - t_n = \Delta t$

and $n\Delta t = T_{AV}$, the averaging period.

The relative magnitudes of the terms (eq. 2.3) may be investigated using "typical" values, as shown in Table 2.1.

The tabulations of Table 2.1 show that even if the time rate of change of c_t is very high locally, the averaging process damps out the variation to the extent that the first term in eq. 2.1 is usually an order of magnitude less than the second. Thus, the averaging process employed provides justification for neglecting the first term in eq. 2.1 unless the averaging period is very short, the spatial change in concentration flux is very small or the time change in concentration is very high. It should be noted that this approximation is not valid when concentrations are uniformly increasing or decreasing at a rapid rate over a long period of time as in curve 1 of Figure 2.1. In the case of uniform changes in concentration $\frac{\partial c^*}{\partial t} \simeq \frac{\partial c}{\partial t}$ where $\frac{\partial c}{\partial t}$ is the instantaneous time rate of change in concentration. Consequently, the steady state approximation will surely not be valid, for instance, when a phytoplankton bloom is in progress if nutrient concentrations are of interest. If, however, local changes in c are either high frequency fluctuations or low frequency ones of small magnitude (for instance, due to seasonal effects) as shown in curves 2 and 3 respectively, of Figure 2.1, the approximation will hold.

Harper (1972) showed that, for steady discharges of wastes the diffusion terms in eq. 2.1 are negligible. This is essentially the case to which we are confined by the approximations made above, as we do not consider short term fluctuations in c. Dropping the diffusion terms, eq. 2.1 reduces to

$$\frac{\partial}{\partial x}(u^* \overline{c^*}) \simeq \overline{r} \qquad (2.1a)$$

Table 2.1: Order of Magnitude Comparison for Steady State Assumption

T_{av}, weeks	ΔX, miles	u, ft/sec	Δt, hrs	$\frac{c_n+c_{n+1}}{2C} - \frac{c_o+c_1}{2C}$	$\frac{c_{x+\Delta x} - c_x}{C}$	$\frac{\frac{\partial c^*}{\partial t}}{\frac{\partial}{\partial x}(u^* c^*)}$
1	10	2	1	0.1	0.1	0.0436
1	10	2	1	0.5	0.1	0.218
0.5	10	2	1	0.1	0.1	0.0872
0.1	10	2	1	0.1	0.1	0.436
1	10	0.5	1	0.1	0.1	0.1744
1	10	2	1	0.1	0.01	0.436

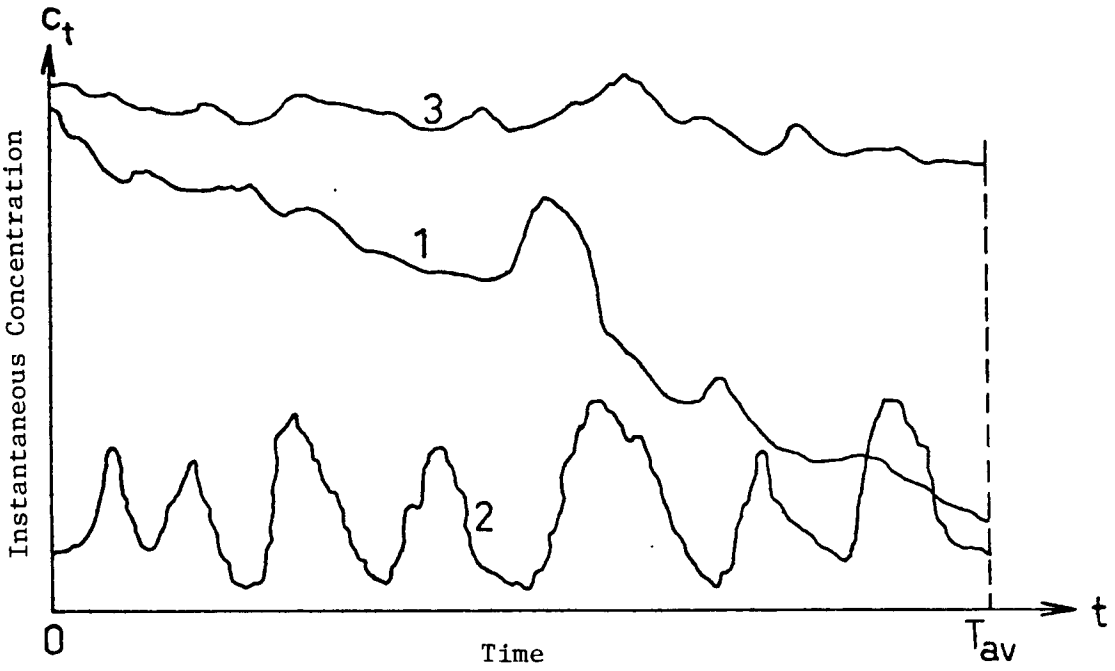

Figure 2.1. Possible Modes of Variation in Instantaneous Concentrations

Here u^* is, in general, a function of space and time. It is desired now to constrain the velocity to also be steady state, i.e., $\frac{\partial u^*}{\partial t} = 0$. The validity of this assumption may be investigated using existing time series of streamflow records. Consider a time series q_i, where q_i is the daily average streamflow on day i at a given station. Now consider the bivariate series (q_i^1, q_i^2) where q_i^1 and q_i^2 are defined as $q_i^1 = q_{i-1}/q_i$, and $q_i^2 = q_{i+1}/q_i$. The joint distribution function, $f_{Q^1Q^2}(q^1, q^2)$ gives a measure of how quickly the daily average flows are varying, where, following standard statistical notation,

$$f_{X_1X_2}(x_1,x_2) = P(X_1 \leq x_1 \leq X_1+dX_1,\ X_2 \leq x_2 \leq X_2+dX_2)$$

$$\text{hence } P(q^1,q^2)\ \varepsilon R = \int_R f_{Q^1Q^2}(q^1,q^2)\ dQ^1dQ^2$$

where R is the region containing flow ratios of interest.

The joint distribution functions of q^1 and q^2 for the Spokane River at Spokane and the Snohomish River near Monroe for water years 1971-73 are given in Figure 2.2. The joint distribution functions were estimated using the method of Tarter, et al. (1967). Within the region $0.87 \leq q^1 \leq 1.13$, $0.87 \leq q^2 \leq 1.13$ the rate of change in average daily velocities is less than 5%, computed on the basis of a rectangular channel with constant Manning's n, whence $U/U_o = (Q/Q_o)^{.4}$ with U_o and Q_o as base velocities and flows respectively. This region is shown in Figure 2.2b; the entire plot area of Figure 2.2a falls within this region. Figure 2.2 shows that both the Spokane and Snohomish River flow regimes may be considered quasi-steady state for the purposes of this investigation. The Spokane River, with some upstream regulation and the damping effect of its source, Lake Couer d'Alene, has an extremely stable flow regime. The Snohomish River is essentially unregulated, and the flow regime is much more sensitive to Pacific Coastal storm fronts. Nevertheless, the flow regime is dominated by the slowly decaying recession limb of the hydrograph, accounting for the relative stability of the flow regime.

Including the steady state flow assumption, eq. 2.1a now becomes

$$\frac{\partial}{\partial x}(u^*(x)\bar{c}^*(x)) = \bar{r} \qquad (2.1b)$$

where both u^* and $\bar{c}^*$ are spatial functions only.

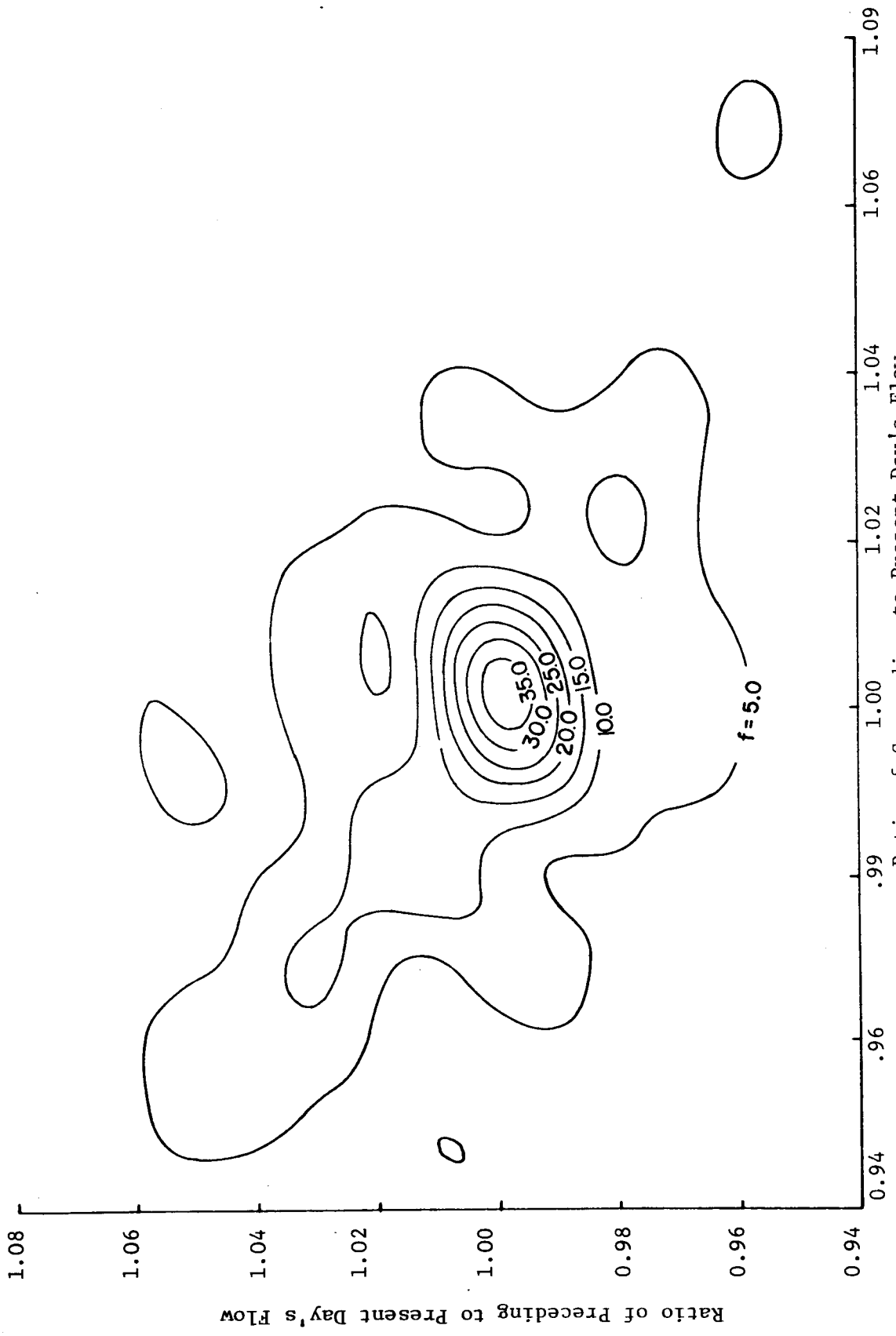

Figure 2.2a Bivariate Probability Density Estimate for Preceding and Succeeding Daily Average Flow Ratios, Spokane River at Spokane, Washington

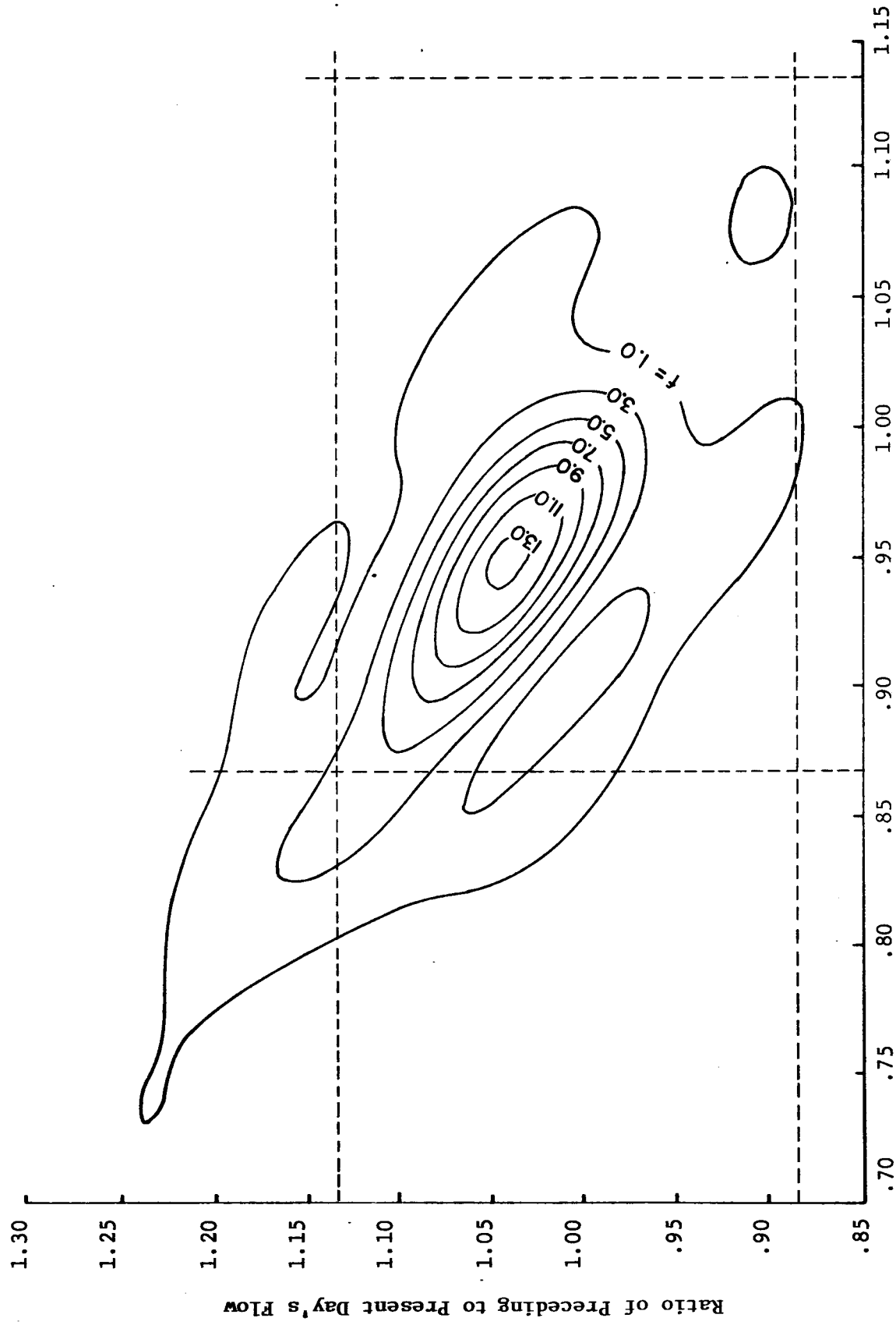

Figure 2.2b Bivariate Probability Density Estimate of Preceding and Succeeding Daily Average Flow Ratios, Snohomish River Near Monroe, Washington

It should be noted that the steady state flow assumption will not hold for small streams, especially those characterized by partial or complete urbanization. In these cases variations in flow rate must be included in the analysis, e.g. the model used must include a rainfall runoff module with channel routing capability, such as the Stanford Watershed Model (Crawford and Linsley, 1966). For large streams such as those investigated here, however, this should not be necessary.

In order to compensate for the assumptions made, it is necessary to introduce an error term $\bar{V}(x)$ in eq. 2.1b, hence,

$$\frac{\partial}{\partial x}\left(u^{*}(x)\bar{c}^{*}(x)\right) + \bar{V}(x) = \bar{r} \tag{2.1c}$$

where the averaging notation has been dropped and it is understood that $\bar{u}^{*}$, $\bar{c}^{*}$, $\bar{r}$, and $\bar{V}$ are spatial functions only. In addition, it is assumed that[a]

$$E(\bar{V}(x_1)\bar{V}^{T}(x_2)) = \underline{Q}(x)\delta_{x_1 x_2} \tag{2.4}$$

where δ is the Kronecker delta function, $\delta_{ij} = \begin{cases} 0 & i \neq j \\ 1 & i = j \end{cases}$ and x_1 and x_2 are discrete spatial locations. These assumptions are not so confining as might be imagined. First, the noise covariance matrix $\underline{Q}$ is normally assumed zero in the absence of divergence (see Chapter 3). Second, if the noise vector is exponentially correlated and spatial locations of interest are sufficiently separated, Jazwinski (1970) has shown that the problem may be treated as if the requirements of eq. 2.4 were met. Nevertheless, the solution of eq. 2.1c is by no means trivial as $\bar{r}$ may

---

[a]The notation $\underline{A}^{T}$ denotes "the transpose of $\underline{A}$".

be very complex, and $\bar{V}$ can only be known, of course, in a statistical sense.

The problem as formulated is to design a network of monitoring stations capable of distinguishing long range changes (trends) in a vector of water quality constituents whose dynamics are described by eq. 2.1c. The assumptions made in reaching this formulation are substantial, and since the validity of the solution cannot be better than the assumptions imply, these assumptions should be emphasized. The monitoring system design optimization is constrained to the detection of long term variations in water quality parameters where the optimization is based on quasi-steady-state flow and steady-state stream quality dynamics and where only cross-sectional average concentrations are considered. In addition the noise vector $\bar{V}$ included to compensate for the assumptions made is assumed to be spatially uncorrelated.

II. Design Methodology

In this section the basis of the overall design methodology is introduced. Details of methods used in design substeps are addressed in Chapters 3, 4, and 5. It is the intent here only to provide the reader with an overview of the relationship of the methods detailed in later sections to the overall methodology.

As the problem has been formulated in the preceding section, temporal and spatial dependence may be treated separately, where the only temporal variations of interest are those measurable as long range trends. Hence, the monitoring design may be optimized subject to a constraint on maximum total samples per unit time, f_c, as follows. First choose a range of candidate numbers of sample stations,

NS_k, k = 1, 2, ..., m. To satisfice[a] sample station locations it is necessary to determine the propagation of uncertainty of estimated quantities downstream from the sample station. For instance, associated with a measurement M_{ji} of a quantity j at station i is a variance σ^2_{ji} which may be used to parametrize the uncertainty, where σ^2_{ji} is determined by the confidence in both the model used (modelling error) and the measurement taken (measurement error). If X_i denotes the i^{th} sample station, a variance $\sigma^2_{jx}|\sigma^2_{ji}$ is associated with each point x where $x_i<x<x_{i+1}$.

Downstream at any point x, where $X_i<x<X_{i+1}$ (the subscripts i and i+1 denote sample station locations) is associated some variance $\sigma^2_{jx}|\sigma^2_{ji}$. Here the conditional notation denotes the value of the quantity j at location x conditioned on the variance based on the measurement at location i, the closest upstream station. Schematically the variance propagation as a function of distance, for arbitrary sample station locations, may resemble that of Figure 2.3. In Figure 2.3 $X_{NS_{k+1}}$ is defined to be the end of the stream stretch, and is not a sample station location, a convention followed throughout the remainder of this work. The point reduction in variance at a sample station corresponds to the additional information given by the measurement, which results in a decrease in uncertainty in the estimate of the true quantity.

---

[a]The term satisfice indicates a loosely defined pseudo-optimization in situations where a strict global optimization is inappropriate. The term is especially relevant in problems where a solution which is preferred to other feasible solutions is readily available, and where the global optimum is only very slightly preferred to this "satisficing" solution. In this work solutions are sought which satisfice, rather than optimize over the design criterion, hence even although the terms optimal, optimize, etc. are used in later sections it should be understood that the solutions are really satisficing, rather than optimizing.

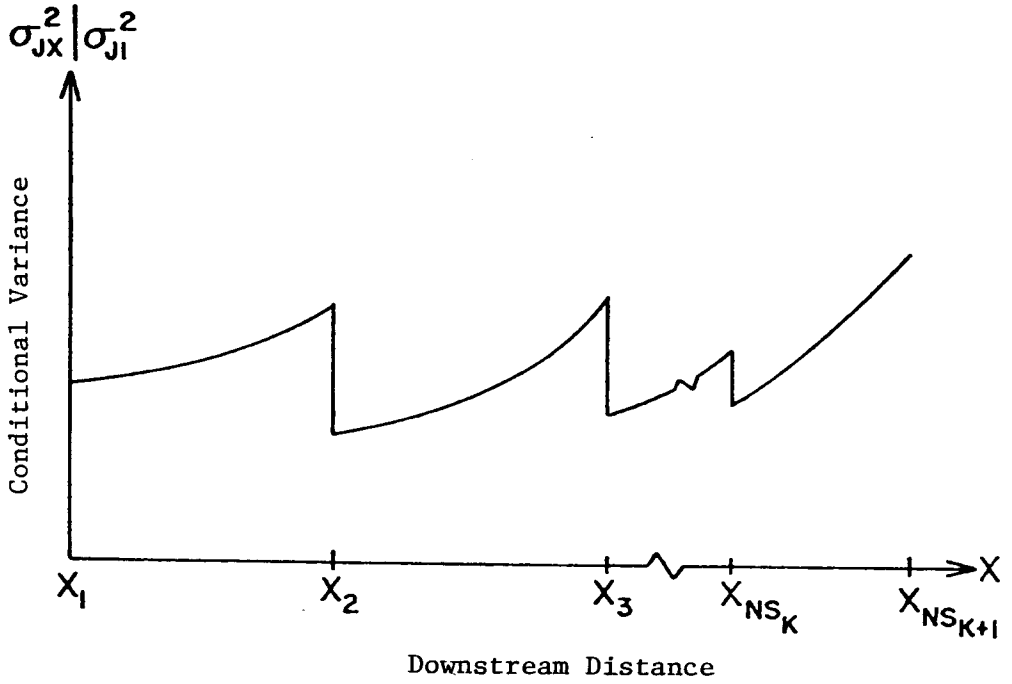

Figure 2.3. Variance Propagation Schematic

State estimation techniques allow the determination of variance propagation and are utilized in this research. The details of this method for determining variance propagation are discussed in Chapter 3.

Given the variance propagation as shown in Figure 2.3, criteria may be developed for satisficing sample station location. The method used here is to equalize the integrated variance associated with each station, i.e., $\int_{X_i}^{X_{i+1}} \sigma^2_{jx} | \sigma^2_{ji} \, dx$ = constant, i = 1, 2, ..., NS_k. Here X_i is the upstream boundary of interest and X_{NS_k+1} is the downstream boundary. An <u>apriori</u> estimate of the variance, σ^2_{j1} is made at X_1. If more than one parameter is included, the criterion is

$$\int_{X_i}^{X_{i+1}} \sum_{j=1}^{NV} \sigma^2_{jx|\sigma^2_{ji}} \cdot w_j \quad dx = \text{constant} \qquad (2.5)$$

where w_j is an arbitrary weighting factor associated with each parameter of interest, and NV is the number of parameters of interest. The choice of the w_j's is analogous to the choice of the weighting factors in a multiple objective optimization and is ultimately, of course, subjective as the w_j's essentially provide an equivalence between "apples and oranges". In some cases, however, the weighting factors may be dictated by legislation which establishes the constituents to be monitored.

The station location criterion of eq. 2.5 was chosen because it provides an equalization of the integrated spatial dependence on each station. Alternatively, a criterion may be selected which specifies equalization of the peak variance magnitudes, as was done by Moore (1971). This assumes, however, that the prediction variance increases between sample station, as shown in Figure 2.3. Preliminary results of this work showed, however, that this need not be the case; in fact, the estimation variance propagation depends on the form of the model dynamics and may actually decay between stations, making a peak variance criterion meaningless. For this reason, the integrated variance criterion was chosen.

Given the sample station locations for candidate numbers of sample stations, NS_k, the temporal sampling frequency may be computed as $f = f_c/NS_k$, where f_c is the constraint on total samples per unit time. Here uniform temporal sampling frequency is assumed and it is assumed that the same parameters are measured at each sampling time.

At this point the introduction of some background from statistical

hypothesis testing theory is necessary. Essentially we require the power curve for each parameter as a function of spatial location, where the power, P_w, following statistical nomenclature, is the probability of detecting a trend given that one really exists. In general, $P_w = P_w(\alpha,n,\sigma^2,T_r)$ where α is the confidence level, or the probability of prediction the existence of a trend given that one does not really exist, n is the sample size, σ^2 is sample variance, and T_r is the trend magnitude. The relationship becomes more complicated if the samples are not independent, which is usually the case. Dependence in time series and implications for hypothesis testing are discussed in detail in Chapter 4. At this point, it is necessary only to recognize the existence of a power curve, usually of the form of Figure 2.4 (curve 1) for each n, where $n = N_y \cdot f$, and N_y is the number of years over which trend detection is desired. Throughout this work a base value of N_y of four years was taken because this is approximately the length of time over which permit renewal decisions must be made. The power P_w is determined at each location x where α, n, σ^2, and T_r are determined as follows. The confidence level α is selected <u>apriori</u>. A base confidence level of 95% was used throughout this report. The sample length n is computed as described above. The variance, σ^2, must be computed using historical information as well as the prediction variance. In general, the variance of an arbitrary historical sequence has two contributions, measurement and prediction error and natural variability. These two contributions may be assumed to be independent, hence $\sigma^2 = \sigma_m^2 + \sigma_n^2$, where σ_m^2 and σ_n^2 are the measurement and prediction, and natural contributions, respectively. At any point x, the variance in the time series of predicted values based on a given selection of sample locations

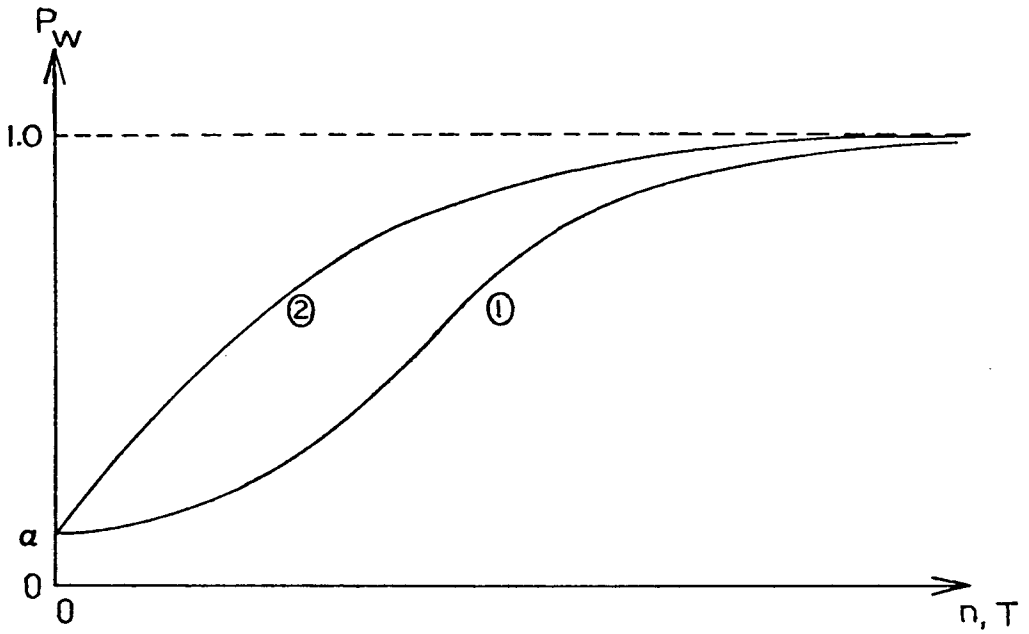

Figure 2.4. Typical Power Curves

is $\sigma^2_{p_{ix}} = \sigma^2_{n_j} + \sigma^2_{jx}$ where the conditional notation has been dropped but it is implied that $\sigma^2_{p_{ix}}$ is the predicted variance in the time series at location x conditioned on the time series at the closest upstream station, i. Finally, the trend magnitude, T_r is selected <u>apriori</u> and is equivalent to the selection of, say, the design storm for a structure. Two forms of trends are considered, linear and step increase. The linear trend is a uniform increase of magnitude T_r over the record length and the step increase is an instantaneous

change of magnitude T_r at the midpoint of the record. Consequently a linear trend of magnitude T_r has the same average change over the record length as a step trend of magnitude $T_r/2$.

Having determined, in a manner specified in Chapter 4, the power at each spatial location, an integrated measure of the power may be computed as

$$P_k = \int_{X_1}^{X_{NS_k+1}} \left[\sum_{j=1}^{NV} P_{w_{jx}} W_j \right] dx \qquad (2.6)$$

where W_j is an arbitrary weighting factor and NV is the number of variables of interest. The optimization is now performed by choosing $P^* = \max_k (P_k)$.

Typical power curves are given in Figure 2.4. Curve 1 shows how the power of detection of a trend of given magnitude (fixed T_r) increases with the number of samples, n, taken. Curve 2 shows the increase in power with increasing trend magnitude T_r for n fixed. Both curves 1 and 2 assume the standard deviation of the series of observations to be fixed.

This introduction has ignored, in the interest of brevity, such difficulties as the choice of design trend (Chapter 5), dependence in the time series of observations (Chapter 4), estimation of σ_n^2 (Chapter 5) and the influence of seasonally driven cycles (Chapter 5).

III. Issues in Model Building

In order to progress beyond a purely kinematic approach to monitoring system design, such as that proposed by Sharp (1970; 1971), it is necessary to incorporate knowledge of the dynamics relating values of water quality parameters. This leads inevitably to the need to conceptualize the form of the interactions between parameters, hence the choice of a model. Some brief comment concerning this choice seems appropriate.

The question of choice of model is often surrounded by controversy, since that decision is, in the end, a subjective one. Recognition of two differing objectives in model building may reduce some of the subjectiveness, however. Models may be used as an aid in conceptualizing physical processes; such conceptualization may be an end unto itself, particularly in scientific research. In engineering research, conceptualization is normally seen as a means toward ultimately building operational models for design application. In either case, if conceptualization is the objective of the model, a reasonably detailed approach is usually taken, and there is a conscious attempt to attach a physical meaning to model components. If, on the other hand, the objective is to build an operational model, one which merely reproduces observed phenomena, it is not always necessary to attach direct physical meaning to components in the modelling process. For instance, some components may be lumped in such a way that their individual contributions cannot be disaggregated, and components which are relatively insignificant may be ignored. Often models of the first type suggest required forms for models of the second type. Dracup,

et al. (1970) provide an extensive analysis of considerations in model building which emphasizes possible pitfalls.

For the purpose of this research, operational models are preferred. This is so because the requirement for monitoring system design is not so much a conceptually accurate understanding of parameter interactions as an adequate basis for describing variance propagation in an operational sense. In fact, a secondary use of the data collected (the primary use is, of course, trend detection) is the development of improved models. The improved models may be used to redesign the monitoring system. The process is an iterative one, as shown in Figure 2.5.

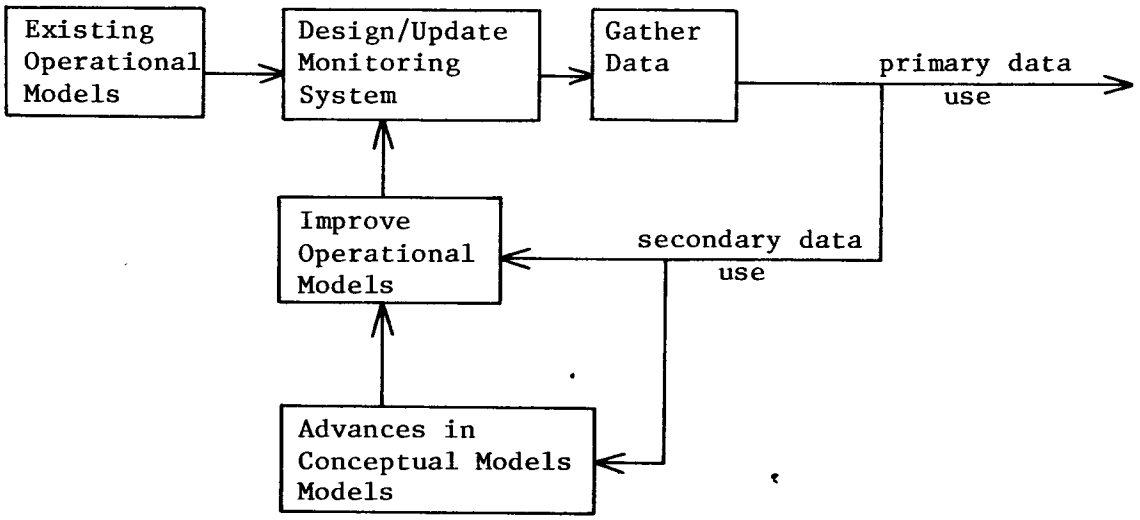

Figure 2.5. Interactions Between Monitoring System Design and Model Building

Harper (1972) conducted a survey of operational water quality models. In general, he found that the more detailed of these were one dimensional, included the BOD-DO-nitrification system with settling and resuspension terms, accounted for phytoplankton photosynthesis and included dynamic flow routing. A more recent review by Systems Control, Inc. (1974) showed that the principal change since Harper's review was conducted has been the incorporation of hydrologic aspects of water quality modelling through coupling of a watershed-hydraulic routing model with water quality modules similar to those reviewed by Harper.

The author is unaware of any quantitative attempt to compare performance of the different operational water quality models on the basis of the limited data usually available for calibration and verification. There is, however, undoubtedly some level beyond which increased complexity results in decreasing performance, i.e. "overfitting" the data.

The methodology developed in this report is not dependent on a particular form for the modelling of parameter interactions. Implementation, however, requires specification of the form of the dynamic interactions using some model as a basis. The model selected has three modules. The primary module includes interactions between biochemical oxygen demand (BOD), dissolved oxygen (DO), orthophosphate ($O\text{-}PO_4\text{-}P$), nitrite ($NO_2\text{-}N$), nitrate ($NO_3\text{-}N$) and ammonia ($NH_3\text{-}N$). Two secondary modules describe coliform and temperature dynamics. The primary module is a simplified form of the DOSCI steady-state stream model developed by Systems Control, Inc. (Finnemore & Shepherd, 1974). The coliform module includes a simple first order die-off with a non-point source supply term, and the temperature model incorporates a simple heat

balance approach. A detailed description of the models used is provided in Appendix A. The DOSCI model was chosen because of its ease of accessibility (the program listing itself is available to the user), because it appears to be representative of the general level of operational models presently available, and because the steady state assumption made in this research is incorporated in the model, reducing computation time considerably. This particular choice of model form does not suggest a judgment of superiority over other available models, in fact the methodology developed here could proceed with the choice of any other available model. The choice is primarily one of convenience to both the author and potential users of the methodology developed in this research.

In the following chapter the basic elements of state estimation theory required to incorporate the dynamics of a deterministic model (e.g., the DOSCI steady state stream model) in a filter (stochastic) model are introduced. The results of this development will ultimately be used in establishing the particular form of the variance trajectories (Figure 2.3) for a vector of water quality variables. These trajectories are necessary to specification of sample station locations as well as to determination of measurement and prediction error as a function of spatial location. The latter result is necessary to derive trend detection power curves at each spatial location along a river reach conditioned on given sample station locations.

CHAPTER 3

USE OF STATE ESTIMATION TECHNIQUES IN DESIGN OF MEASUREMENT SYSTEMS

I. Introduction

State estimation theory has long been a topic of interest in the aerospace field. Before the landmark work of Kalman and Bucy (Kalman, 1960; 1963; Kalman and Bucy, 1961), however, the theory was essentially incompatible with numerical techniques. The work of Kalman and Bucy, while originally limited to linear time-invariant systems, gave impetus to more recent work, the result of which has been numerous filtering approaches applicable to more general nonlinear, time-variant systems. It is the purpose of this section to briefly review the theory, to present several of the more well known nonlinear filtering techniques, and to discuss their adaptability to measurement system design.

The general model considered in all the filtering schemes discussed here is:

$$d\bar{X}(t) = \bar{f}(\bar{X},t)\,dt + d\bar{n}(t) \tag{3.1}$$

$$d\bar{Z}(t) = \bar{h}(\bar{X},t)\,dt + d\bar{w}(t) \tag{3.2}$$

where $\bar{n}(t)$ and $\bar{w}(t)$ are Wiener processes and

$$E(d\bar{w}(t)d\bar{w}^{T}(t)) = \underline{R}(t)dt \tag{3.3}$$

$$E(d\bar{n}(t)d\bar{n}^{T}(t)) = \underline{Q}(t)dt \tag{3.4}$$

Here $\bar{X}(t)$ is the system state vector and $\bar{Y}(t) = \frac{d\bar{Z}(t)}{dt}$ is the measurement vector.

Special cases of eqs. 3.1 and 3.2 are:

1. $\bar{f}(\bar{X},t) = \underline{f}(t)\bar{x}(t)$ linear state equation.
2. $\bar{f}(\bar{X},t) = \underline{f}\bar{x}(t)$ linear time-invariant state equation.
3. $\bar{h}(\bar{X},t) = \underline{h}(t)\bar{X}(t)$ linear measurement equation.
4. $\bar{h}(\bar{X},t) = \underline{h}\bar{X}(t)$ linear time-invariant measurement equation.

It should be noted that in aquatic systems measurements are almost always linearly related to the system state. For instance, a typical application is the estimation of a state vector of concentrations of water quality indicators where some or all of the indicators are measured directly. Consequently, in the applications of interest the measurement equation is almost always linear and often time-invariant. Equations 3.1 and 3.2 may be written (formally only, as the derivatives $\frac{d\bar{n}}{dt}$ and $\frac{d\bar{w}}{dt}$ do not exist in a strict mathematical sense) in the more familiar form

$$\frac{d\bar{X}}{dt} = \bar{f}(\bar{X},t) + \frac{d\bar{n}(t)}{dt} \tag{3.5}$$

$$\frac{d\bar{Z}}{dt} = \bar{Y}(t) = \bar{h}(\bar{X},t) + \frac{d\bar{w}}{dt} \tag{3.6}$$

where $\frac{d\bar{n}}{dt}$ and $\frac{d\bar{w}}{dt}$ are independent Gaussian white noise processes with zero mean and covariances $\underline{Q}(t)$ and $\underline{R}(t)$, respectively.

Two criteria form the backbone of almost all filtering schemes. The first, and that used in the original Kalman-Bucy papers, is the minimum expected loss (MEL) criterion. The second is the maximum aposteriori (MAP) criterion motivated by a maximum likelihood

approach. The more familiar MEL criterion is discussed first.

A necessary concept to the use of state estimation techniques is that of a loss function. A loss function is a quantitative description of the weight given to each data value in arriving at the estimate of a state variable. The state estimate chosen is that which minimizes some statistic of the loss functions of the data, often the mean. A simple example is that of finding the "best" estimate of a given functional form through a given data set. If the function f is specified by a parameter θ, the problem is to choose θ so as to minimize the mean loss between the data and the function, i.e.

$$\min_{\theta} \sum_{i} L(X_i - f(X_i)) \qquad \text{where L is the loss function.}$$

Two frequently used loss functions are the squared error $L(\xi) = \xi^2$ and absolute value $L(\xi) = |\xi|$ loss functions. Squared error loss functions are generally optimal in a classical statistical sense (i.e. they yield estimates with minimum variability) if the data are normally distributed. For other distributions, particularly those with much heavier tails than the normal distribution, squared error loss functions may be much less efficient than loss functions which weight the extreme data parts less heavily, such as the absolute value loss function. The squared error loss function is chosen here primarily because the existing state estimation algorithms are based on its use. Modifications are, however, possible (if necessary) to avoid overweighting the extreme data (Martin, 1974).

A more rigorous definition of the concept of a loss function is as follows (McGarty, 1974):

Define a loss function L to be any function belonging to a class having the properties that:

1. $\rho(0) = 0$
2. $\rho(\xi_2) \geq \rho(\xi_1) \geq 0 \Rightarrow L(\xi_2) \geq L(\xi_1) \geq 0$

If we choose $\rho(\xi) = k\xi^2$, k a constant, we have the familiar quadratic form which leads to minimum mean square error (MMSE) estimates. Jazwinski (1970) proves that for any real, non-negative loss function ρ, the optimal estimate of a state random variable X_t is the conditional mean $E(X_t|Y_t)$, where Y_t are measurements of the state X_t up to and including time t.[a] Here "optimal" is defined as the estimate which minimizes the expected loss. Jazwinski's proof requires the additional assumption that the probability density function of X_t conditioned on Y_t be symmetric and unimodal. This restriction is not necessary, however, and a more elegant proof which does not require this assumption is possible through the use of orthogonal projection theory (McGarty, 1974). Consequently, the conditional mean is the MEL estimate for all systems of the form of equations 3.1 and 3.2, linear and nonlinear, subject to the general assumptions made as to the form of the loss function.

Although the theoretical derivation of the filter equations requires only that the loss function satisfy the requirements given above, in practice most MEL filter algorithms require in addition that the loss function be minimum squared error and that the apriori distribution of the state variable (vector) be Gaussian. This condition allows

---

[a] The notation X_t is used as a contraction of the notation X(t) used elsewhere in this work.

propagation of the covariance matrix using the basic property of random variates that linear combinations of normally distributed random variables are themselves normal. Hence, choice of the squared error loss function is implied by the filter algorithms used in this work.

Equations 3.5 and 3.6 for the case of a linear state-linear measurement system lead to the well-known Kalman filter algorithm:

$$\hat{\underline{X}}(k+1|k) = \underline{\Phi}(k+1,k)\ \hat{\underline{X}}(k|k) \tag{3.7}$$

$$\underline{P}(k+1|k) = \underline{\Phi}(k+1,k)\ \underline{P}(k|k)\ \underline{\Phi}^{T}(k+1,k) + \underline{Q}(k+1) \tag{3.8}$$

$$\underline{K}(k+1) = \underline{P}(k+1|k)\ \underline{M}^{T}(k+1)(\underline{M}(k+1)\ \underline{P}(k+1|k)\ \underline{M}^{T}(k+1) + \underline{R}(k+1))^{-1} \tag{3.9}$$

$$\hat{\underline{X}}(k+1|k+1) = \hat{\underline{X}}(k+1|k) + \underline{K}(k+1)(\underline{Y}(k+1) - \underline{M}(k+1)\ \bar{\underline{X}}(k+1|k)) \tag{3.10}$$

$$\underline{P}(k+1|k+1) = (\underline{I} - \underline{K}(k+1)\underline{M}(k+1))\ \underline{P}(k+1) \tag{3.11}$$

where $\underline{\Phi}$ is the solution to $\dot{\underline{\Phi}} = \underline{F}(t)\underline{\Phi}$ and $\underline{F}(t)$ is the (linear) coefficient matrix in eq. 1. In eqs. 3.7-3.11 $\underline{P}$ is the estimated state covariance matrix and $\underline{K}$ is the gain matrix. $\underline{M}$ is the measurement matrix corresponding to the linearized form of eq. 3.2. The notation $(k+1|k)$ indicates an estimate at time k+1 based on measurements to time k. Equations 3.8, 3.9, and 3.11 are sufficient to yield an estimate of the state covariance matrix at any time, and are independent of the measurements. However, this independence breaks down for non-linear systems. For a detailed derivation of the Kalman filter, see Jazwinski (1970).

An alternative approach to the filtering problem is to use the maximum likelihood approach, that is, to ask the question: Which

estimate of the system state maximizes the posterior density of the state estimate conditioned on the measurements? By making use of Bayes' theorem, this conditional density may be written as a functional of the probability density function of the measurements conditioned on the state estimate and the unconditional probability density function of the state. The desired estimate of the state maximizes this functional. Cox (1964) presents an approach which makes use of the method of Lagrange multipliers and dynamic programming to maximize the functional. For a linear system the solution is much more straightforward; McGarty (1974) shows that for a linear system the maximum aposteriori (MAP) filter is identical to the Kalman filter given in eqs. 3.7-3.11. For nonlinear systems the MAP estimate may be quite close to the MMSE estimate so long as the posterior density is unimodal. The primary disadvantage of the MAP approach is that it is essentially a modal technique and may give spurious results if the posterior density is multimodal. This is a serious problem since without a much more complex analysis, it is normally not known if the posterior density is unimodal or not.

II. Difficulties in Implementation

Although the Kalman and related filter algorithms appear quite straightforward, difficulties are often encountered. The most significant of these are the effect of nonlinearities and the divergence problem. These problems are often not mutually exclusive; the method used to handle nonlinearities may be responsible for divergence. The effect of nonlinearities is discussed first.

Filtering of nonlinear systems may be accomplished in several ways. The most obvious is to make use of the Kalman filter linearized about a nominal trajectory. Hence eq. 3.7 is replaced by

$$\frac{d\hat{\underline{X}}}{dt}(t|t_k) = \underline{f}(\hat{\underline{X}}(t|t_k)) \qquad t_k \leq t \leq t_{k+1} \tag{3.7a}$$

and the state transition matrix is the solution to

$$\frac{d\underline{\Phi}}{dt} = F\underline{\Phi} \tag{3.12}$$

$$\text{where } \underline{F} = \left\{F_{ij}\right\} = \left\{\frac{\partial f_i}{\partial X_j}\right\}\Bigg|_{\underline{X} = \hat{\underline{X}}(k|k)} \tag{3.13}$$

In essence, this method involves expanding the nonlinearity as a Taylor series about the estimated value and retaining only the linear term. Equations 3.7-3.11, with 3.1 replaced by 3.7a and 3.12 and 3.13 used to generate the state transition matrix constitute the extended Kalman filter.

Several more sophisticated filters which retain higher order terms are presented by McGarty (1974). Schwartz and Stear (1968) presented a comparison of several nonlinear filters applied to two simple nonlinear problems with and without nonlinear measurements. In general, as would be expected, the more complex filters performed better than did the extended Kalman. Under some conditions, however, notably when the measurement system was linear, the superiority of the nonlinear filters was not marked. In such situations the computational simplicity of the extended Kalman filter may dictate its use.

The problem of divergence results frequently in filter application. Divergence manifests itself in the decay of the gain matrix ($\underline{K}$ in eq. 3.9) which causes measurements to be virtually ignored. If the dynamic model is inexact, which is often the case, the filter estimates may

diverge from the true values, with the actual estimate error becoming inconsistent with the estimation error. The source of the problem usually lies in estimating the system noise covariance matrix, $\underline{Q}$. The $\underline{Q}$ matrix is difficult to estimate, while the measurement noise covariance matrix, $\underline{R}$ is relatively straightforward to obtain. Unlike the measurement noise, (for which the modeller usually has some feel) the system noise cannot usually be readily estimated from experience. Examination of eq. 3.9 shows that the gain matrix $\underline{K}$ depends directly on the value of the conditional state covariance matrix, $\underline{P}(k+1|k)$, which is composed in part of the system noise covariance matrix, $\underline{Q}$. Several methods are available for estimation of $\underline{Q}$, although none of them has a strong theoretical basis. The most straightforward approach is trial and error. The value of $\underline{Q}$ chosen is that which yields actual mean square errors between the observations and predicted values which are consistent with the measurement error covariance matrix $\underline{R}$. This approach is probably the most convenient for systems with state vectors of small dimension. For large dimensional systems, however, complicated search techniques will be required to find the optimal value of $\underline{Q}$, and computational efficiency may be greatly impaired.

A more elegant approach to the estimation of $\underline{Q}$ has been proposed by Jazwinski (1968; 1970). His method makes use of the expected mean square residual, defined as the expected mean square difference between the measured values and the predicted state, to yield $\underline{Q}$. So long as the actual residuals are less in absolute value than their one standard deviation (1σ) limits, $\underline{Q}$ is taken as zero, otherwise it is taken as the excess of the actual residual squared over the expected mean square residual, scaled appropriately. A problem sometimes arises in obtaining

a statistically significant estimate of $\underline{Q}$ using this method. One approach is to smooth several such estimates. The biggest disadvantage of the method is that it requires processing of the measurements first to obtain the $\underline{Q}$ matrix, then reprocessing to yield the filter state estimates. Alternatively, an "old" estimate of $\underline{Q}$ may be used in processing new measurements, potentially resulting in a lag in filter response to divergence.

The author has experienced stability problems in the use of the adaptive filter. A large residual tends to heavily weight the smoothed estimate of $\underline{Q}$ toward large values, hence the filter "follows" the measurements very closely. This reduces the residuals and results in the local estimate of $\underline{Q}$ being zero ($\underline{0}$). The filter slowly recovers under the influence of these small estimates of $\underline{Q}$ until another large residual occurs once again resulting in a large $\underline{Q}$. One possible approach to this problem is to design an appropriate rejection rule for processing the residuals. However, the computational requirements of the adaptive filter are already substantial, particularly since measurements must be processed as scalars. More sophisticated filters such as the optimally driven filter discussed below aid in eliminating linearization errors as a source of filter divergence, and were implemented in this research. Since, in general, only a very few measurements were actually processed, the diagonal elements of the state covariance matrices remained quite large and filter divergence was not found to be a significant problem.

The optimally driven filter was proposed by McGarty (1974). This filter makes use of a forcing term added to the right hand side of the nonlinear state prediction equation 3.7a:

$$\frac{d\bar{X}}{dt}(t|t_k) = \bar{f}(\bar{X}(t|t_k)) + \bar{\Psi}(t) \qquad (3.7b)$$

The forcing function $\bar{\Psi}$ is chosen to eliminate the bias resulting from linearizing the non-linear system. The system nonlinearity is expanded as a Taylor series, retaining terms through second order for use in the solution for $\bar{X}$. Equation 3.7b is iterated to continually provide the linearization point used in the solution for $\bar{X}$. Hence, the filter is essentially a second order approximation to the nonlinear system with a corrector for the linearization error. Consequently, the optimally driven filter should reduce linearization error as a source of divergence. This is, however, no guarantee that divergence will not occur; linearization error is only one cause of divergence. A detailed derivation of the optimally driven filter is presented in McGarty (1974).

III. Applications in Measurement System Design

The use of state estimation or filtering techniques described above offers a useful tool for measurement system design. All of the filters discussed provide an estimate of the conditional state covariance matrix, that is, the second central moment of the probability density of the state estimate conditioned on a given number of measurements. Hence, we are provided with a measure of the propagation of uncertainty through the system, which allows the measurement points to be chosen in some optimal manner.

Several possible optimality criteria are feasible. In what follows, we consider that the number of sampling points has been fixed by some given constraint, and the problem is to optimally locate the given number of stations. One possibility is to locate the stations at the points at

which the uncertainty or sum of estimated variances of the given parameters reaches a threshold value. The uncertainty chosen may be either that provided by the covariance measure at a given point conditioned on a new measurement ($\underline{P}(k+1|k+1)$) or that conditioned on an old measurement ($\underline{P}(k+1|k)$). Moore (1971) used the former criterion. The latter criterion seems more realistic since, as a measure of the uncertainty conditioned on the last measurement it gives an estimate of how well the previous (upstream) estimate may be extrapolated to estimate downstream conditions; it is not site-specific. The criterion used by Moore is specific to the location at which the new measurement is taken; it tells only how much uncertainty remains after taking a new measurement if one is taken; if no measurement is taken the estimate has no meaning. Since an entire reach of river is being searched for the optimal measurement station location, it seems appropriate to assume that a measurement will not be taken at any given location, hence the use of the covariance conditioned on the previous measurement. The criterion used here of choosing station locations which equate the space integrated variance sums between stations is more meaningful than choice of a maximum variance threshold in cases where the conditional variance decays, rather than grows with time for the reasons indicated in Chapter 2.

As discussed earlier in this chapter the measurement and state prediction equations (eqs. 3.7 and 3.10) do not enter directly into the measurement problem. They are, however, indirectly present in the case of a nonlinear system if the predicted state is used in the linearization trajectory or in estimating $\underline{Q}$. Since parameter uncertainty is often a substantial contributor to estimation error, systems which are

linear in the state variables are usually nonlinear when the parameters themselves are taken as state variables. Hence, even if the variable interactions at first glance may appear to be linear, extension of the theory to nonlinear systems is of interest if parameter uncertainty is to be modelled. In the nonlinear case, the measurements enter into the determination of the linearization point and the estimate of the state transition matrix only if linearization about the filter estimate is used. The linearization point may be determined using a nominal trajectory, thus eliminating the requirement for measurements in estimating the state covariance matrix. The error introduced by doing this depends on how closely the true trajectory follows the nominal trajectory. The $\underline{Q}$ matrix enters only as an additive term, hence the specification of station locations will not be affected so long as $\underline{Q}$ is time-invariant if the covariance conditioned on previous measurements (eq. 3.8) is used to estimate propagation of uncertainty. If the updated state covariance estimate (eq. 3.11) is used, however, $\underline{Q}$ enters in a more complex manner and the analysis becomes measurement dependent. The simulation alternative does provide a method of obtaining an *apriori* estimate of $\underline{Q}$, however, so that with some additional effort the entire analysis may be carried out independent of the measurements.

IV. Example of Propagation of Conditional State Covariance Matrix

As an example of the propagation of the conditional state covariance matrix (eq. 3.8) the simplified Streeter-Phelps equations have been treated as a nonlinear problem using an extended Kalman filter. The system may be written in vector form as:

$$\frac{d}{dt}\begin{bmatrix} X_1 \\ X_2 \\ X_3 \\ X_4 \\ X_5 \end{bmatrix} = \begin{bmatrix} \frac{X_3X_2 - X_4X_1}{X_5} \\ \frac{X_3X_2}{X_5} \\ 0 \\ 0 \\ 0 \end{bmatrix} + \begin{bmatrix} W_1 \\ W_2 \\ W_3 \\ W_4 \\ W_5 \end{bmatrix}$$

where X_1 = DO deficit

X_2 = BOD remaining

X_3 = BOD decay constant

X_4 = reaeration coefficient

X_5 = stream velocity

W_i = Gaussian white noise process with variance Q_{ii}

The extended Kalman filter introduced earlier was implemented using as the initial uncertainty values ($\underline{P}(0|0)$) a diagonal matrix consisting of the initial values used by Burges and Lettenmaier (1975). The measurement system consisted of linear measurements of DO and stream velocity only. The measurement error in DO was taken to be 0.25 ppm^2 and in velocity 36 $(mi/day)^2$.

The results of the simulation are shown in part in Figure 3.1. The general character of the curves is close to that provided by the first order approach used by Burges and Lettenmaier. Sensitivity tests

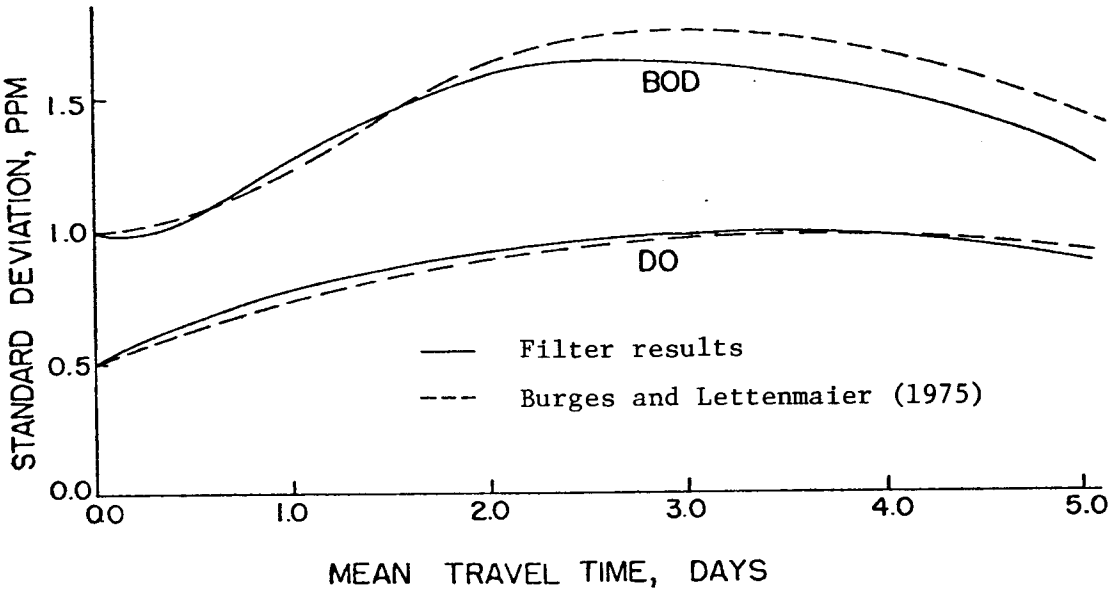

Figure 3.1. Comparative Plot of Uncertainty in DO and BOD for Conditions of Burges and Lettenmaier (1974)

indicated that the maximum uncertainty in DO is about the same regardless of the initial conditions, so long as the initial uncertainty is not too large. If the initial uncertainty is very large, the maximum moves to the initial time and decays rather than increases as in Figure 3.1; assymptotically, however, the behavior becomes independent of the initial conditions. It is the potential for this decaying behavior that resulted in selection of the criterion measure of eq. 2.5 for

locating sample stations.

The use of state estimation techniques to aid in sample station placement is particularly helpful in the design of trend detection networks since not only are the sample station locations provided but the (conditional) variance trajectory itself is specified. This is especially important as the variance (more accurately, the standard deviation) of the estimate of the state variable trajectory is required for determination of the power of trend detection. This issue is explored in detail in Chapter 4. The application of state estimation theory is not constrained to use in trend detection alone. Sample station locations for other types of monitoring may also be determined using this method. The coupling of the state estimation methodology with the theory of hypothesis testing necessary to implement a trend network design approach is described in Chapters 4 and 5.

CHAPTER 4

USE OF STATISTICAL TREND DETECTION TECHNIQUES IN DESIGN OF AMBIENT WATER QUALITY MONITORING NETWORKS

I. Introduction

The primary reason for the existence of ambient water quality monitoring networks is the detection of trends or their absence. A fundamental tradeoff exists between temporal sampling frequency and spatial sample station location; in general the total number of samples taken per unit time, i.e., the temporal frequency times the number of stations is constrained by budget and manpower. A preliminary requirement necessary to any optimization scheme is the identification of the performance of a given sample station in detecting trends as a function of temporal sampling frequency.

The statistical problem of detecting trends is the well known hypothesis testing problem of the classical statistics. As hypothesis testing nomenclature is used throughout this section, a brief review of the theory is included here.

The standard form of an hypothesis test is to test a data set on the null hypothesis H_o versus an alternative hypothesis H_1, where H_1 is the complement of the null hypothesis, or the hypothesis that H_o is not true. In the tests of interest in this work H_o is the hypothesis that there is no trend in the population from which the data are drawn while H_1 is the hypothesis that a trend does exist in the population. Hence we have two possibilities of truth and two possible conclusions which might be drawn from the data set. Logically, two of the possible

conclusions will be incorrect, representing two different types of error. The possible states of truth and test outcomes may be shown schematically in the table below taken from Conover (1971):

		Decision: Accept H_o	Decision: Reject H_o
State of Nature (truth)	H_o True	$p = 1-\alpha$	$p = \alpha$ (Type I error)
	H_o False	$p = \beta$ (Type II error)	$p = 1-\beta$

Type I error is the rejection of H_o when H_o is really true and is parametrized by α, the significance level of the test.

While the probability of type I errors is certainly an important consideration, it gives no indication of how successful a test is in establishing differences in the population. For example, in our case α only gives the probability of stating that a trend is present when none really is; we are more interested in knowing how effective a test is in establishing the existence of a trend when one really exists. This probability is $1-\beta$, and is known, appropriately, as the power of the test. The power of a test, unlike the confidence level, is not constant for a given population size; it can vary with parameters (specified or otherwise) of the population. This does not seem unreasonable, since, for instance, the probability of making a type II error, or of stating that no trend is present when one really is, will most likely depend (at least) on the trend magnitude.

II. Parametric and Nonparametric Tests

If the underlying probability distribution is known, a test tailored to fit that distribution may be designed. Perhaps the best known of these parametric tests is the family of t-tests for normally distributed data. If the parametric test is well designed, it will have power at least as great as any nonparametric competitor. However, the parametric tests usually are not robust to changes in the distribution. In practice, sample sizes are often moderate to small, so the underlying distribution is almost never known with high confidence (most goodness-of-fit tests require very large sample sizes to distinguish between distributions with moderately similar characteristics), therefore the use of parametric tests is often dangerous. In fact, nonparametric tests (tests which do not require knowledge of the probability distribution of the data) exist which have high efficiency relative to the tailored-to-fit tests for many families of distributions, where efficiency is defined as the ratio of the number of samples required for given power for the best tailored-to-fit test to the number required of the nonparametric competitor.

Statisticians often use the assymptotic relative efficiency (A.R.E.) which is simply the limit of the efficiency as defined above as the sample size approaches infinity. The A.R.E. of nonparametric tests is most often stated with respect to the power function of the analogous t-test for normal random variates. The appeal of A.R.E.'s is their ease of computation; unfortunately their usefulness is limited since the finite (small to medium) size sample behavior is most often of interest. Finite sample efficiencies usually are most easily determined using Monte Carlo sampling techniques as a result of mathematical intractability of the manipulation required. The Monte Carlo approach

is pursued below with respect to the nonparametric tests investigated.

One set of parametric tests which lends itself to fairly straightforward computation of the power function is the family of t-tests. The computation of the power functions for the t-tests for step trends as well as for linear trends are carried out in the following section. The computation of power for the t-tests allows a base against which the power of the nonparametric tests may be compared.

III. The Case for Nonparametric Statistics

Of great interest in many cases is performance of a candidate test under some family of distributions removed from normality, particularly those with tails that are heavy compared to the normal distribution with, say, identical location (e.g. mean, median) and scale (e.g. standard deviation, inner quartile distance). Distributions with heavy tails are important in any work dealing with natural systems where occasional very extreme events (e.g. occasional instrumentation errors or extreme natural events such as floods) result from a population different from that generating the majority of events recorded. Gross (1973) presented Monte Carlo results which showed that two nonparametric tests (the sign and Wilcoxon tests) performed nearly as well as an approximately tailored-to-fit test (the wave test) for heavy tailed deviations from normality in cases in which use of the standard t-test resulted in confidence interval lengths which were up to 55 times too long. This worst case resulted when the second population contributed a relatively large proportion of the random variates and where the second population had very large scale compared to the first. Substantial errors were also shown to result, however, when the second population contributed

a relatively small proportion of the total sample and had scale not greatly larger than the dominant population.

The performance of the nonparametric tests, on the other hand, broke down only for sample sizes smaller than about 20 and for very heavy tailed distributions; for larger sample sizes the nonparametric tests approached the performance of Gross's wave test while the t-test fell apart completely. The nonparametric tests had a further advantage in that no assumptions of symmetry in the generating distribution are required in contrast to the wave test. This is an especially important consideration in water resource applications where symmetric distributions are the exception rather than the rule.

It is not surprising that the nonparametric tests perform reasonably well under heavy tailed alternatives, since these tests make use of signs and ranks rather than the data itself. For instance, Spearman's Rho test uses a statistic

$$N_s = \sum_{i=1}^{n} (R_i - i)^2$$

where R_i denotes the rank of i in the pool of n observations. The null hypothesis is rejected if N_s lies outside a given range. Mann Whitney's test uses a statistic based on sums of ranks (Conover, 1971). When ranks, rather than the data values themselves are used, a single extreme value has the same incremental effect on the test statistic as does a moderate value, whereas in the case of a least squares estimate a single value can overwhelm the test statistic. Because it is extremely difficult to distinguish between, for example, a Gaussian and a moderately contaminated Gaussian distribution for small to medium sample sizes, there is a great deal to be said for the use of nonparametric statistics.

A final point concerning robustness of test statistics is the result that the performance of both parametric and nonparametric statistics with respect to heavy tailed alternatives tends toward an increase in type II errors and a decrease in type I errors, i.e. the power decreases and the true confidence level tends to be less than the stated level. Hence, the tests always behave more conservatively when used against heavy tailed distributions.

IV. Power of Some Parametric Tests

Because nonparametric tests are robust against small to moderate deviations from normality, they are used throughout this work. It is useful, however, to parametrize the power curves of the parametric t-tests since the power (determined by Monte Carlo methods) of the non-parametric tests may be described in terms of the analytical results derived for the t-tests. The power of the t-tests against step and linear trends are derived in the following two sections for the type I error probability, α, fixed.

The parameter of principal interest for the statistical tests we select as candidates is the β error, the probability of acceptance of the null hypothesis if false. The type II error, or alternatively the power of a given test, will, in general, be a function of the true trend magnitude, the record length, the underlying probability distribution of the time series being tested, and the magnitude of some specified scale estimate of the distribution. For the two t-tests of interest, this functional dependence may be derived analytically. The derivation is presented in the following sections. A Kalman filter approach is used in this derivation of the power curves for the two t-tests. The Kalman filter approach was chosen in lieu of a more classical method because it offers an insight into the application of the Kalman filter algorithm for two systems with very simple dynamics, which should prove helpful in reading the following chapters.

IV.1. Step Change, Kalman Filter Approach

We consider first the case of an underlying generating mechanism which includes a step increase in the mean of the distribution only. A convenient method of approaching the problem is as a filtering problem; we attempt to filter out the noise present to allow a possible distinction between the two levels in the process. The problem may be formulated as a linear (Kalman) filter if the underlying probability distribution is normal, which is, of course, implicit in use of the t-test.

The true process in this case is:

$$x_i = \varepsilon_i$$
$$\sigma^2 = R$$

where ε is normally distributed with mean zero and variance R, i.e., $\varepsilon \sim N(\cdot|0,R)$.

Hence the linear filter is (see Chapter 3):

$$\frac{dX}{dt} = 0 \qquad (4.1)$$

$$\Phi = 1 \qquad (4.2)$$

$$\text{whence } P_{k+1} = \frac{P_k(1-P_k)}{P_k + R} \qquad (4.3)$$

Here R is the measurement noise variance, which in this case is equivalent to the process noise, and P_{k+1} is the estimate of the variance of the mean at step k+1. At step zero, we take P_o as our *apriori* estimate of the process variance. Hence it can easily be shown that

$$P_n = \frac{P_o R}{nP_o + R} \tag{4.4}$$

We note that if $P_o = \infty$ (no apriori information) $P_n = R/n$ as expected. In addition, for n large, the effect of the apriori estimate is negligible, also as expected.

For convenience define $\sigma^2 = P_n$. Now for $N = 2n$ = total record length and for independent observations X_i, we are testing

$$H_o: \quad \mu_1 = \mu_2$$

$$\text{vs.} \quad H_1: \quad \mu_1 \neq \mu_2$$

where μ_1 and μ_2 are the population means of the first (and the second) halves of the data set.

We make use of the fact that $\bar{X}_1 = \frac{1}{n} \sum_{i=1}^{n} X_i$ and $\bar{X}_2 = \frac{1}{n} \sum_{i=n+1}^{N} X_i$ are independent, hence

$$\text{Var}(\bar{X}_1 - \bar{X}_2) = \text{Var}(\bar{X}_1) + \text{Var}(\bar{X}_2) = 2\sigma^2 = \sigma_*^2 \tag{4.4a}$$

Now we desire, for fixed α, the probability of detecting differences in the mean values. The problem may be schematized as below for the two tailed test:

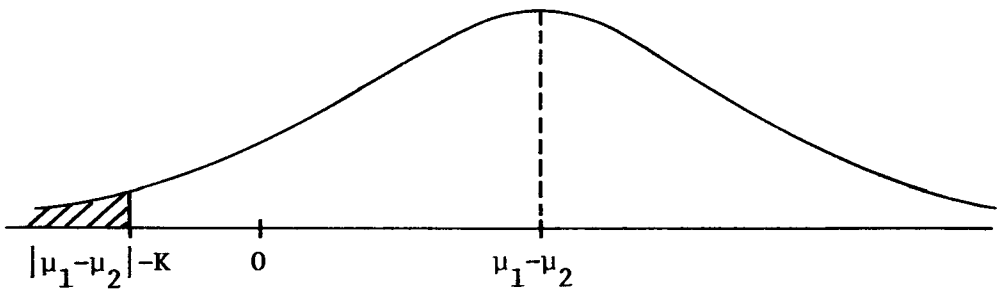

Here $K = \sigma_* w_{1-\alpha/2}$ and $w_{1-\alpha/2}$ = standard normal deviate for $100(1-\alpha/2)\%$ probability. The above curve may be transformed to a standard normal by translating by $\mu_1-\mu_2$ and dividing by σ_*, shown schematically below:

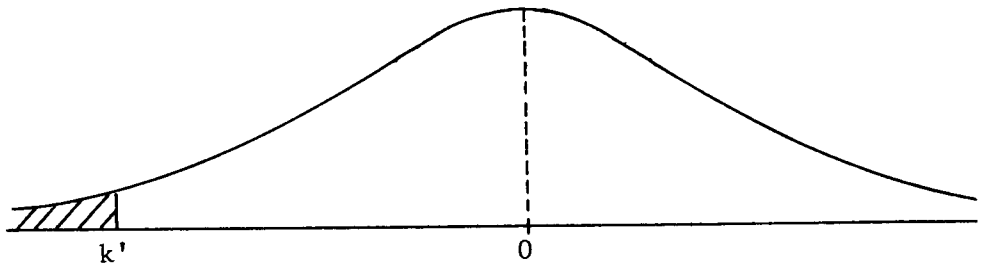

Here $k' = \dfrac{|\mu_1-\mu_2|}{\sigma_*} - w_{1-\alpha/2}$

Hence at confidence level $1-\alpha$, and assuming σ^2 known, Pr(detection)

$$= \Pr\left(\frac{\bar{X}_1-\bar{X}_2}{\sigma_*} > w_{1-\alpha/2}\right)$$

$$= 1 - F_x\left(w_{1-\alpha/2} - \frac{|\mu_1-\mu_2|}{\sigma_*}\right) \qquad (4.5)$$

where $x \sim N(\cdot|0,1)$ and F_x is the cumulative distribution function of x. We note that the test may be parametrized by

$$w_{1-\alpha/2} - \frac{|\mu_1-\mu_2|\sqrt{n}}{\sqrt{2}\,\sigma_\varepsilon} \qquad \text{where } \frac{\sigma_\varepsilon^2}{n} = \frac{\sigma_*^2}{2}$$

or, for a given confidence level simply by

$$\frac{|\mu_1-\mu_2|\sqrt{n}}{\sqrt{2}\,\sigma_\varepsilon}$$

since $w_{1-\alpha/2}$ is independent of n.

If the variance is not known, the test may be parametrized by

$$\frac{|\mu_1-\mu_2|\ \sqrt{n}}{\sqrt{2}\ S_\varepsilon} - t_{1-\alpha/2}$$

where $t_{1-\alpha/2}$ is the student's t deviate for n-1 degrees of freedom at confidence level $1-\alpha/2$ and S_ε is the sample standard deviation of ε.

In the case where variance is known, a dimensionless number

$$N_T = \frac{T_r\ \sqrt{N}}{2\sigma_\varepsilon} \qquad (4.5a)$$

may be defined where $T_r = |\mu_1-\mu_2|$ and $N = 2n$ = total record length.

A plot of power versus N_T for a step trend is shown in Figure 4.1.

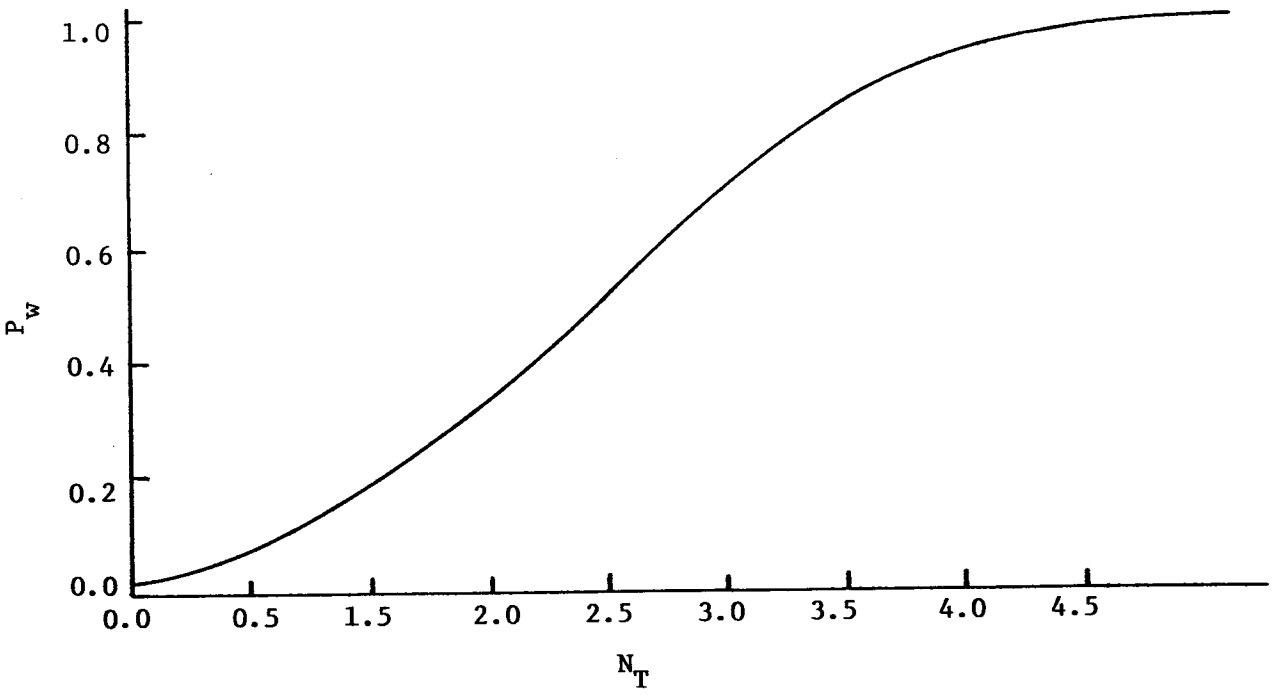

Figure 4.1. Normalized Power Curve for t-Test (Variance Known) Against a Step Trend

In the results presented, σ^2 was taken as R, the true variance. For moderate sample sizes (greater than about 30) the power for the case of variance unknown is less than but almost identical to that plotted.

IV.2. Linear Increase, Kalman Filter Approach

We consider now the case of a linear trend with superimposed Gaussian white noise. The true process in this case is:

$$X_i = i\tau + \varepsilon_i \tag{4.6}$$

and the Kalman filter is:

$$\frac{d}{dt}\begin{bmatrix} X_1 \\ X_2 \end{bmatrix} = \begin{bmatrix} X_2 \\ 0 \end{bmatrix} \tag{4.7}$$

$$\Phi = \begin{bmatrix} 1 & 1 \\ 0 & 1 \end{bmatrix} \tag{4.8}$$

$$P_{k+1} = \begin{bmatrix} \dfrac{R(P_{11_k} + 2P_{12_k} + P_{22_k})}{D_k} & \dfrac{R(P_{12_k} + P_{22_k})}{D_k} \\ \dfrac{R(P_{12_k} + P_{22_k})}{D_k} & \dfrac{P_{22_k}(P_{11}+R)}{D_k} + P^2_{12_k} \end{bmatrix} \tag{4.9}$$

where $D_k = P_{11_k} + 2P_{12_k} + R$.

We are primarily interested in P_{22_k}, the estimated variance in the trend magnitude at time step k. For the general case with estimated apriori (k=0) values of P_{11}, P_{12}, and P_{22} the general expression for the covariance matrix at any time step becomes extremely messy. If, however, we choose $P_{11_o} = P_{22_o} = \infty$, $P_{12_o} = 0$, the relationship is much easier to handle. This corresponds to the case of no apriori information, as is assumed in the classical statistical tests. In this case it can easily be shown that the succession is as follows:

time step, k	P_{22}/R
0	∞
1	∞
2	2
3	1/2
4	1/5
5	1/10
6	2/35
7	1/28

For the classical regression of Y on X (not to be confused with notation used elsewhere in this paper) the variance of $\hat{\tau}$, where $Y_i = \gamma + \tau X_i + \varepsilon_i$, and $\hat{\tau}$ is the sample estimate of τ, is

$$\mathrm{Var}(\hat{\tau}) = \frac{\sigma_\varepsilon^2}{\sum_{i=1}^{n} x_i^2} \qquad (4.10)$$

where $x_i = X_i - \bar{X}_n$ and $\bar{X}_n = 1/n \sum_{i=1}^{n} X_i$.

Here σ_ε^2 is the variance of the noise process, and is equivalent to R in the filter problem above. Also, in our case $X_i = i$, hence we can compute $\mathrm{Var}(\hat{\tau})$ as a function of n as below:

n	$\mathrm{Var}(\hat{\tau})/\sigma_\varepsilon^2$
1	∞
2	2
3	1/2
4	1/5

It is apparent that the variance of the classical regression estimate is identical to that of the Kalman filter. A straightforward proof by finite induction will establish that the filter result is identical to the classical regression result for all n. Hence the use of the linear filter to test for the existence of a linear trend will be identical to the standard t-test.

The values for the power of the t-test based on the filter approach derived below are based on the assumption that R is known, hence they give an upper limit for the power of the test. For $n \gtrsim 30$, the standard t-test will have very nearly identical power to the values derived below assuming variance known.

The power of a test is, by definition, the probability of detecting a trend when one really exists. Hence if a two sided test is used, and if the trend magnitude is τ, we desire $\Pr(|\hat{\tau}| - w_{1-\alpha/2}\sqrt{\mathrm{Var}(\hat{\tau})} > 0)$

$= 1 - F_x(w_{1-\alpha/2} - \frac{|\tau|}{\sigma})$ where $x \sim N(\cdot|0,1)$,

$\sigma = P_{11}$ = predicted standard deviation in trend estimate, and $w_{1-\alpha/2}$ = normal deviate at probability $1-\alpha/2$.

Using eq. 4.10 it may be shown making use of the identity

$$\sum_{i=1}^{n} i^2 = \frac{1}{6} n(n+1)(2n+1) \tag{4.11}$$

that

$$\sigma^2 = P_{11} = \frac{12\sigma_\varepsilon^2}{n(n+1)(n-1)} \tag{4.11a}$$

Hence the t-test against a linear trend with variance known may be parameterized by

$$N_T' = \frac{\sqrt{n(n+1)(n-1)}\,\tau}{\sqrt{12}\,\sigma_\varepsilon} \tag{4.12}$$

The normalized power curve using N_T' in place of N_T is identical to the curve for the case of a step increase plotted in Figure 4.1. It should be noted that the denominator in the variance equation for the linear estimator (eq. 4.11a) behaves as $1/n^3$, whereas for the step estimator (eq. 4.4a) the variance behaves as $1/n$. However, for the case of a linear trend the trend magnitude must be redefined for each n if the total difference in the record length is to be kept constant, e.g., $T_r = \tau n$ in eq. 4.10 and the curves may be parameterized by

$$N_T' = \frac{\sqrt{n(n+1)(n-1)}\,T_r}{\sqrt{12}\,n\,\sigma_\varepsilon} \tag{4.12a}$$

which, if the approximation $\sqrt{n(n+1)(n-1)} \approx n^{3/2}$ is made, is identical to eq. 4.5a except for a constant.

V. Power of Some Nonparametric Tests

A number of nonparametric tests exist for the testing of hypotheses relative to the existence of trends. Two of these (Spearman's Rho and Mann-Whitney) were introduced earlier. Some analytic results are available for the power curves of nonparametric tests (for example, Dixon (1953; 1954), and Hayman and Zakkula (1966)), however, the power functions are usually very difficult to derive analytically for a general underlying probability density function. For this reason, Monte Carlo sampling has been used here. Results are presented for the two tests which show the best power curves: Mann-Whitney's test (against step trends) and Spearman's Rho test (against linear trends). Both have A.R.E.'s of around 95% relative to the t-test against a Gaussian alternative (Breiman, 1973) and hold up well with respect to a number of commonly used distributions.

Monte Carlo test results are presented in Figures 4.2 and 4.3 for the Mann-Whitney and Spearman's Rho tests against Gaussian alternatives for linear and step trends. The results were derived from 200 test runs for each statistic. Curves of the form $P_w = 1 - e^{-a(n-b)}$ were fitted to the raw values for constant T_r and σ_ε using classical regression. These curves appeared to give a good fit for all but small (i.e., less than about 20) n, below which the behavior became erratic. Curves were computed for $\sigma_\varepsilon^2 = .25, .5, 1, 4$, and 16 and for trend magnitudes of .3, .6, .9 and .15, .3, .45 for linear and step increases, respectively. From each curve a maximum of 9n values were calculated for N_T from 0.5 to 4.5 in increments of 0.5, and were plotted as "pox diagrams" (Mandelbrot and Wallis, 1969) in Figures 4.2 and 4.3. It can be seen from Figures 4.2 and 4.3 that each test is substantially better than the other with respect to the alternative for which it is designed, e.g.,

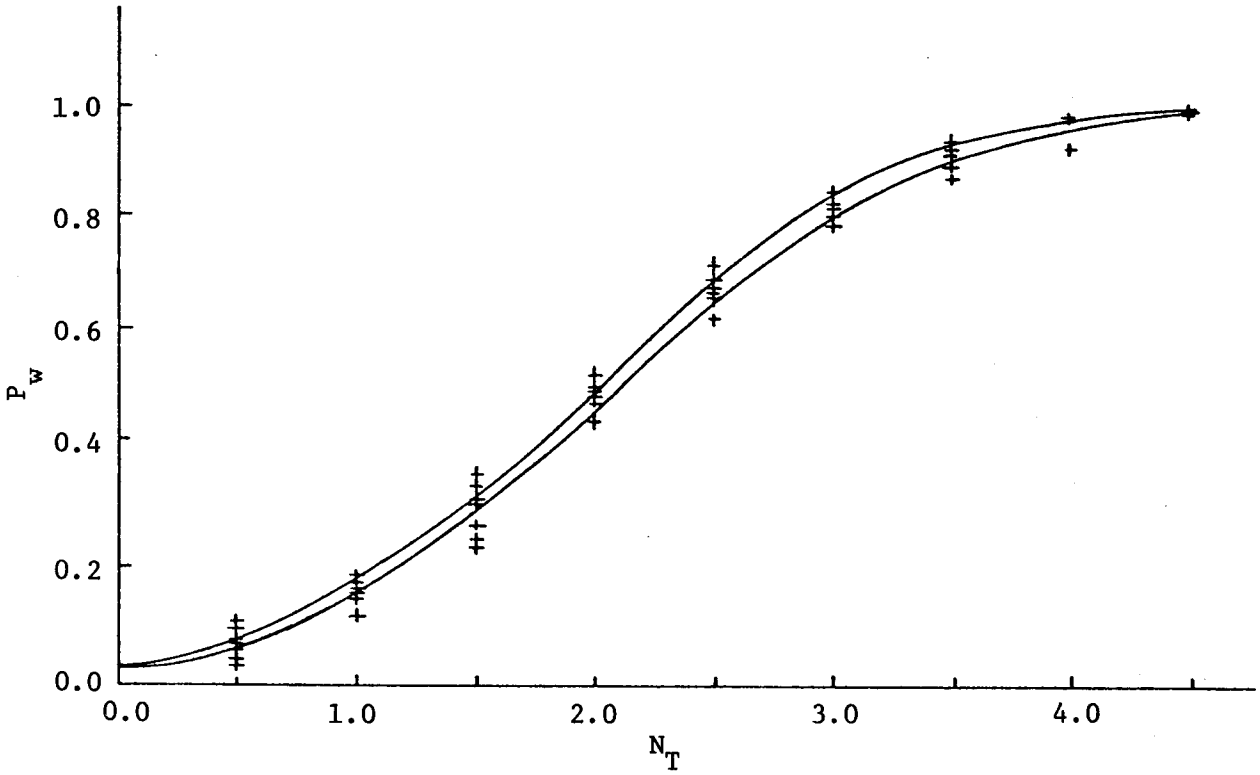

Figure 4.2a. Estimated Dimensionless Power for Mann-Whitney's Test (lower curve) Compared to t-test (upper curve) for a Step Trend with Gaussian Distribution

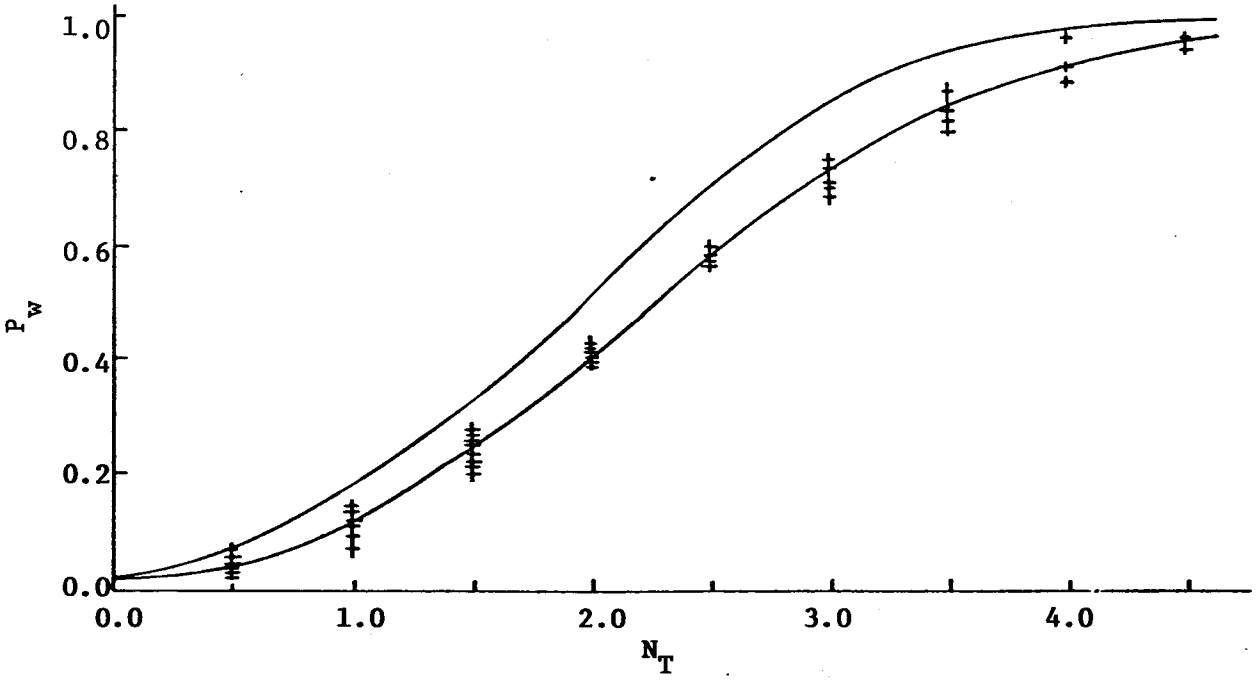

Figure 4.2b. Estimated Dimensionless Power for Spearman's Rho Test (lower curve) Compared to t-test (upper curve) for a Step Trend with Gaussian Distribution

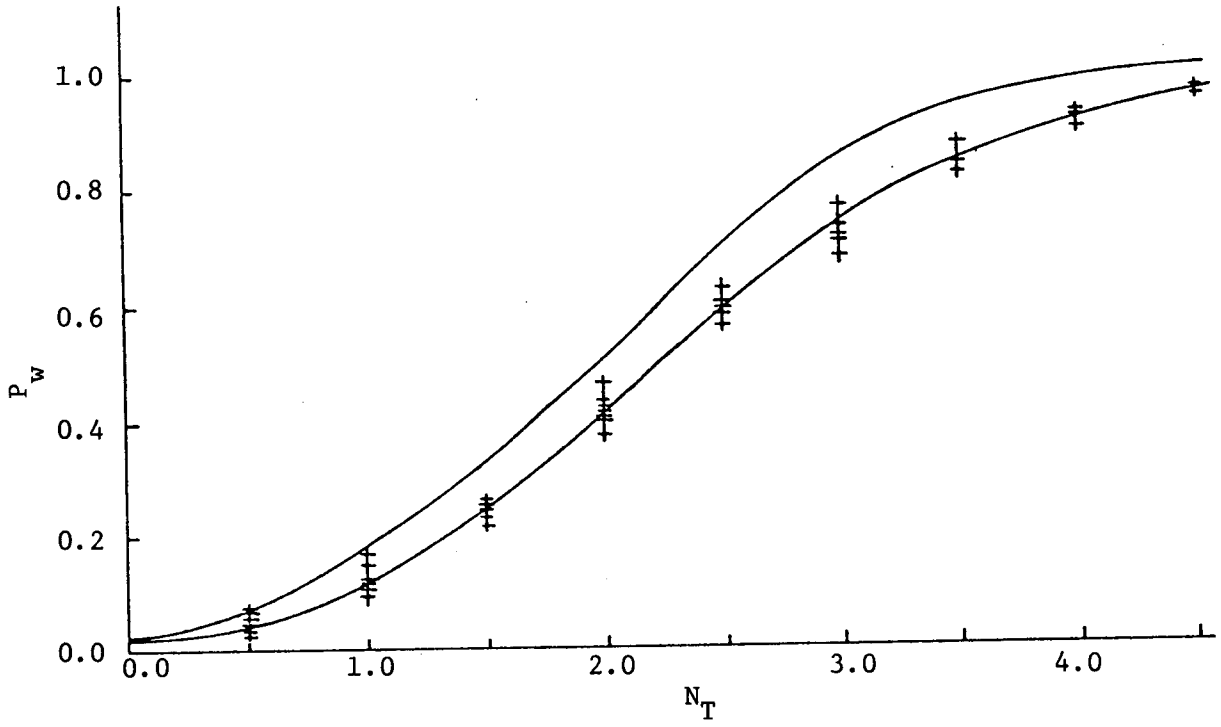

Figure 4.3a. Estimated Dimensionless Power Curve for Spearman's Rho Test (lower curve) Compared to t-test (upper curve) for a Linear Trend with Gaussian Distribution

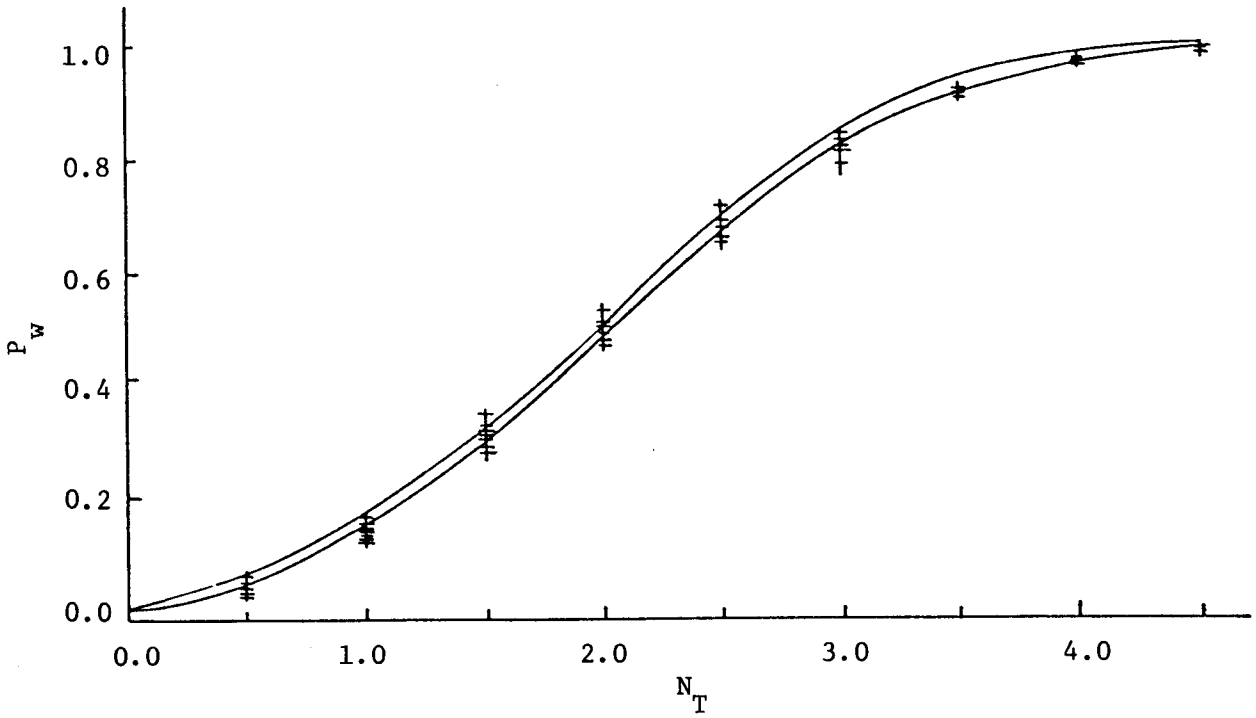

Figure 4.3b. Estimated Dimensionless Power Curve for Mann-Whitney's Test (lower curve) Compared to t-test (upper curve) for a Linear Trend with Gaussian Distribution

the Mann-Whitney test is substantially more powerful than Spearman's Rho when the underlying population does in fact include a step change.

VI. Extension to Time Series with Dependence of Certain Kinds

All of the tests, parametric and nonparametric, reviewed above include an assumption of independence of some kind. The Mann-Whitney test, for example, requires explicitly that the variables be independently (not necessarily identically) distributed. Spearman's Rho test, on the other hand, tests a null hypothesis of independence against a certain kind of dependence, but will not yield meaningful results if the data are known to be correlated in the absence of a trend. Parametric tests require even more stringent assumptions; an assumption that the data are independently identically distributed with a specified distribution is usually made. These assumptions tend to be very restrictive in water resource applications, particularly in examination of time series for trends. Unless temporal sample spacing is very large, there is usually significant correlation between the observations. Consequently the tests introduced above may not be used unless this correlation can somehow be eliminated. A further complication, usually ignored, is that unless the underlying distribution is Gaussian, lack of correlation does not imply independence. For distributions other than Gaussian, it is necessary to show independence of all the moments to infer independence of the distributions. For small sample sizes it is virtually impossible to estimate dependence higher than second order, and one can only hope that lack of correlation will prove adequate for the purposes of the tests.

One analytical technique which will yield essentially uncorrelated values is to take averages over sufficiently long periods, for instance

yearly average values (of water quality parameters) are often essentially uncorrelated. This procedure will be unacceptable, however, if record lengths are relatively short, say five years or so. (It should be noted that trends over record lengths on the order of five years are extremely important, since this is often approximately the renewal period for waste discharge permits.) A similar complication results if the data are initially uncorrelated but some kind of smoothing of a local family of data is performed. The tests introduced earlier will not be applicable in this case.

The necessary theory to handle dependence of the kinds discussed above was presented by Sen (1963; 1965). This work presented test statistics which are assymptotically applicable for large sample sizes (although "large" was not defined in the original work, the author has found that on the order of several hundred samples are required) to two cases:

1. $$X_t = \sum_{j=1}^{m} \alpha_j Y_{t+j-h} \qquad (4.13a)$$

where $h = 1 + [\frac{m}{2}]$, α_j is an arbitrary weighting factor, and $[\frac{m}{2}]$ is defined to be $\frac{m}{2}$ for m even and $\frac{m}{2} - \frac{1}{2}$ for m odd.

In eq. 4.13a Y_t is defined as $Y_t = M_t + \varepsilon_t$ with M_t a deterministic component and

$$E[\varepsilon_t \varepsilon_s] = \sigma^2 \delta_{ts}$$

$\{X\}$ (the time series of values X_i) consists of n-(m-1) values, where m is the span of dependence. Hence $\{X\}$ is a time series consisting of values derived from another time series with independent values by linear smoothing over a finite data window.

2. $$X_t = M_t + \sum_{j=0}^{m} \alpha_j \varepsilon_{t-j} \qquad (4.13b)$$

with α, M, and t as defined above and

$$E(\varepsilon_t \varepsilon_s) = \sigma^2 \delta_{ts}.$$

Thus $\{X\}$ consists of a deterministic part plus a linear combination of m independently distributed random variables.

In both cases M is assumed to be a systematic component and the tests are designed to test the null hypothesis that M_t is constant versus an alternative that M_t is a monotonic function of t. The results presented by Sen (1965) allow use of a modified form of the Cox-Stuart test and a modification of Kendall's tau test, a rank correlation test which has performance characteristics almost identical to Spearman's Rho (Conover, 1971). In addition, results presented in an earlier paper (Sen, 1963) provide for use of a modified Mann-Whitney test.

Because the power of the nonparametric tests for dependent time series has not been published, a Monte Carlo sampling program was designed to estimate the power curves for two nonparametric tests against trend in dependent time series. The form of the power curves for tests against trend in a dependent time series is a function of the trend magnitude to noise ratio, the sample size, a vector of parameters relating observations, and the probability distribution of the data, i.e., for the probability distribution known.

$$P_w = P_w\ (T_r/\sigma,\ n,\ \underline{\theta}) \qquad (4.14)$$

where in general

$$X_k = f(\overline{\theta},\ \{X_j,\ j = 1, 2, \ldots k-1\}\ ) + \varepsilon_k \qquad (4.14a)$$

i.e. the current observation is the sum of a function of the parameter vector $\overline{\theta}$ and the preceding observations plus a noise term.

The parameter vector $\underline{\theta}$ is a function of the actual form of the dependence of the data. In order to determine the power, P_w, then, this dependence must be modelled. A particularly useful set of time series models are the autoregressive integrated moving average (ARIMA) models given in Box and Jenkins (1970). The general ARIMA model is:

$$\phi_p(B)\nabla^d(Z_t-\bar{Z}) = \theta_q(B)A_t \qquad (4.15)$$

where $\nabla Z_t = Z_t - Z_{t-1}$

$$\phi_p(B) = 1 - \phi_1 B - \phi_2 B^2 - \ldots\ldots \phi_p B^p$$

$$\phi_q(B) = 1 - \phi_1 B - \phi_2 B^2 - \ldots\ldots \phi_q B^q$$

$$B^k Z_t = Z_{t-k}$$

and ϕ_i and θ_j are elements of the model parameter vector.

In simulation studies, it is desired to fit models such that d=0 in order to maintain stationarity, a necessary condition for stability of a synthetic time series (Watts, 1972). Hence any nonstationarity must be eliminated prior to modelling, possibly by extracting pseudo-deterministic components such as seasonal cycles. The principal tool in identification of autoregressive moving average (ARMA) models (ARIMA models with d=0) are the autocorrelation and partial autocorrelation functions. For a comprehensive discussion of model fitting, the reader is referred to Box and Jenkins (1970). Briefly, however, the general ARMA model has the property that both the autocorrelation and partial autocorrelation functions die off gradually with increasing lags, whereas pure AR (ARMA (p,0)) models have partial autocorrelation functions which vanish after p lags and decaying autocorrelation functions and pure MA (ARMA(0,q)) models have autocorrelation functions which vanish after q lags and decaying partial autocorrelation functions.

In order to determine the model complexity which might be required to adequately describe the dependence in time series of water quality observations, long records of water quality parameters with frequent observations were sought. Through the cooperation of the U.S. Geological Survey (USGS) and the Municipality of Metropolitan Seattle (METRO) some of the longest available time series of daily water quality records were analyzed. A summary of these records is given in Table 4.1.

Table 4.1. Water Quality Records Analyzed (Daily observations)

location	parameter	period*	Source	years data
Duwamish R. at Renton Junction, Wash.	Dissolved	1970-74	METRO	5
Duwamish R. at Renton Junction, Wash.	Temperature	1970-74	METRO	5
Delaware R. at Trenton, New Jersey	Suspended Solids	1949-73	USGS	25
Delaware R. at Trenton, New Jersey	Temperature	1954-73	USGS	18**
San Juan R. near Bluff, Utah	Specific Conductivity	1942-60	USGS	19
San Juan R. near Bluff, Utah	Suspended Solids	1942-73	USGS	32
Arkansas R. at Little Rock, Arkansas	Specific Conductivity	1946-60	USGS	15

*USGS data are for water years indicated, METRO data for calendar years.

**Missing water years 1962, 1964.

Suitable transformations were sought to yield approximately normally distributed data. An approximately normal distribution is a necessary condition for the use of least squares estimation techniques (Breiman, 1973). Different transformations of the data were assessed using quantile-quantile plots of the transformed observed data against a normal distribution as proposed by Wilk and Gnanadesikan (1968). After a suitable transformation was obtained, two Fourier components corresponding to a six month and twelve month cycle were estimated and residualized data obtained by subtracting these pseudodeterministic Fourier components from the transformed data. Partial autocorrelation and autocorrelation functions were then estimated. Due to the large computational requirements, the autocorrelation and partial autocorrelation functions were estimated using the first five years of data only. Although the numerical values of the autocorrelation and partial autocorrelation functions were affected by this choice, the general form (e.g. cutoff points for partial autocorrelation functions and decay rates for autocorrelation functions) of the functions required for model identification did not, and the savings in computational time appeared to outweigh the loss of accuracy. The lag one correlation coefficient was estimated based on the entire data record. Missing data were filled in after removal of the Fourier components by disaggregating the data into four seasons and estimating seasonal means, variances, and lag one correlation coefficients. Missing data were synthesized using a lag one Markov model,

$$X_t = \phi(X_{t-1} - \overline{X}) + \sigma\sqrt{1-\phi^2}\, A_t \qquad (4.15a)$$

where $\overline{X}$, σ, and ϕ were the estimated seasonal mean, standard deviation, and lag one correlation coefficient, respectively, and A_t was a

pseudo-random number generated from a normal distirubtion with mean zero and variance one. Equation 4.15a was used as the basis for filling in missing values in order to create a pseudohistoric trace with the same low order moments (mean, standard deviation, and skew) as the historic data.

The estimated autocorrelation and partial autocorrelation functions for the augmented data are shown in Figures 4.4-4.10. With the exception of the Renton Junction dissolved oxygen and possibly the Delaware River Temperature series, the data appear to indicate that the use of a simple lag one Markov (AR(1)) model is sufficient. The results of the investigation are summarized in Table 4.2.

Some of the records showed oscillation of the autocorrelation function at large lags, particularly in the case of the logarithms of the San Juan River conductivity data (Figure 4.7) which are shown, for convenience, on a scale twice the length of the other correlation and partial autocorrelation plots. This oscillation is apparently the result of a low frequency component in the data not removed by the residualization process. These oscillations are of little importance to the model fitted except where sample frequencies on the order of the cycle length are specified. In this case, a suitable transformation to remove the nonstationarity evidenced by the oscillation of the autocorrelation function would be required.

A cursory examination of the number of variables in equations 4.14 and 4.15 indicates that a comprehensive Monte Carlo testing program would be extremely expensive, especially since the computation time is approximately proportional to m in eq. 4.13. However, if some relationship could be found allowing the dependence to be summarized in such

Table 4.2 Summary of Results of Investigation of Daily Water Quality Records

station	parameter	transformation	suggested model	lag one correlation
Duwamish	D.O.	$Y_t = X_t$	AR(2)	0.809
"	Temp.	$Y_t = X_t$	AR(1)	0.876
Delaware	S.S.	$Y_t = \log(1+\log(X_t))$	AR(1)	0.782
"	Temp.	$Y_t = X_t$	AR(2)	0.866
San Juan	Spec. Cond.	$Y_t = \log(X_t)$	AR(1)	0.830
"	S.S.	$Y_t = \log(1+\log(X_t))$	AR(1)	0.818
Arkansas	Spec. Cond.	$Y_t = \log(X_t)$	AR(1)	0.869

a manner that the power curves for independent time series could be used, considerable savings might be realized. Relationships between the actual number of samples and the effective number of independent samples for an autocorrelated time series were presented by Bayley and Hammersley (1946). They defined a relationship

$$\text{Var}\ (\bar{X}) = \frac{\sigma^2}{n_b^*} \tag{4.16}$$

for the variance of the mean estimate of an autocorrelated time series of the form of eq. 4.14a, where σ^2 is the variance of X and n_b^* is the equivalent number of independent samples. This number can be shown to be related to the correlation structures of the time series by

$$\frac{1}{n_b^*} = \frac{1}{n} + \frac{2}{n} \sum_{j=1}^{n-1} (n-j)\rho(jt) \tag{4.17}$$

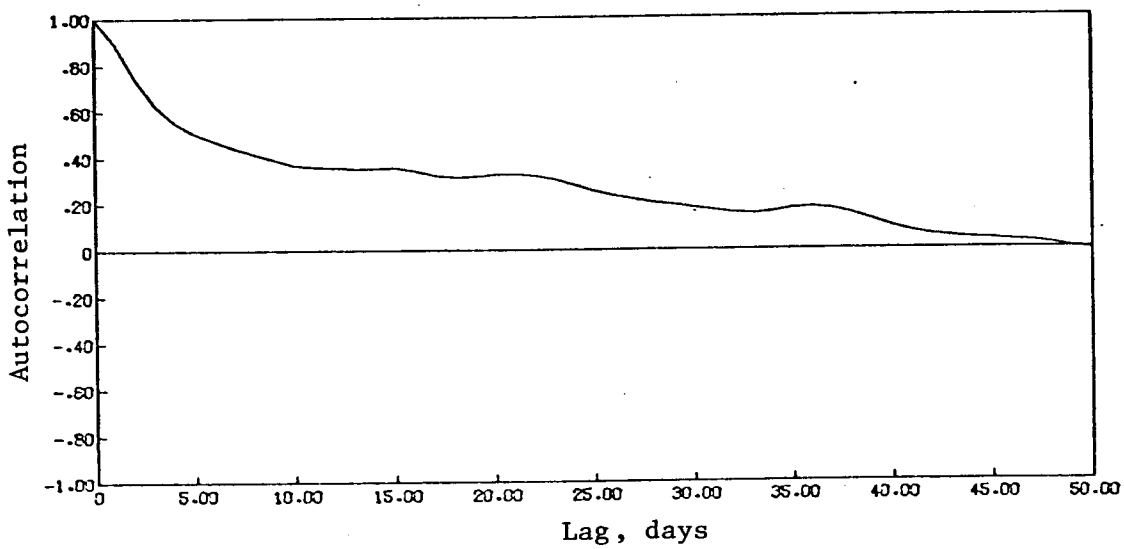

Figure 4.4a. Estimated Autocorrelation Function for Duwamish River Dissolved Oxygen Data

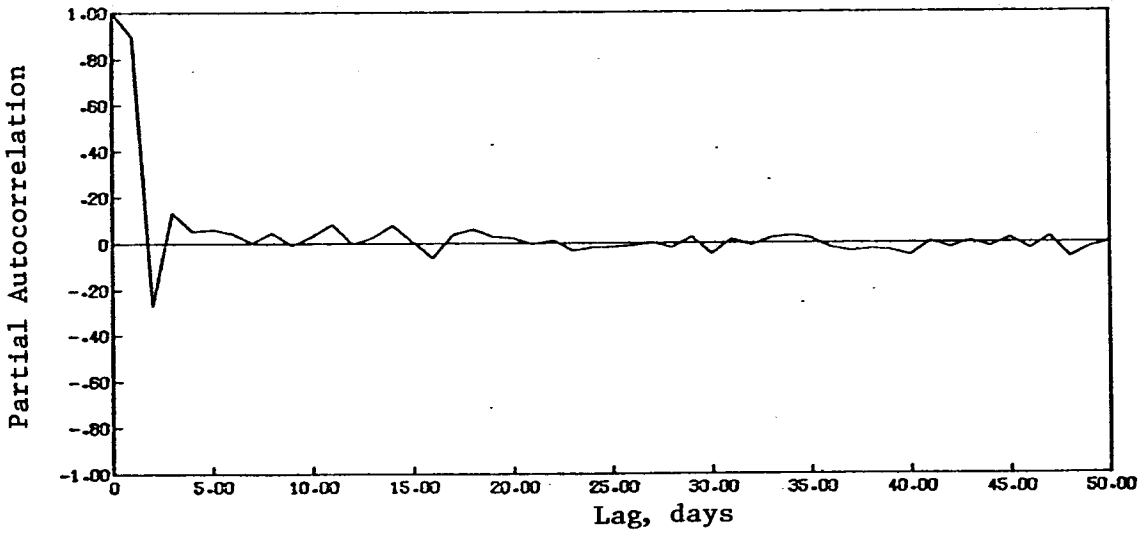

Figure 4.4b. Estimated Partial Autocorrelation Function for Duwamish River Dissolved Oxygen Data

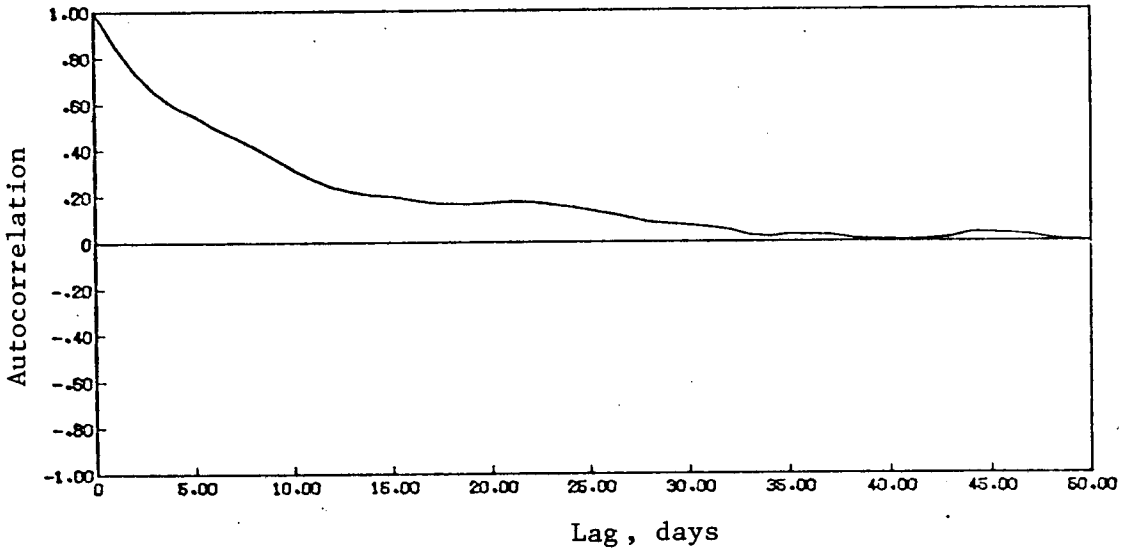

Figure 4.5a. Estimated Autocorrelation Function for Duwamish River Temperature Data

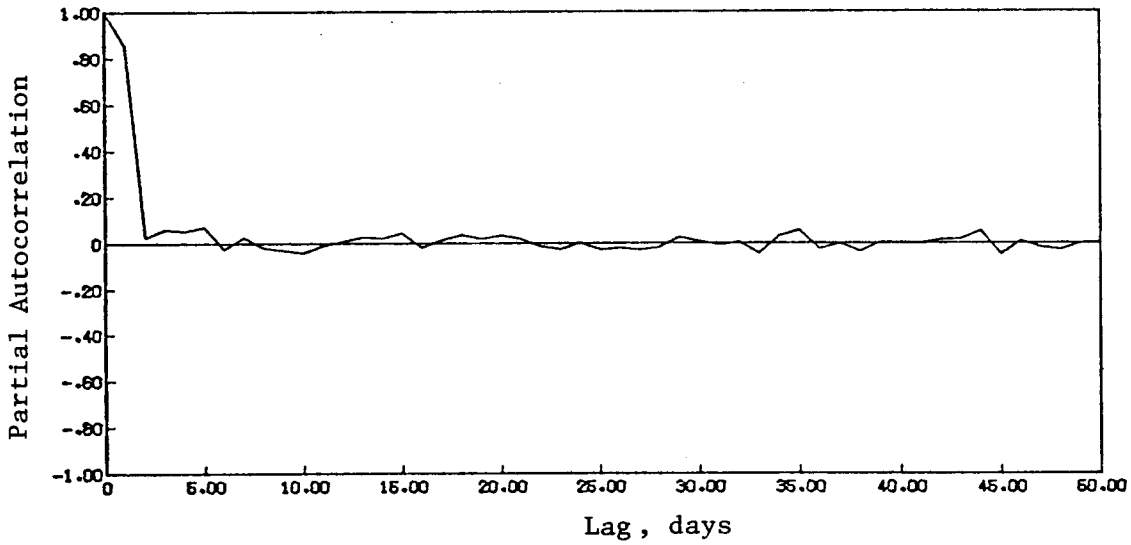

Figure 4.5b. Estimated Partial Autocorrelation Function for Duwamish River Temperature Data

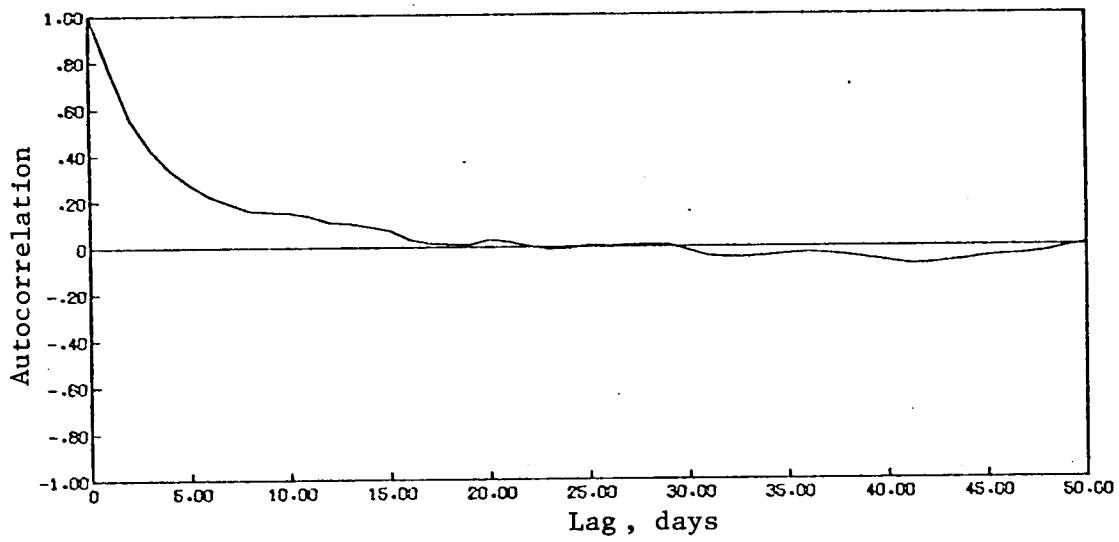

Figure 4.6a. Estimated Autocorrelation Function for Delaware River Suspended Solids Data

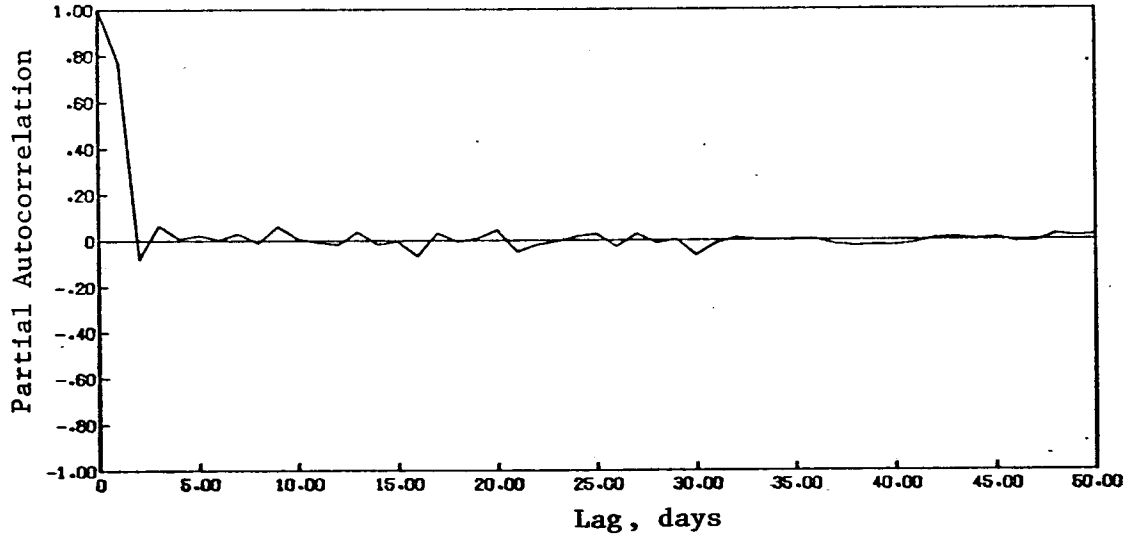

Figure 4.6b. Estimated Partial Autocorrelation Function for Delaware River Suspended Solids Data

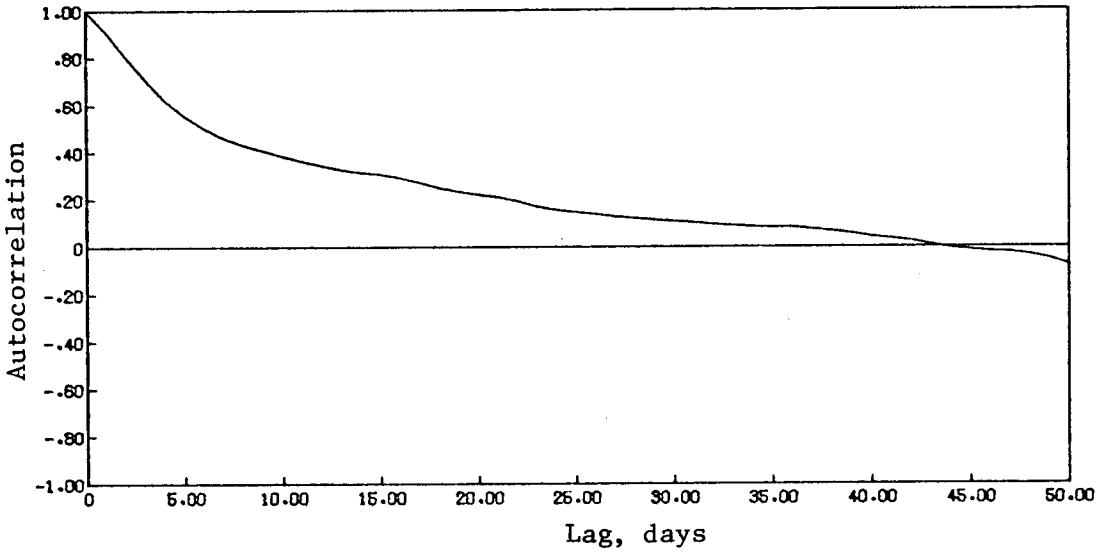

Figure 4.7a. Estimated Autocorrelation Function for Delaware River Temperature Data

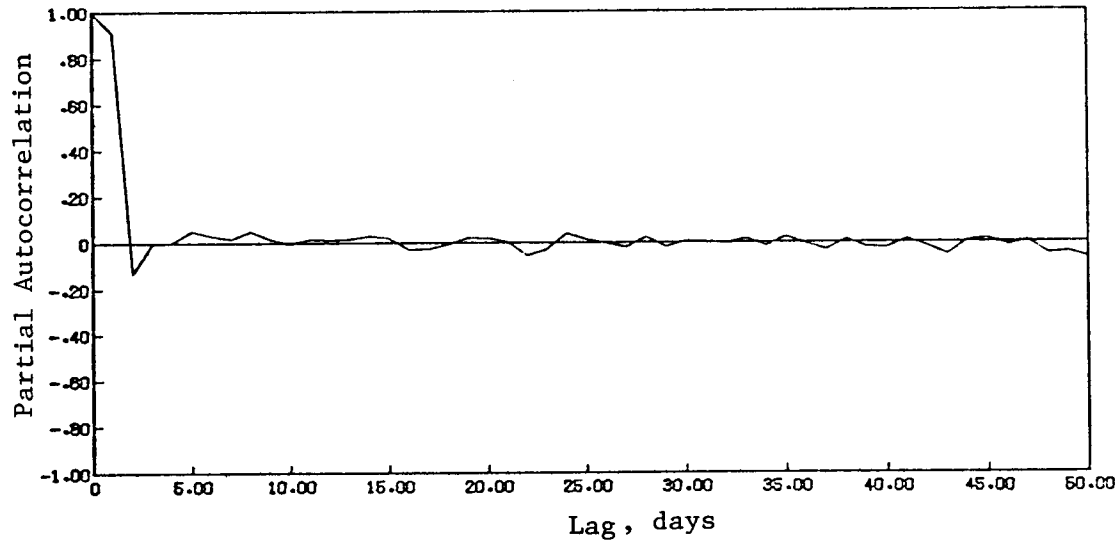

Figure 4.7b. Estimated Partial Autocorrelation Function for Delaware River Temperature Data

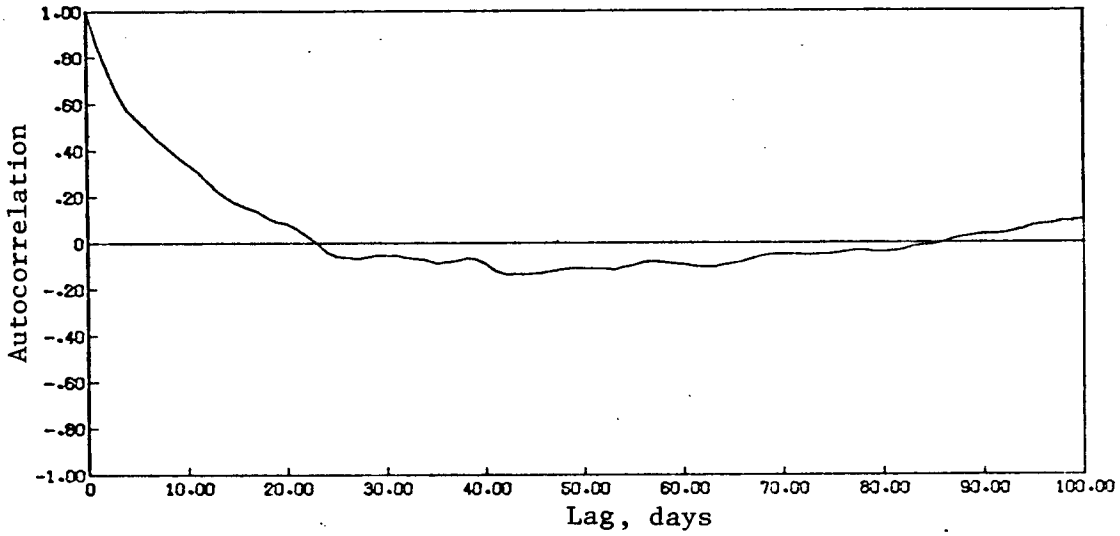

Figure 4.8a. Estimated Autocorrelation Function for San Juan River Specific Conductivity Data

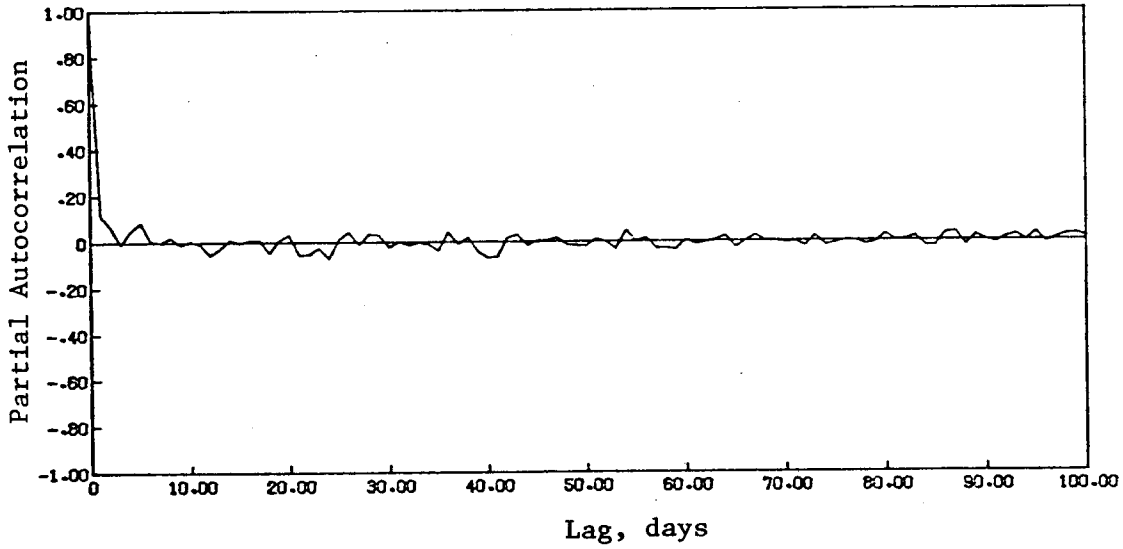

Figure 4.8b. Estimated Partial Autocorrelation Function for San Juan River Specific Conductivity Data

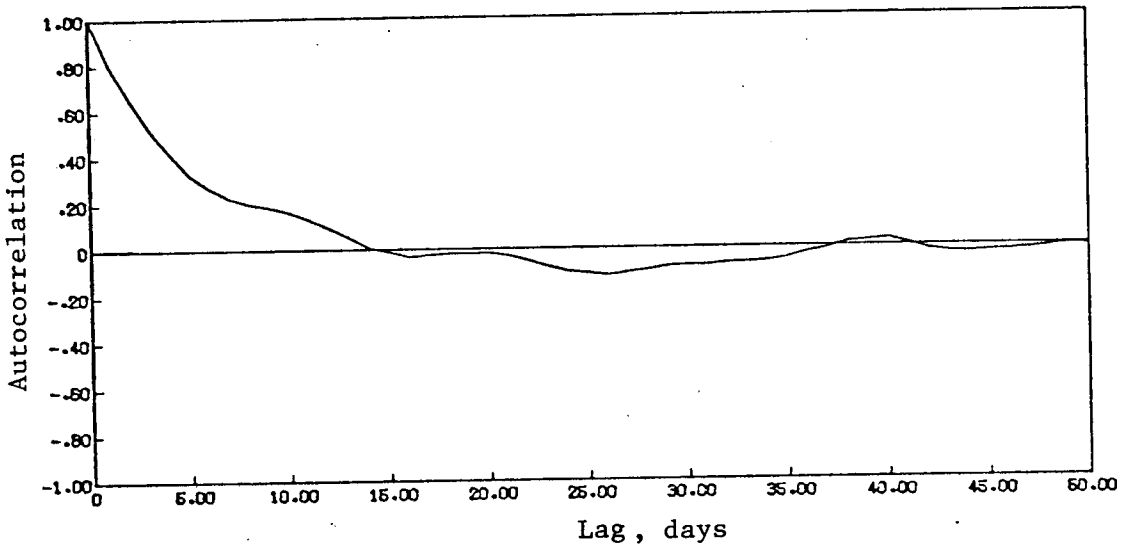

Figure 4.9a. Estimated Autocorrelation Function for San Juan River Suspended Solids Data

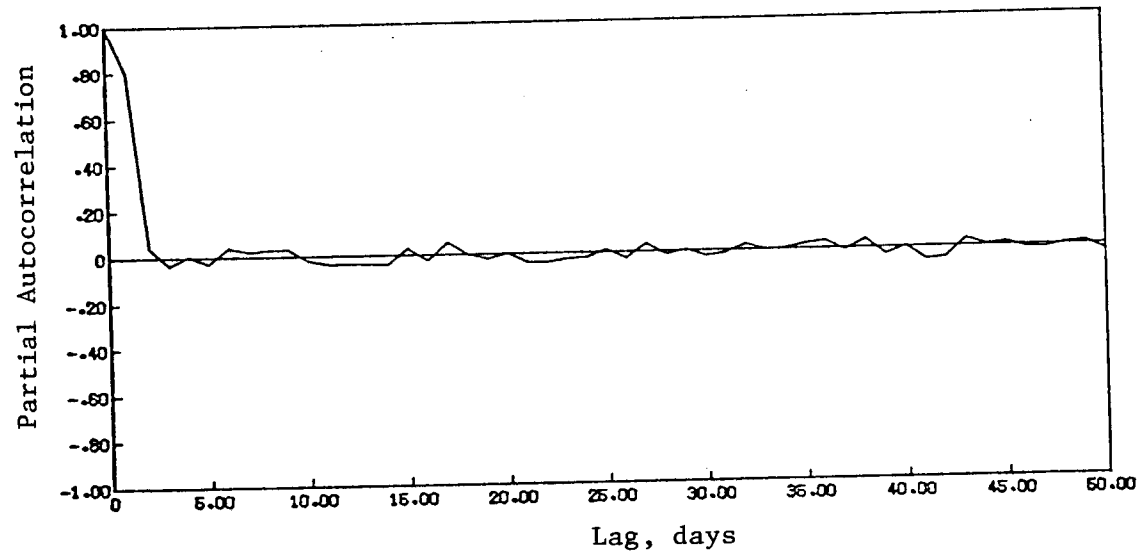

Figure 4.9b. Estimated Partial Autocorrelation Function for San Juan River Suspended Solids Data

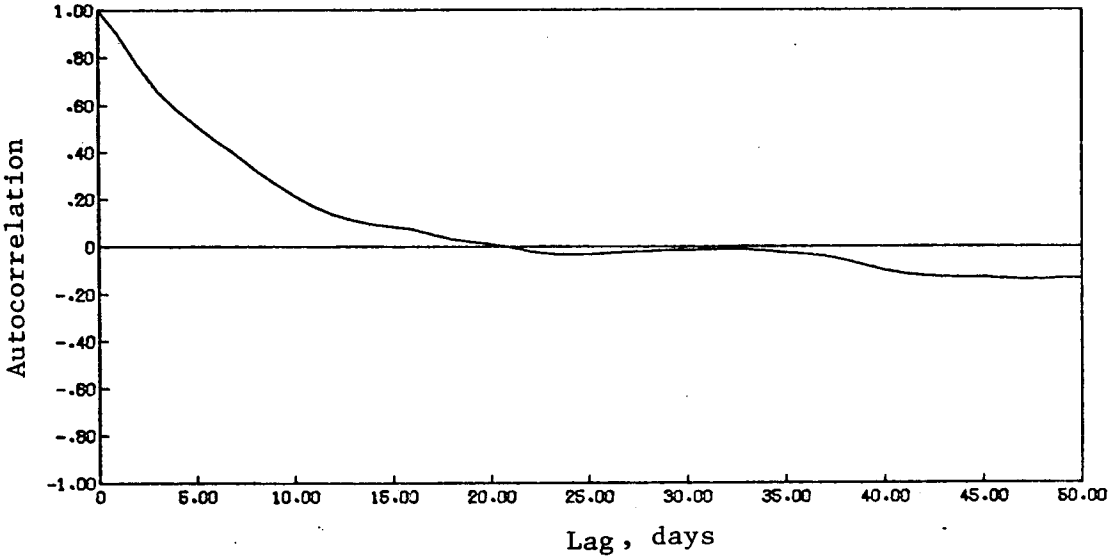

Figure 4.10a. Estimated Autocorrelation Function for Arkansas River Specific Conductivity Data

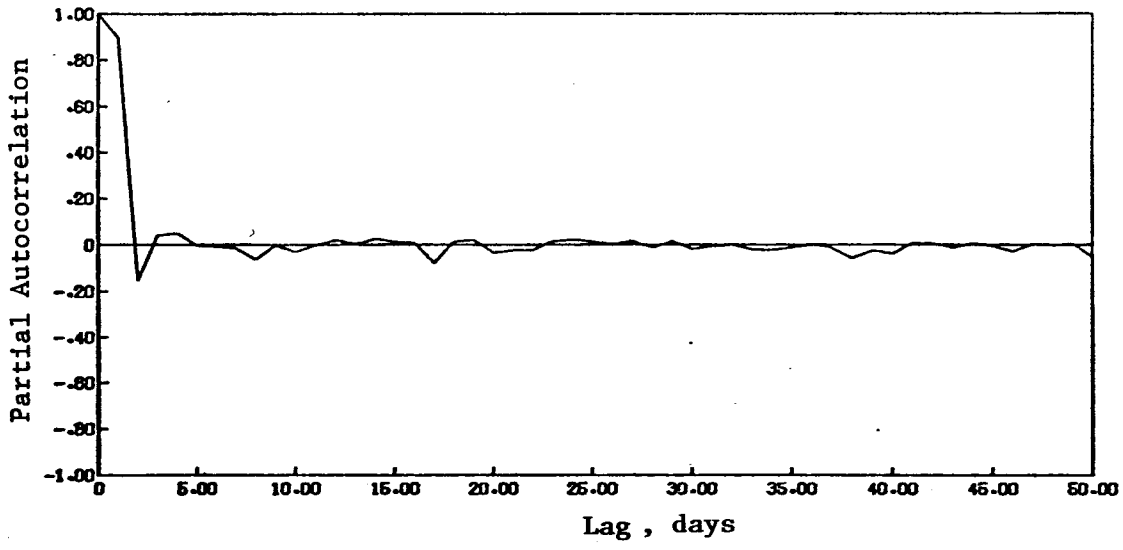

Figure 4.10b. Estimated Partial Autocorrelation Function for Arkansas River Specific Conductivity Data

where t is the sample interval and $\rho(jt)$ is the lag jt correlation coefficient. It should be noted that eq. 4.17 is completely general and does not require a specific form of dependence (e.g., an ARMA model). For an AR(1) (lag one Markov) model, eq. 4.17 can be approximated (Bayley and Hammersley, 1946) as

$$1/n_b^* = 1/n \left\{\frac{1/\rho-\rho}{1/\rho+\rho-2} - 2/n \left[\frac{1/\rho+\rho-2}{(1/\rho+\rho-2\cos(\rho))^2}\right]\right\} \qquad (4.17a)$$

in which ρ is the lag one correlation coefficient.

The concept of using equivalent independent sample sizes was expected to yield useful results based on the mechanism used in the classical t-test for the difference between two means. Since the t-test for a step trend (eq. 4.5) essentially is no more than a method of setting confidence bounds on the difference between two means, a t-test for an autocorrelated time series is possible by simply substituting the expression 4.16 for the standard error of the mean. The t-test for linear trend uses the same type of expression with only numerical factors changed. The observation was made earlier that the power curves for the nonparametric tests appear to follow the same general behavior as those for t-tests (Figures 4.2 and 4.3), e.g., summarization using the same dimensionless "trend numbers" N_t appears to hold. This observation allowed planning of a limited Monte Carlo testing program to assess the hypothesis that the nonparametric tests for trend in an autocorrelated time series can be summarized using the power curves for an independent time series with an equivalent sample size determined from eq. 4.17.

Equation 4.17 has several interesting properties which are summarized

graphically in Figures 4.11 and 4.12. A base sample frequency of 1 day^{-1} was selected to afford compatibility with the historical records investigated. It may be shown that equation 4.17 implies a maximum effective number of independent samples which may be collected in a specified time period n_o, i.e.,

$$\frac{1}{n_{max}} = \lim_{n\to\infty} \{\frac{1}{n} + \frac{2}{n^2} \sum_{j=1}^{n-1} (n-j)\rho(jt) \qquad (4.17b)$$

Here n_o was taken as 365 days. The maximum effective sample number varies with the base lag one correlation coefficient for a lag one Markov process, $\rho_t = \exp(\ln(\rho)t)$, where t is an (arbitrary) sample interval. It is interesting to note in Figure 4.11 that for a daily lag one correlation coefficient of about 0.14 (much lower than any of the historical data assessed) a maximum of 365 equivalent independent samples are possible per year. For daily correlations of the order of magnitude of those observed in the historical data, maximum equivalent independent sample sizes on the order of only about 25-35 per year are possible. Figure 4.12 shows the relationships between effective independent sample size and actual sample size, for instance, for a series with a base (daily correlation coefficient of 0.75, 50% of the maximum equivalent independent samples are collected if only about .06 x 365 = 22 samples per year are taken. Hence, approximately bimonthly sampling yields about 50% of the maximum possible information in this case if n'/n_{max} is considered as a kind of relative information measure. This result has important implications for sample system design and is implemented in Chapter 5.

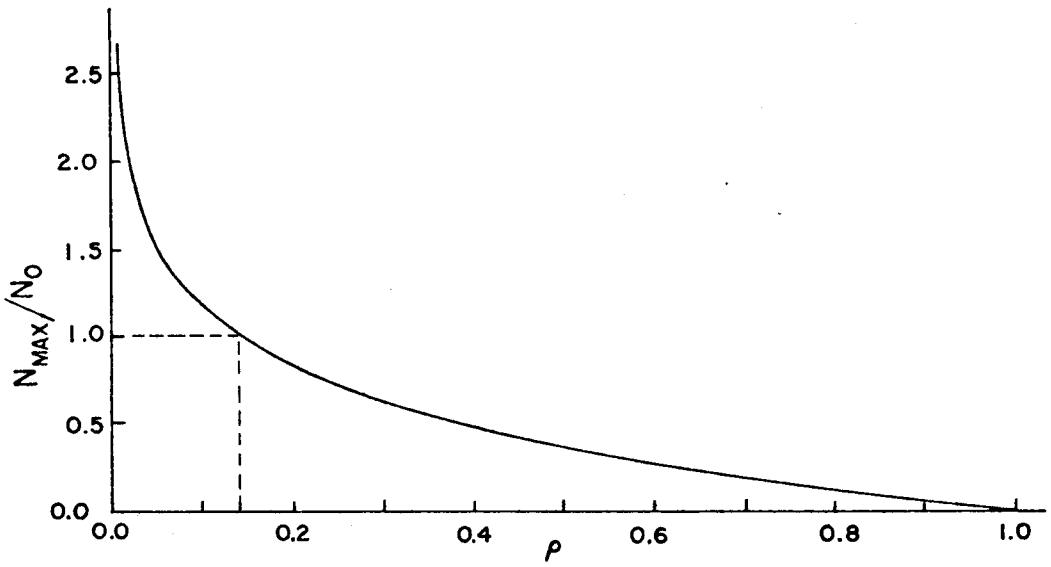

Figure 4.11. Normalized Maximum Effective Independent Sample Size as a Function of One Day Lag One Correlation Coefficient for a Lag One Markov Model

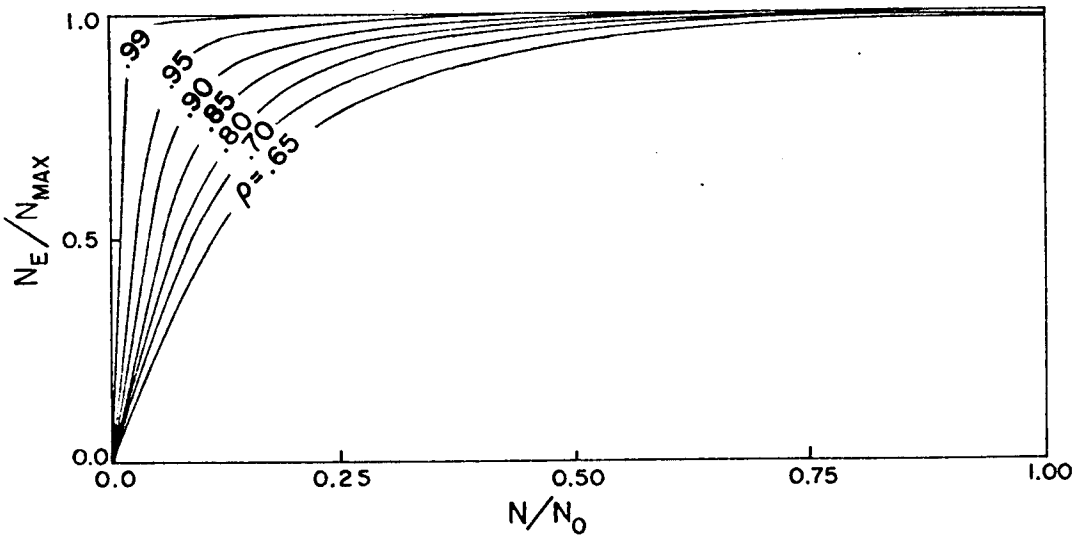

Figure 4.12. Effective Sample Ratio as a Function of Normalized Sample Frequency. N/N_o = 1 corresponds to daily sampling.

VII. Monte Carlo Test Results

Initial pilot tests of the two tests proposed by Sen (1965) indicated that neither was effective for small to medium sample sizes (e.g. $n \sim 10$-100). The problem encountered was that the test statistic, T is estimated as

$$T = \frac{r - \frac{1}{2}n'}{a_o\sqrt{n'}} \tag{4.18}$$

for the Cox-Stuart analogue, where

$$a_o^2 = b_o + \sum_{h=1}^{m} b_n - (2m+1)\left(\frac{r}{n'}\right)^2 \tag{4.19}$$

$$b_h = \frac{1}{n'-h} \sum_{i=1}^{n'-h} \phi(X_i)\phi(X_{i+h}) \tag{4.20}$$

with r = number of values of X_i greater than the preceding value,

$$n' = n-1$$

and

$$\begin{aligned} \phi(X_i) &= 1 \quad \Big| \quad X_i - X_{i-1} \geq 0 \\ &= 0 \quad \Big| \quad X_i - X_{i-1} < 0 \end{aligned} \tag{4.21}$$

The problem which arises in small samples is that the covariance estimates b_h in 4.20 become erratic causing the variance estimate (eq. 4.19) to sometimes assume negative values, especially for large trend magnitudes. This was a frequent occurrence for small samples (e.g., $n \lesssim 20$) but persisted for samples as large as 200. In addition, although the sample statistic T was demonstrated by Sen (1965) to have assymptotic normality, for small samples the distribution has extremely heavy tails, making estimation of rejection values very difficult. Similar problems were

encountered using the analogue to Kendall's Tau test proposed by Sen (1965), which uses an estimate of the variance of the test statistic similar to eq. 4.19.

Only the Mann-Whitney analogue was found not to yield negative variance estimates. The test statistic for this test, however, had extremely heavy tails, as shown in a quantile-quantile plot (Wilk and Gnanadesman, 1968) in Figure 4.13. A straight line in Figure 4.13 would indicate normality of the test statistic; the deviation at the ends indicates tails heavier than normal. This heavy tailed behavior makes estimation of the rejection values at confidence levels of

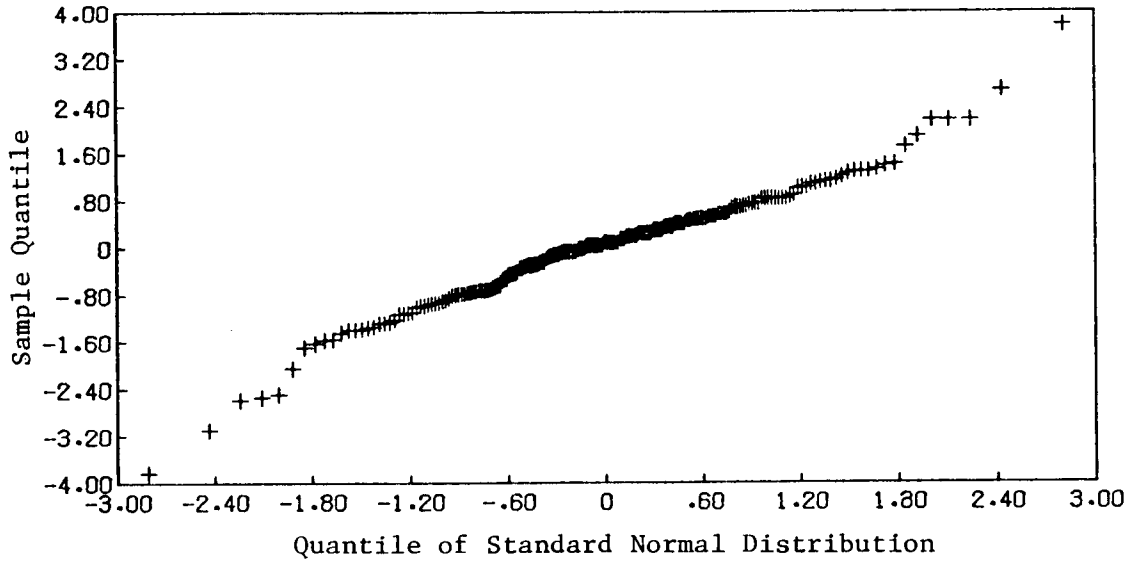

Figure 4.13 Quantile-Quantile Plot for Generated Test Statistics of Modified Mann-Whitney's Test Against Normal Lag One Markov Series of Length 100, $\rho = 0.50$

interest (95% in this work) extremely difficult without very large sample sizes. However, use of the special tests for dependent samples derived by Sen has no apparent advantage when sample sizes are small, since the assymptotic normality of the test statistic is of no help in estimating rejection values. Also, the power of these tests should not be superior to the classical tests for independent samples applied to the dependent case as the basic mechanism of estimating the test statistics is the same. For instance, the numerator in eq. 4.18 is the same as that used in the classical tests (known in the statistical literature as U-statistics), only the method of estimating the scale (the denominator in eq. 4.18) differs.

An alternative approach, then, to the use of the tests proposed by Sen (1963; 1965) is to use the classical tests (Spearman's Rho and Mann-Whitney) with rejection values estimated from Monte Carlo samples. Since the Mann-Whitney and Spearman's Rho test statistics have finite upper and lower bounds, the distribution tails are relatively stable for small sample sizes. For sample sizes of 200, power curves were estimated for lag one Markov models with correlation coefficients of 0.25, 0.5, and 0.75. Equivalent values of

$$N_T = \frac{T_r\sqrt{n_b^*}}{2\sigma} \qquad \text{and} \qquad \frac{T_r\sqrt{n_b^*(n_b^*+1)(n_b^*-1)}}{\sqrt{12}\, n_b^*\sigma}$$

for step and linear trends, respectively were calculated. The results are plotted for Spearman's Rho test against a linear trend and Mann-Whitney's test against a step trend in Figures 4.14 and 4.15. The solid lines in each case are the estimated normalized power curves from Figures 4.2a and 4.3a. Allowing for estimation errors due to the small sample sizes used, the results fall closely about the estimated line for

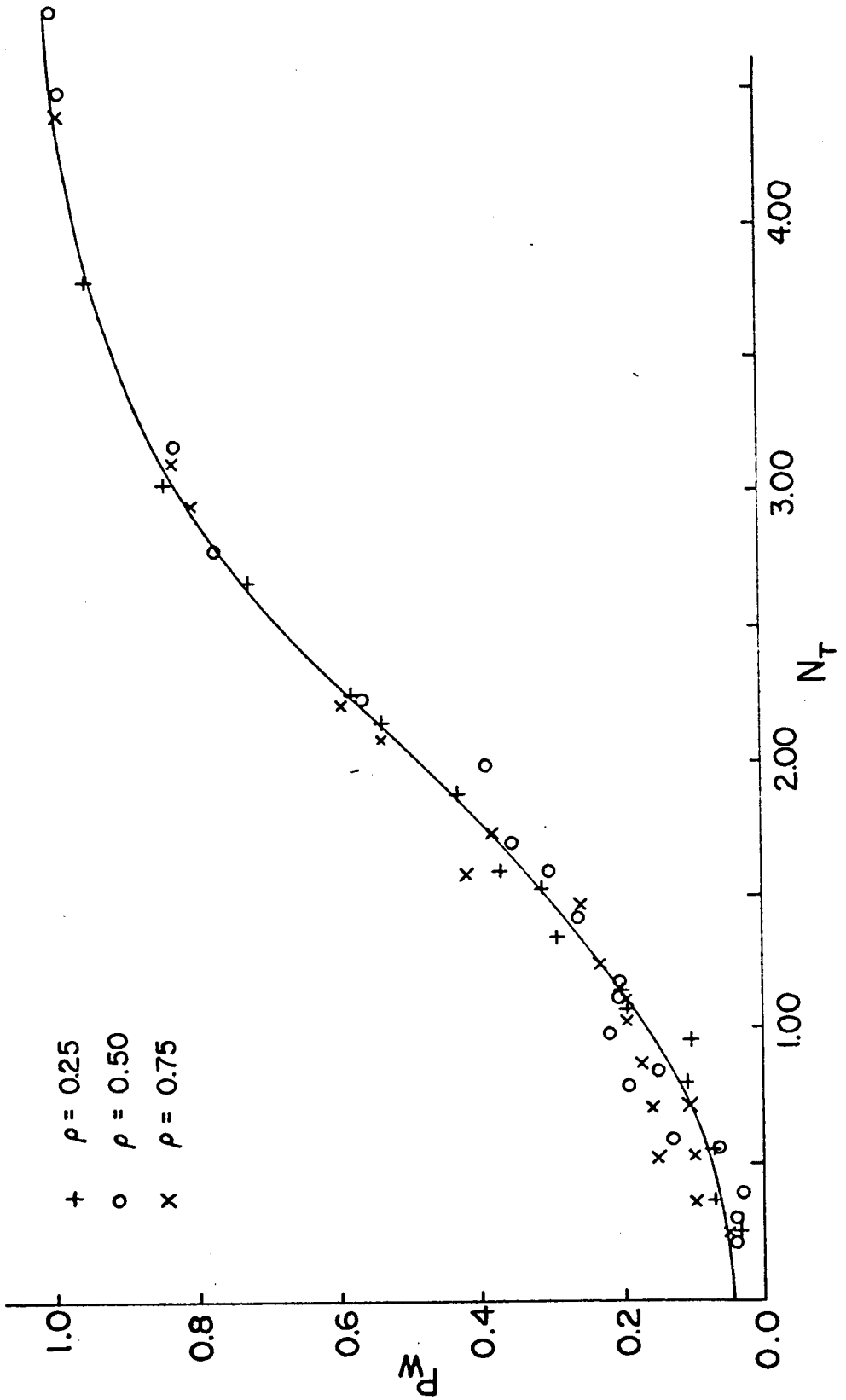

Figure 4.14 Monte Carlo Test Results for Spearman's Rho Test Against a Linear Trend With Lag One Markov Dependence. Data Distribution Is Gaussian.

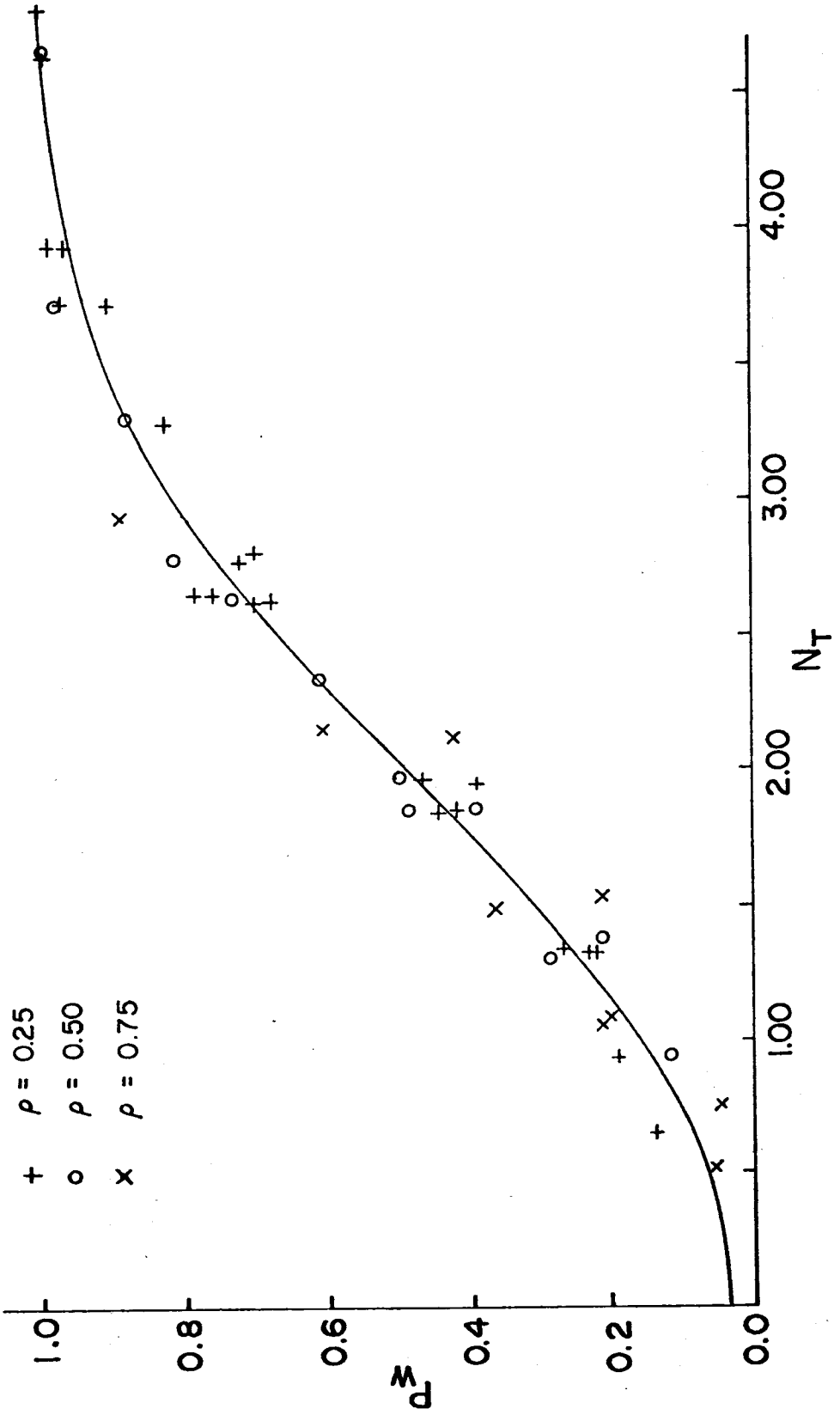

Figure 4.15 Monte Carlo Test Results for Mann-Whitney's Test Against a Step Trend with Lag One Markov Dependence. Data Distribution is Gaussian.

independent samples. Based on these results, it appears that the power curves for the nonparametric tests investigated are relevant for the dependent sample case if an equivalent number of independent samples, as defined by eq. 4.17, is used in specifying the dimensionless trend number, N_t. This result is used throughout the remainder of this investigation.

We may make use of this result to transform the curves of Figures 4.11 and 4.12 for normalized equivalent independent samples as a function of actual sample size to curves for normalized power against sample size. We may define (for a step trend)

$$P_{max} = F\left(\frac{T_r\sqrt{n_{max}}}{2\sigma}\right) \tag{4.22}$$

where F is the normalized power function of Figure 4.14, with n_{max} defined by eq. 4.17b, T_r the trend magnitude, and σ the standard deviation of the time series. We may also define

$$P_w = F(T\sqrt{n_b^*}/2\sigma) \tag{4.23}$$

with n_b^* defined by eq. 4.17. Dimensionless results for P_w/P_{max} versus n/n_o and P_{max} versus daily lag one correlation coefficient are plotted in Figures 4.16 and 4.17. Clearly, the resulting curves depend also on the trend to standard deviation ratio. For $T_r/\sigma = 0.2$ as shown in Figure 4.17 there is little advantage, for any of the correlation coefficients plotted, in sampling at a frequency of greater than about $n/n_o = 0.25$ or once every four days. This method of parametrizing power curves will be of great help in the network optimization method illustrated in the following chapter.

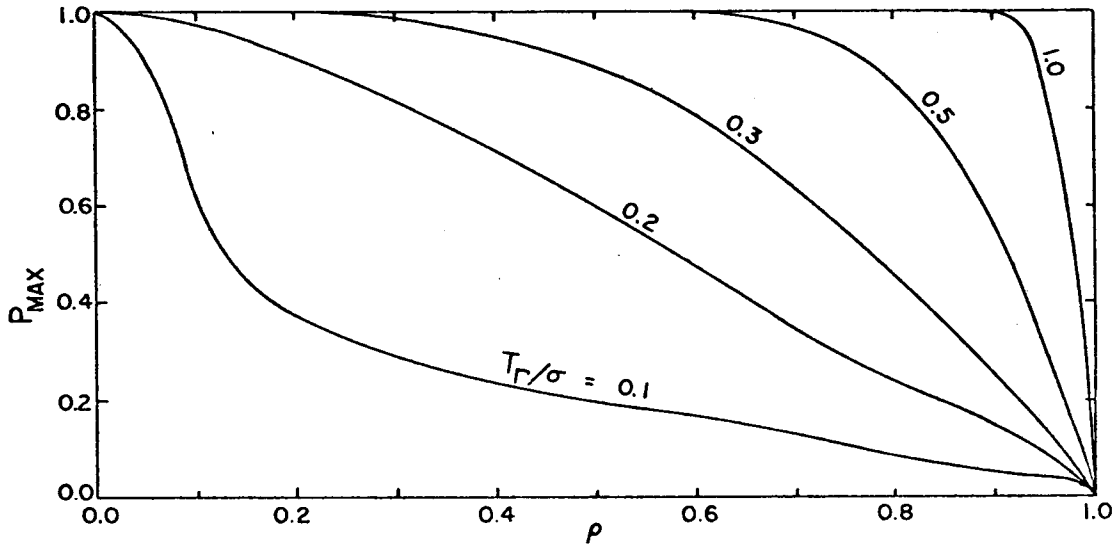

Figure 4.16 Maximum Power vs. Lag One Correlation Coefficient and Trend to Standard Deviation Ratio for a Lag One Markov Model for Mann-Whitney's Test Against a Step Trend

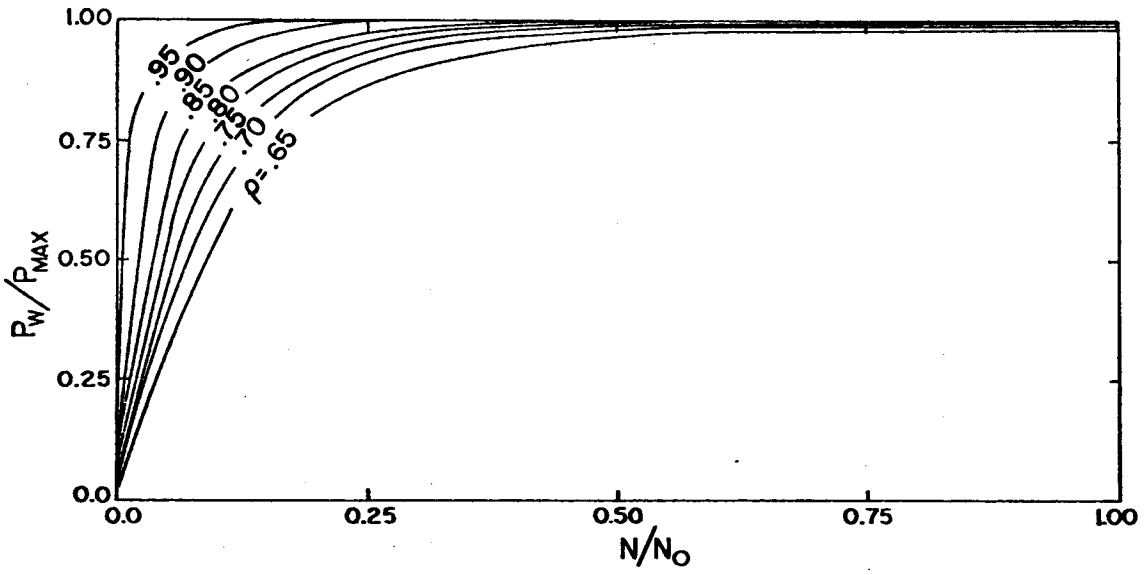

Figure 4.17 Relative Power Ratio vs. Normalized Sample Size and Lag One Correlation Coefficient for a Lag One Markov Model Using Mann-Whitney's Test Against a Step Trend. Trend to standard deviation ratio is 0.2.

CHAPTER 5

APPLICATION TO NETWORK DESIGN

I. Design Method

The results of Chapters 3 and 4 for sample station location and specification of sample frequency may be combined in a comprehensive design approach. Given a constraint, NSAMP, on the total number of samples which may be taken in a given reach per year, various optimal sample station configurations specified in the manner described in Chapter 2 may be analyzed for power against detection of a given trend magnitude. The power used here for comparison is a weighted spatial average power over the river basin,

$$P_{w_i} = \sum_{j=1}^{N_r} W_j \int_{X_{l_j}}^{X_{u_j}} P_{w_i}(X_j)dX_j \Big/ \int_{X_{l_j}}^{X_{u_j}} dX_j \qquad (5.1)$$

where N_r is the number of reaches in the river basin, X_{l_j} and X_{u_j} are the upstream and downstream reach boundaries, W_j is a normalized weighting factor for each reach such that

$$\sum_{j=1}^{N_r} W_j = 1$$

and i denotes the i'th water quality constituent. At present sampling stragegies are constrained to include a sample of each constituent in every sample event, hence each "sample" included in NSAMP includes one sample of each constituent. Consequently, the sample network chosen is not globally optimal, as variable sample strategies are not admitted.

This requirement is, however, compatible with operational considerations.

The sample station location algorithm (Chapter 3) requires specification of a linearization trajectory as well as the upstream boundary estimates of constituent variances and the effluent constituent variances. In addition, stream and effluent flow variances are required. The sample station selection method assumes complete mixing, hence variance estimates immediately downstream of an effluent discharge point are updated (assuming Q and Q_e uncorrelated) by

$$\sigma^2_{Q'} = \sigma^2_Q + \sigma^2_{Q_e} \tag{5.2a}$$

and

$$\sigma^2_{c_i} = \left[\frac{Q_e}{Q+Q_e}\right]^2 \sigma^2_{c_{e_i}} + \left[\frac{Q}{Q+Q_e}\right]^2 \sigma^2_{c_i} + \left[\frac{Q(c_i - c_{e_i})}{(Q+Q_e)^2}\right]^2 \sigma^2_Q + \left[\frac{Q_e(c_i - c_{e_i})}{(Q+Q_e)^2}\right]^2 \sigma^2_{Q_e} \tag{5.2b}$$

where eq. 5.2b is the first order approximation for uncorrelated random variates (Cornell, 1972) to the variance of the downstream concentration of constituent i, with Q = upstream flow, Q_e = effluent flow, c_i = i'th upstream constituent concentration, and c_{e_i} = i'th constituent concentration in the effluent, and where σ^2_x denotes the variance of x. Between tributaries the state estimation methods of Chapter 3 allow estimation of the variances of the estimates of each of the constituent concentrations. These variances are the estimation variances at a given time, and do not include time variability of the sequence of observations.

For any observed water quality record at a specified sample station, the variance of the record is composed of a contribution from

measurement and prediction (estimation) error and a contribution from natural effects, primarily climatalogical. Further, the two contributions may reasonably be assumed independent, i.e., climatological variations bear no influence on measurement error, hence

$$\sigma^2_{c_{ij}} = \sigma^2_{c_{ij}}(m) + \sigma^2_{c_{ij}}(n) \tag{5.3}$$

where c_{ij} is the i'th constituent concentration at the j'th spatial location, and the superscripts m and n signify measurement (and prediction), and natural, respectively. It should be noted that where location j is a sample station, $\sigma^2_{c_{ij}}(m)$ will not exceed the measurement error, but for estimation between sample stations the measurement error may be exceeded. Equation 5.3 reflects the fact that the variance of a historical trace may not be reduced below a lower limit specified by natural conditions. This lower limit may be estimated from historic records as

$$\sigma^2_{ij_L} = \sigma^2_{ij} - \sigma^2_{ij_m} \tag{5.4}$$

where $\sigma^2_{ij_L}$ is the lower variance bound of the historic trace of constituent i, σ^2_{ij} is the observed historic variance, and $\sigma^2_{ij_m}$ is the estimated measurement error in constituent i. The historic variance is assumed to be constant with time, seasonal variations are ignored. Methods for transforming data to conform to this restriction are discussed in Section III of this chapter.

In addition to specification of the historic variance lower bound, the parameters relating dependence in time of the estimated constituent values must be specified, as well as a design trend magnitude for each

constituent. Given the values of this parameter vector, the maximum number of effective samples over a given time horizon may be computed for each constituent. Using the results of Chapter 4, a maximum power over the time horizon may be specified, using the normalization

$$N_{T_{ij}}^{(M)} = \frac{T_{r_i}\sqrt{n_{max}}}{2\sigma_{ij_L}} \tag{5.5a}$$

where T_{r_i} is the design trend magnitude, σ_{ij_L} is estimated from eq. 5.4 or is specified apriori, and n_{max} is the maximum effective number of independent samples described in Chapter 4. The estimated actual power may be based on the trend number

$$N_{T_{ij}} = \frac{T_{r_i}\sqrt{n_e}}{2\sigma_{ij}} \tag{5.5b}$$

with n_e the effective independent sample size and σ_{ij}^2 the total variance of the estimated time series ($\sigma_{c_{ij}}^2$ in eq. 5.3). It should be noted that eqs. 5.5 are strictly applicable for a step trend only, but yield results very nearly equivalent (if the approximation $\sqrt{n(n+1)(n-1)} \sim n^{3/2}$ is made in eq. 4.12) to the case of a linear trend with magnitude $T'_{r_i} = T_{r_i}\sqrt{12/2}$, hence design for a linear as opposed to a step trend simply involves changing the design trend magnitude. The power corresponding to $N_{T_{ij}}(M)$ of eq. 5.5a may be defined $P_{w_{ij}}(M)$, the maximum power in detecting the i'th constituent while the actual power $P_{w_{ij}}$ corresponds to $N_{T_{ij}}$. Hence the efficiency of a trend network may be defined as

$$E_i = \tilde{P}_{w_i} / \tilde{P}_{w_i}^{(M)} \tag{5.6}$$

where $\tilde{x}$ denotes the spatial average of x.

This normalization allows a convenient method for summarizing results. E_{ij} may be considered as a sort of relative information measure as well as a measure of network efficiency.

The prototype network consists of a single reach of length 100 miles with two point source effluents and one tributary, as shown schematically in Figure 5.1.

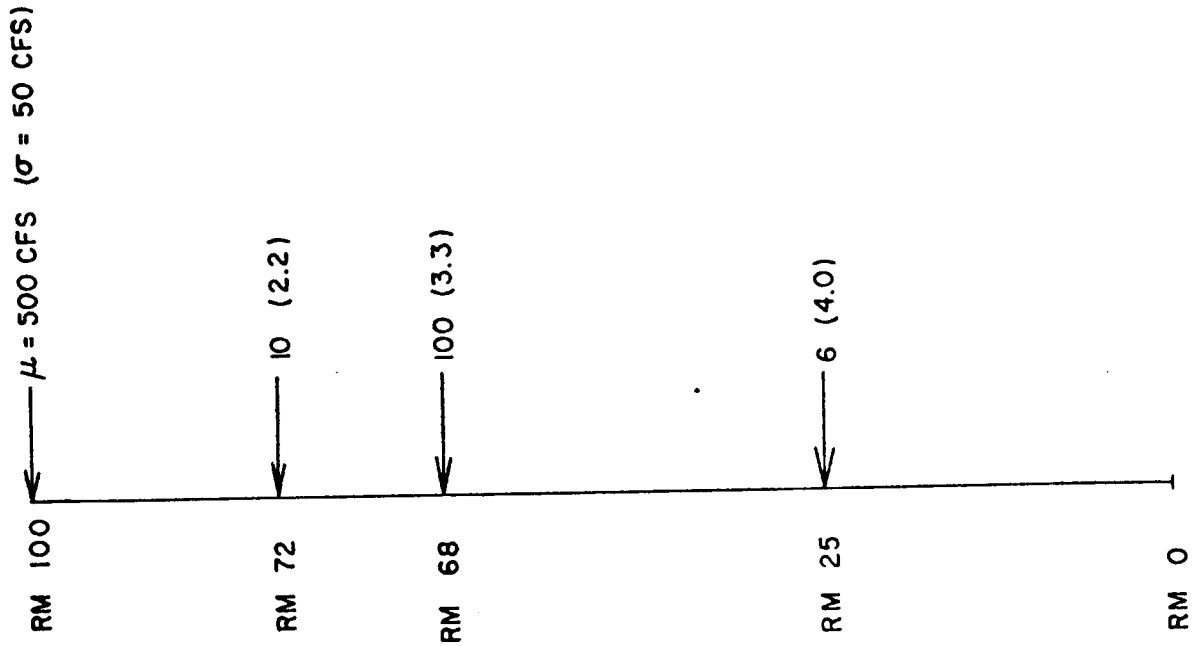

Figure 5.1. Test Stream Reach with Effluent Locations, Flows, and Standard Deviations

The system has been purposely simplified to allow easier identification of the primary factors influencing the design. A set of upstream boundary values was specified as well as tributary and effluent concentrations and variances. These values, and the secondary variable (parameter) values used are given in Tables 5.1 and 5.2.

The historical variances and lag one correlation estimates and measurement errors are given in Table 5.3. Where appropriate,

Table 5.1 Upstream Boundary, Effluent, and Linearization Trajectory Concentrations

Inflow location (river mile)	Flow (cfs)	PO (mg/l)	BOD (mg/l)	DO (mg/l)	NH_3 (mg/l)	NO_2 (mg/l)	NO_3 (mg/l)	Temp (°F)	FCX** (MPN/100ML)
				Effluent Mean Values					
25.0	6.0	12.0	30.0	5.0	8.0	1.0	6.0	60.0	12.0
68.0	100.0	0.1	0.1	9.0	0.1	0.0	0.5	65.0	2.0
72.0	10.0	5.0	40.0	7.0	8.0	2.0	10.0	90.0	15.0
100.0*	500.0	0.1	2.0	9.0	0.1	0.05	0.1	60.0	1.0
				Effluent Variances					
25.0	15.0	35.0	225.0	25.0	16.0	25.0	9.0	36.0	5.0
68.0	10.0	0.01	1.0	1.0	0.01	1.0	0.25	2.0	5.0
72.0	5.0	5.0	5.0	10.0	5.0	5.0	2.0	5.0	5.0
100.0*	2500.0	10^{-4}	1.0	0.25	0.01	2.5×10^{-4}	0.01	4.0	4.0
				Linearization Trajectory (In-Stream Concentrations)					
0		.39	2.42	7.95	.22	.068	.39	64	3.0
15		.39	2.44	8.16	.245	.060	.39	63.4	3.0
30		.34	2.18	8.34	.178	.062	.34	63.0	3.0
45		.34	2.20	8.49	.196	.080	.34	62.4	3.0
60		.34	2.24	8.66	.024	.043	.30	61.4	3.0
80		.10	1.94	8.78	.01	.045	.11	60.4	3.0
100		.10	1.98	9.0	.01	.050	.11	60.0	3.0

* upstream boundary conditions

** natural logarithmic units

Table 5.2 Means and Variances of Secondary State Variables

Variable*	Description	Mean	Variance
K_s	BOD settling constant	0.03	9×10^{-4}
K_n	BOD nitrogen decay coefficient	3.33×10^{-3}	2.5×10^{-5}
K_p	BOD phosphorus decay coefficient	4.0×10^{-4}	9.0×10^{-6}
K_c	BOD carbonaceous decay coefficient	0.3	9.0×10^{-2}
K_{bb}	benthal nonpoint source BOD supply constant	8.0×10^{-3}	6.4×10^{-5}
K_a	reaeration constant	0.7	0.5
K_2	NO_2 decay coefficient	0.5	0.36
K_1	NH_3 decay coefficient	4.8×10^{-2}	1.5×10^{-2}
K_v	NH_3 volatization constant	0.3	4.0×10^{-2}
K_{bn}	benthal NH_3 supply constant	8.0×10^{-3}	6.4×10^{-5}
K_3	NO_3 settling coefficient	3.6×10^{-2}	10^{-3}
K_{bp}	benthal nonpoint source PO_4 supply constant	5.0×10^{-3}	6.4×10^{-5}
K_{ps}	PO_4 settling constant	2.2×10^{-2}	5.0×10^{-4}
K_{bd}	benthal DO demand constant	1.7×10^{-2}	6.4×10^{-5}
R_{bb}	benthal BOD supply rate	61.0	3.6×10^{3}
R_{bd}	benthal DO demand rate	31.0	2.25×10^{2}
R_{bn}	benthal NH_3 supply rate	0.11	10^{-2}
R_{bp}	benthal PO_4 supply rate	6.5×10^{-2}	1.5×10^{-2}
U	cross-section mean stream velocity	25.0	50.0
Q_i	net incident heat flux	5.0	25.0
C_1	net incident heat flux change rate	0.2	0.01
H	upstream boundary stream depth	2.0	1.0
C_2	stream depth change rate	0.05	4×10^{-4}
K	coliform decay constant	0.4	0.01
R	coliform supply rate	0.0	0.0

*for a more complete description see Appendix A.

Table 5.3 Constituent Variances and Lag One Correlation Coefficients

Constituent	Units	Variance: Measurement	Variance: Historical minimum	Lag one correlation
PO_4	mg/l	0.01	0.4**	0.835
BOD	mg/l	1.0	0.75	0.835
DO	mg/l	0.25	1.0	0.835
NH_3	mg/l	0.01	0.3**	0.835
NO_2	mg/l	0.0025	0.4**	0.835
NO_3	mg/l	0.04	0.35**	0.835
Temp	^oF	4.0	16.0	0.835
FCX	MPN*	1.0	3.0	0.835

*natural logarithmic units

**coefficient of variation

especially for nutrient values, variances are specified as coefficients of variation where the linearization trajectory (Table 5.1) provides the mean values for calculating the standard deviation.

Measurement errors were assumed to include both laboratory analysis and sampling errors and the error present due to characterizing a cross-sectional average property from a single sample. The lag one correlation coefficient represents the average over all the records investigated in Chapter 4. A simple lag one Markov model of temporal dependence of each water quality constituent was used to determine equivalent independent sample sizes. The constituent variances were chosen to be realistic in terms of historical data actually observed and reported in U.S. Geological Survey Water Supply Papers. The values are not taken from an actual sampling station, however,

The linearization trajectory was formed by running the simplified DOSCI filter model described in Appendix A for a case with no sample stations. This is equivalent to use of one of the many available deterministic stream quality models to specify constituent trajectories. A polynomial fit was then made to the estimated constituent trajectories to yield the linearization trajectory.

II. Sensitivity Tests

The monitoring network design optimization (satisficing) requires specification of a number of parameters. Included are historic time series parameters (coefficient of variation or variance, and lag one correlation coefficient), model parameters (linearization trajectory, stream velocity, and measurement error) and design specifications (number of samples or constraint level, and design trend level). A

series of sensitivity tests designed to determine which parameters merit the most effort in estimation and to determine the general character of the design efficiency response to increased sample size are reported in this section.

The initial runs were made using the base conditions of Tables 5.1, 5.2, and 5.3. Table 5.4 shows the locations of each candidate sample station computed using eq. 2.5. Table 5.5 shows the design trend levels used. Where coefficients of variation are specified (e.g., PO_4 and other nutrients) trend magnitude is expressed as the ratio of trend magnitude to mean. Fig. 5.2 shows the resulting average efficiencies over all eight primary state variables for varying constraint (sample size) values using the base conditions. The constraint level, NSAMP, represents the total number of samples taken over a four year period for each primary state variable. The most striking implication of the results shown in Figure 5.2 is the loss of efficiency at small samples sizes with increased numbers of stations. For instance, at the lowest constraint level of 20 samples/year (or NSAMP = 80 samples over the four year base period) increasing the number of sample stations from one to three approximately halves the network efficiency. At higher constraint levels, the maximum efficiency shifts toward multiple station configurations, for instance,at the highest constraint value (NSAMP = 1280) four stations should be used. Possibly more important is the observation that with increased NSAMP the configuration efficiencies become less sensitive to the number of stations specified.

If a moderate to large number of stations is specified, time series of water quality constituents at intermediate points may be

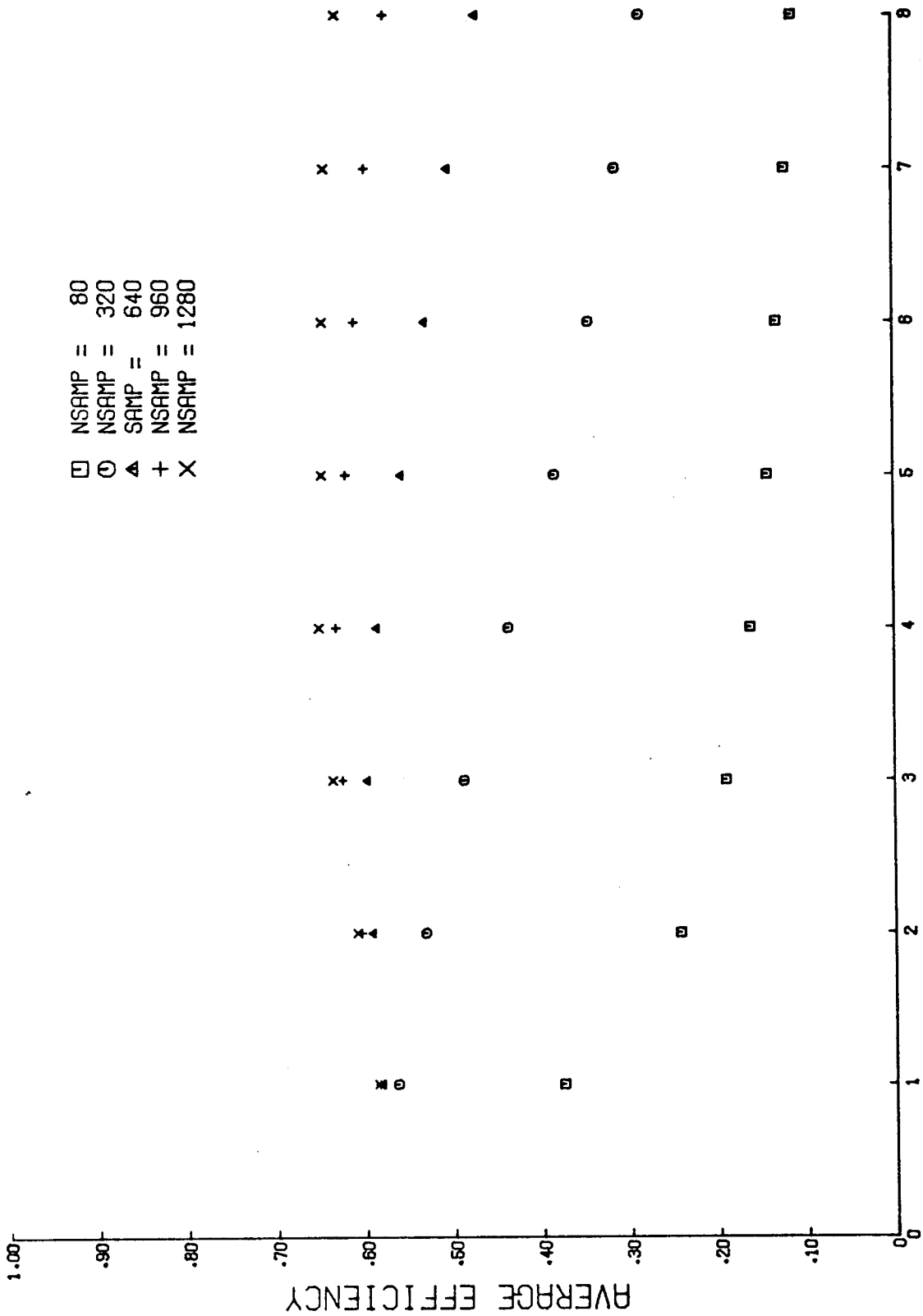

Figure 5.2. Efficiency vs. Number of Sample Stations and Sample Frequency for Base Conditions

Table 5.4 Base Sample Station Locations (River Mile)

Number of Stations	Station Number 1	2	3	4	5	6	7	8
1	48.8							
2	32.1	68.8						
3	23.4	50.9	76.6					
4	19.0	39.8	61.9	82.0				
5	16.4	33.9	51.5	85.2				
6	14.3	28.6	44.0	58.8	73.9	87.6		
7	12.3	25.2	38.7	52.1	64.8	77.6	89.5	
8	10.6	21.9	33.5	45.4	57.3	68.7	80.0	90.6

Table 5.5 Design Trend Magnitudes for Sensitivity Tests

	PO_4[a]	BOD[b]	DO[b]	NH_3[a]	NO_2[a]	NO_3[a]	Temp[c]	FCX[d]
base	0.2	0.4	0.4	0.2	0.2	0.2	1.0	0.75
low	0.1	0.2	0.2	0.1	0.1	0.1	0.5	0.375
high	0.4	0.8	0.8	0.4	0.4	0.4	2.0	1.5

[a] expressed as trend to mean ratio

[b] ppm

[c] ^oF

[d] MPN (natural log units)

estimated using relatively unsophisticated methods, such as linear interpolation. If few stations (perhaps only one) are specified, a more sophisticated method of extrapolating measurement results is required. Since, in general, few stations are associated with low constraint levels, the implication is that for small constraint levels a substantial premium is placed on using a water quality model to augment the data collected at a single station. At higher constraint levels, substantially equivalent efficiencies result from large sample networks with relatively low sample frequencies at each station. Hence, if large sample sizes may be taken, little additional benefit accrues from augmenting the monitoring values with model predictions, whereas the benefit from sample augmentation is great when small sample sizes are available.

The parameter ranges tested for sensitivity are listed in Tables 5.5 and 5.6. The results of the sensitivity tests are presented in Table 5.7. The efficiency losses are defined as

$$E_L = \frac{E_2 - E_1}{E_2} \times 100 \qquad (5.7)$$

where E_1 is the maximum efficiency for the given parameter values, E_2 is the efficiency for the same parameter values but with the number of sample stations which are optimal for the base conditions (Table 5). In all cases investigated in this section, station locations are those given in Table 5.4.

A single sample station was always associated with low constraint levels, hence no efficiency loss was found at these levels for any of the parameter perturbations. The actual efficiency levels, however, associated with the different parameter combinations do vary widely. It is important to recognize that while the actual efficiency levels

Table 5.6 Parameter Ranges for Sensitivity Tests

Parameter		PO_4	BOD	DO	NH_3	NO_2	NO_3	Temp	FCX
σ^a or CV^b	low	0.267	0.589	0.667	0.2	0.267	0.237	2.670	1.178
	high	0.6	1.299	1.5	0.45	0.6	0.525	6.0	2.598
lag one corr.	low	0.75	0.75	0.75	0.75	0.75	0.75	0.75	0.75
	high	0.9	0.9	0.9	0.9	0.9	0.9	0.9	0.9
meas. error	low	.0134	0.5	.0158	0.04	.0126	.05	2.0	1.0
mean stream velocity	low	12.5 mile/day							
	high	50 mile/day							
linearization trajectory[c]		+0.1	+2.0	-2.0	+0.1	+0.1	+0.1	+10.0	+3.0

[a] standard deviation for BOD, DO, Temp., FCX, coefficient of variation for others

[b] all units are mg/l except Temp (^oF) and FCX (MPN/100 ml; log units)

[c] amount added or subtracted uniformly from base linearization trajectory (Table 5.1)

Table 5.7a Optimal Numbers of Stations in Test Network[a]

Parameter Changed[a]		NSAMP 80	200	320	480	640	800	960	1120	1280
base conditions		1	1	1	1	2	3	4	4	4
lag one correlation coefficient (ρ)	low	1	1	1	1	1	1	3	3	4
	high	1	1	2	3	4	4	7	7	7
standard deviation or coefficient of variation (σ or CV)	low	1	1	1	3	3	3	4	4	7
	high	1	1	1	1	1	1	3	4	4
trend (Tr) trend (Tr)	low	1	1	1	1	3	3	4	4	4
	high	1	1	1	1	4	4	4	4	7
measurement error (R)	low	1	1	1	3	4	4	4	4	4
linearization trajectory		1	1	1	2	3	4	4	4	4

[a] The table shows the optimal number of sample stations for the base run, and for each additional run with only the parameter indicated perturbed. For instance, for the base conditions 4 sample stations are optimal if the constraint is 1280 samples, whereas 7 stations are optimal if the lag one correlation is changed to 0.90 with all other parameters held constant.

[b] See Tables 5.5 and 5.6 for magnitudes of changes.

Table 5.7b Relative Efficiency Losses for Sensitivity Tests[a]

Parameter Changed		NSAMP 80	200	320	480	640	800	960	1120	1280
ρ	low	0	0	0	0	2.1	0.9	1.6	0.6	0
	high	0	0	0.7	5.3	5.3	2.7	1.5	2.5	3.5
σ or CV	low	0	0	0	2.4	6.1	0	0	0	1.6
	high	0	0	0	0	2.0	0	0	0	0
Trend	low	0	0	0	0	0.5	0	0	0	0
	high	0	0	0	0	1.8	0.8	0	0	0
Meas. Err.	low	0	0	0	1.3	5.1	3.3	0	0	0
Lin. Trajectory		0	0	0	3.2	2.5	0.5	0	0	0

[a] The table shows the losses resulting if the optimal number of stations for the base run are used, rather than the optimal number for the case indicated.

predicted are sensitive to changes in the parameters (especially lag one correlation coefficient) the network design configuration specified (i.e., sample station locations and number of samples) is quite insensitive to these parameters.

The effects of parameter variations are discussed below by group. Only model parameters have any influence on the station location algorithm, as may be seen from investigation of eq. 2.5. In reporting sensitivity to the model parameters, however, station locations reported in Table 5.4 were retained. A separate investigation of the effect of changes in sample station location (for other parameters at base levels) is reported in Section II.3. of this chapter.

II.1. Historic Parameters

The lag one correlation coefficient and the variance ($\sigma^2_{c_{ij}}(n)$ in eq. 5.3) or coefficient of variation are denoted historic parameters since, in practice they must be estimated from historic records. In this work the historic parameters are assumed population values. This choice was made to avoid obfuscation resulting from estimation problems. Several lag one correlation coefficients were selected to cover the range of values observed in the data investigated in Chapter 4. Figure 5.3 shows efficiencies as a function of sample constraint for three values of the daily lag one correlation coefficient ρ. The same data are plotted in Figure 5.4 as a function of the number of sample stations specified for NSAMP = 320. An apparent anomoly exists at low constraint values where efficiency increases with increased ρ. This effect may be traced to the manner in which efficiency is defined in eq. 5.6 which results in the maximum power being a decreasing function of ρ.

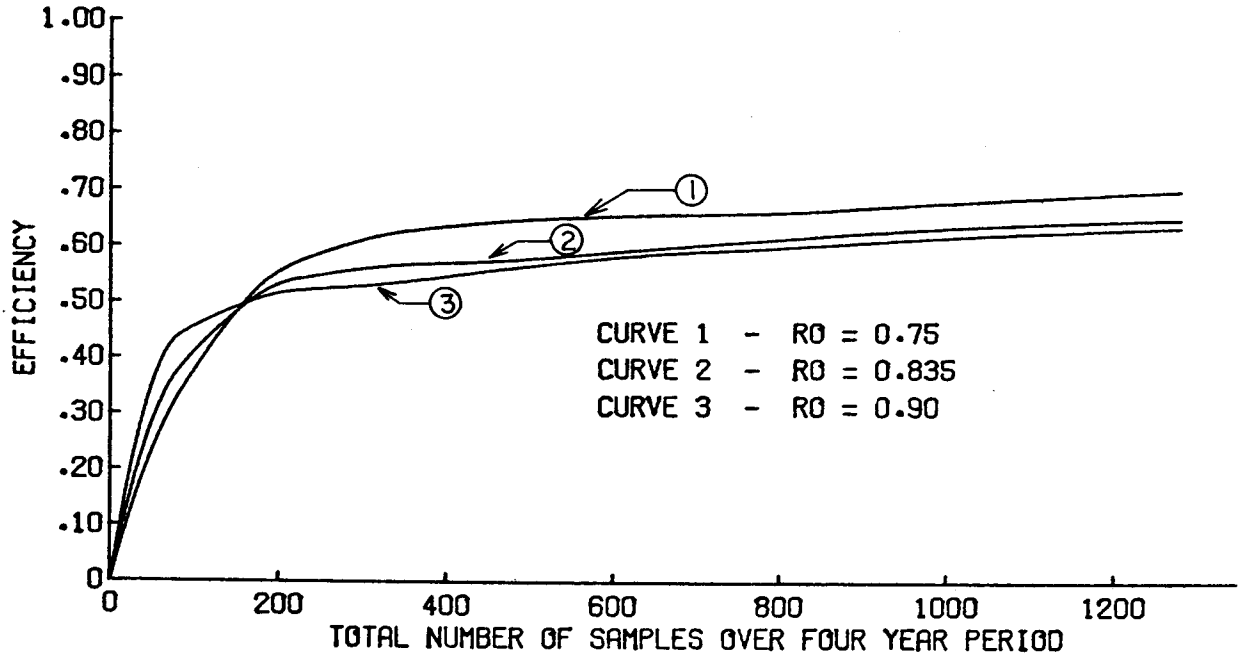

Figure 5.3. Maximum Spatial Average Efficiency vs Sample Size and Lag One Correlation Coefficient for Base Conditions

The absolute powers for the high value of ρ are much less than for the low value, only the efficiencies show the reverse behavior at low values of NSAMP.

Sensitivity of the design network to lag one correlation is surprisingly low, as shown in Table 5.7b. This is a welcome result since, based on the limited data presently available, accurate summarization (perhaps using regionalization techniques) of daily lag one correlation coefficients for most water quality indicators would be an extremely difficult task (Lenton, et al., 1974).

The effect of perturbing the coefficient of variation on design network efficiency is shown in Figure 5.5. As with lag one correlation coefficient, a change in coefficient of variation changes the maximum power as well as the actual power (curves 3 and 4 of Figure 5.5),

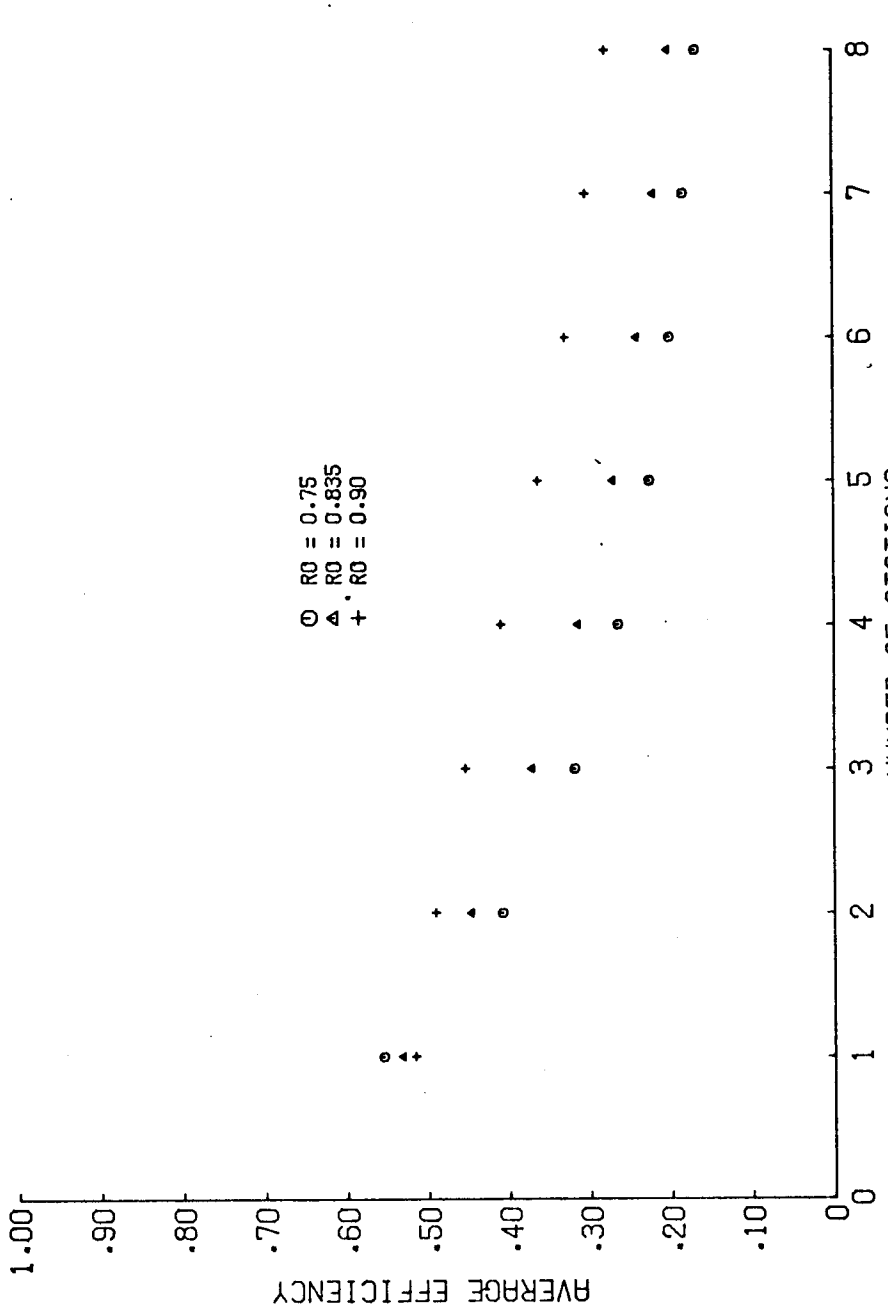

Figure 5.4. Efficiency vs. Number of Stations and Lag One Correlation Coefficient for Base Conditions and NSAMP = 320. The given lag one correlation coefficients are the assumed (identical) values for all water quality constituents.

resulting in increased efficiency with increasing coefficient of variation for small sample sizes. As sample size increases, this effect is reversed, and lower efficiencies are associated with higher coefficients of variation. Relative network efficiencies show little effect from changes in coefficient of variation although small coefficients of variation require networks with relatively larger numbers of sample stations for a constant value of the constraint NSAMP.

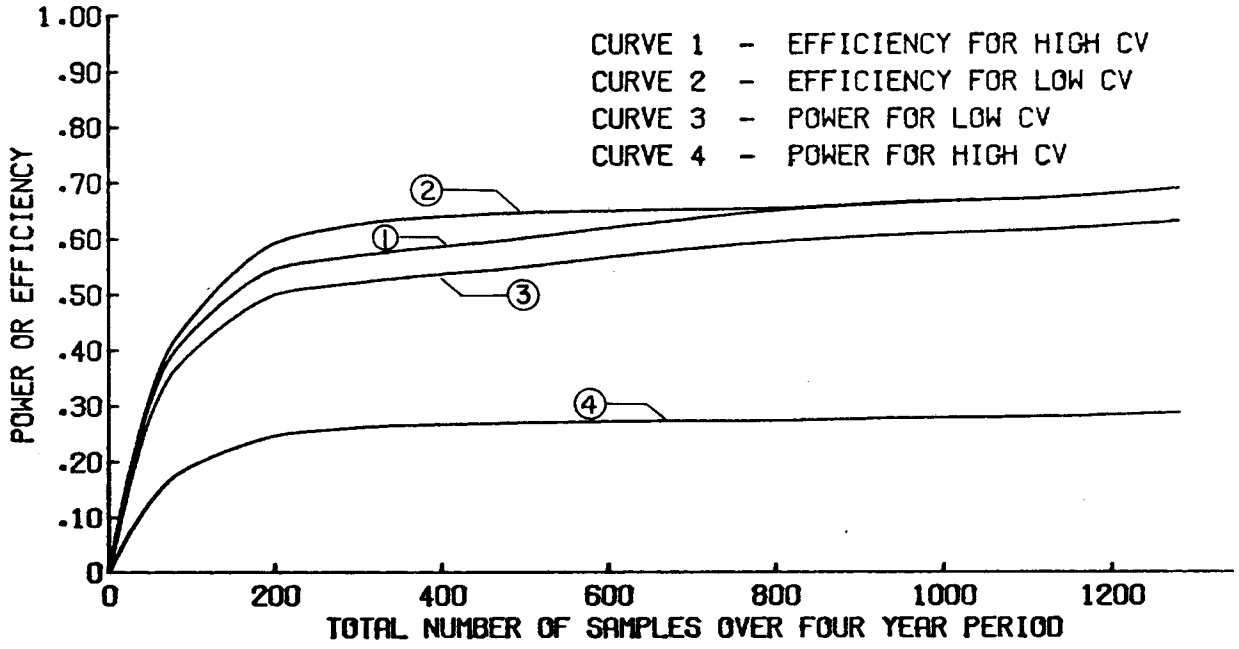

Figure 5.5. Maximum Spatial Average Power and Efficiency vs Sample Size and Coefficient of Variation or Standard Deviation for Base Conditions

II.2. Model Parameters

Unlike historical parameters, changes in model parameters result in changes in location of the specified sample stations. In these sensitivity studies, changes in sample station location were suppressed, and are investigated separately in the following section. All the results given in this section are for the station locations of Table 5.4.

Sample network efficiencies for several stream velocities are shown in Figure 5.6 for a single station. These curves show less variation than do efficiency curves for either of the two historical parameters, even although changes of stream velocity by a factor of two above and below the base value are represented. Based on these results it may be concluded that stream velocity is not a critical design parameter for the range of parameter combinations investigated.

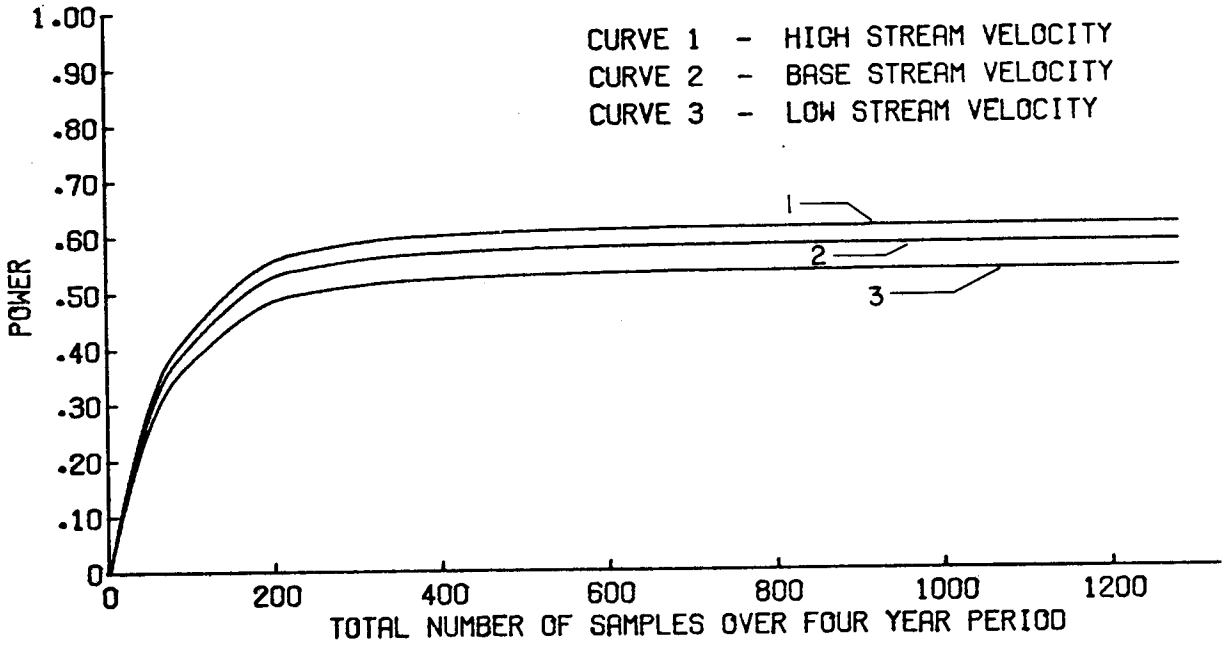

Figure 5.6. Spatial Average Power vs Sample Size and Stream Velocity for Base Conditions and One Sample Station

The results of Table 5.7b indicate that the optimal trend network efficiencies are quite insensitive to changes in measurement error and linearization trajectory except for moderate values of NSAMP where the transition to multiple sample station occurs. Even for these sample sizes, however, the maximum efficiency loss experienced was only about 5%. Based on these results, the effect of model parameter errors on network design appears to be negligible. This is especially apparent when viewed in comparison to efficiency losses resulting from an incorrect choice of the number of stations, particularly when too many stations are specified when NSAMP is small.

II.3. Design Parameters

Two parameters affecting network design are denoted design parameters. The first of these is the design trend magnitude. Two approaches to the choice of the design trend are possible. If the value of NSAMP is known, the trend magnitude should be chosen to result in a maximum power near one, say in the range 0.7 - 0.95. This choice is appropriate because design trend magnitudes which are too low result in a maximum power of near zero, which implies that very few trends of that magnitude may be detected regardless of the level of sampling effort. If trend magnitudes are specified which result in very high values of $N_T^{(M)}$ (eq. 5.5a), maximum power of essentially one results and efficiencies of near one are yielded by almost any sampling strategy even for small sampling efforts, affording no useful basis for comparison of alternate strategies.

It should again be emphasized that the measure of efficiency used

here is useful only as a basis for comparison of alternate sampling strategies for the same river basin. Efficiency comparison between river basins are not useful since the maximum power levels will vary for the same trend magnitudes because of climatological influences on the relevant time series parameters (standard deviation and lag one correlation coefficient).

In some cases the value of the design trend magnitude may be fixed by threshold values of changes for which detection is desired (Cunningham, 1970; Enviro Control, 1972). In this case, NSAMP will not be fixed, but will depend on the trend detection power desired for the given trend magnitude. In either case the sensitivity of the design network to trend magnitude is important, as it is desired that the specified network be efficient (relative to other candidate networks) over a range of possible trend magnitudes.

Figure 5.7 shows network efficiency as a function of constraint level for the "high" and "low" trend levels of Table 5.5. As expected, efficiency is highly sensitive to trend magnitude, since the dimensionless trend numbers N_T and N_T' in eqs. 4.5a and 4.12a are directly proportional to trend magnitude. The relative network efficiencies, however, are very insensitive to design trend magnitude as shown in Table 5.7b.

The remaining variable which is classified as a design parameter is sample station location. Station location is not strictly a design parameter as it is specified by the station location algorithm developed in Chapter 3. Nevertheless, if errors are made in specifying the model parameters, or if the station locations must be changed from those

determined theoretically for practical reasons (e.g. bridge or waterfront access locations) the station locations will be perturbed.

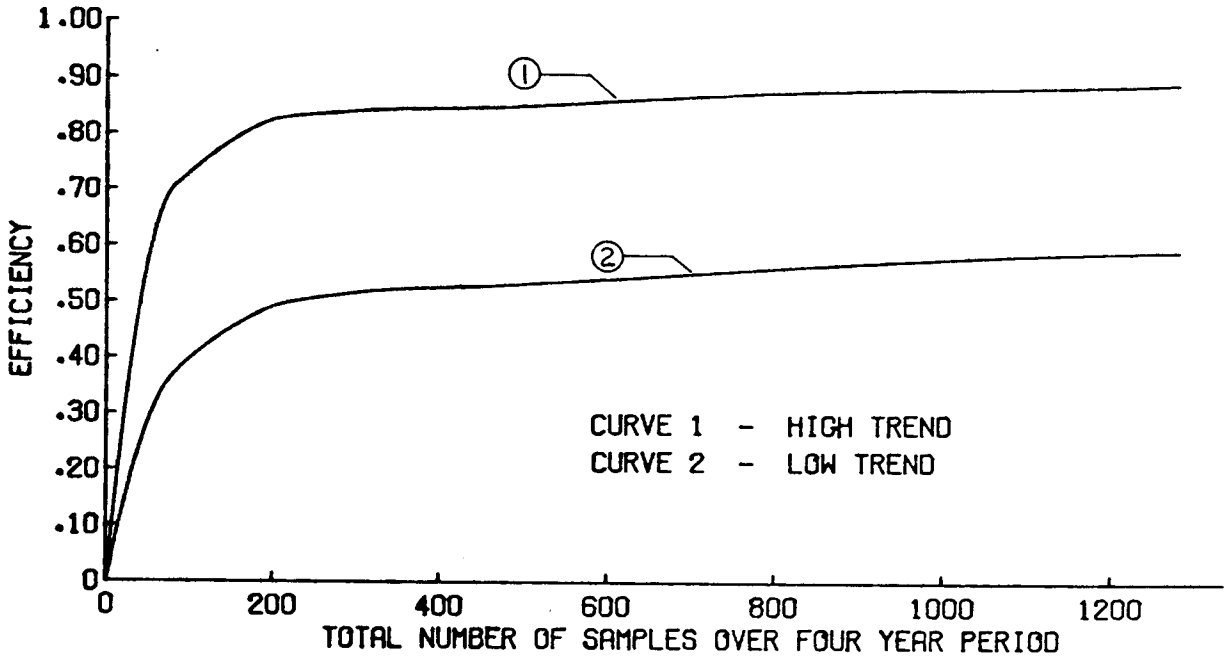

Figure 5.7. Maximum Spatial Average Efficiency vs Sample Size and Trend Magnitude for Base Conditions

Table 5.8 lists the station locations for up to six stations specified by the "low measurement error" case of Table 5.6 This class of networks in general specifies station placements further upstream than the base locations of Table 5.4. As the number of stations increases, the station locations for the two cases become nearly identical, hence, the single station case is investigated here. Table 5.9 shows efficiency losses using the base parameter values when the single station location of Table 5.8 instead of that specified by Table 5.4 is used. The losses are only about 1% for all values of constraint NSAMP investigated, implying low sensitivity of the optimal design network efficiency to station location about the base conditions.

Table 5.8 Station Locations for Low Measurement Error (river mile)

Total No. of Stations	Station # 1	2	3	4	5	6
1	57.1					
2	37.0	73.6				
3	25.5	54.6	81.0			
4	20.8	32.8	64.8	85.5		
5	17.2	35.0	54.3	70.8	87.6	
6	14.7	29.1	44.2	59.7	73.7	88.4

Table 5.9 Sensitivity Test for Errors in Station Location

NSAMP	Efficiency for large measurement error sample locations	Efficiency for small measurement error sample locations	Loss, %
80	.380	.376	1.1
200	.538	.532	1.1
320	.570	.564	1.1
480	.583	.577	1.0
640	.588	.582	1.0
800	.590	.584	1.0
960	.591	.585	1.0
1120	.592	.586	1.0
1280	.592	.586	1.0

III. Issues in Data Analysis

The principal emphasis of this work has been on the design of monitoring systems rather than the analysis of data derived from such systems. The data analysis problem is, however, an integral part of the design problem, in fact, the limited usefulness of much existing data has resulted from poor design of sampling systems. In this light, the decision was made to require fixed sample station locations and frequencies. Fixing station locations avoids the problem of analyzing inhomogeneous time series, i.e., those whose elements may be drawn from different statistical populations. Setting constant sample frequencies enhances the ease of use of such techniques as spectral analysis.

Requiring constant sample frequencies implies that data sets taken in different seasons have essentially equivalent information content. This conflicts with a tendency of some researchers to emphasize critical periods, especially low flow. The importance of low flow for such parameters as dissolved oxygen and temperature is countered by the importance of high flow periods for such other parameters as suspended solids and turbidity. In analyzing time series of water quality parameters for trend, suitable normalization techniques will allow use of high as well as low flow data, if the data are normalized to a base flow level. The author has found, for instance, that linear regression of dissolved oxygen on the logarithms of daily flow values removed almost all of the annual periodicity in dissolved oxygen data from the Spokane and Duwamish Rivers, Washington. Extraction of the six and twelve month Fourier components (Delleur, et al., 1974) from the daily water quality reported in Chapter 4 resulted in time series which were essentially time

homogeneous in level. Inhomogeneity in variance may be removed, after suitable data transformation, using the residualization techniques of Young and Pissano (1968), although homogeneity in variance is not required for use of the suggested nonparametric statistics discussed in Chapter 4.

IV. Synopsis

The network design methodology developed in the preceding chapters appears to be relatively insensitive to all design parameters except the number of stations selected to detect trends in a river basin. This result comes about because network efficiency increases rapidly with increasing sample size, whereas decreasing estimation variance by increasing the number of sample stations has essentially a second order effect on efficiency. This may be observed in the curves of Figure 5.3 which all show an inflection point after a large initial increase in efficiency. The initial rise corresponds to increasing N_T through increased sample size at a single station, the secondary rise is caused by an increase in N_T due to the reduction in estimation variance resulting from multiple sample stations. Consequently, all parameters other than those which affect the number of samples taken at each station (i.e. number of sample stations in the network) have a secondary effect for the range of parameters investigated herein.

It is important, in view of this result, to recall the basic assumption made in utilizing the state estimation approach to sample network design. It was assumed that, given a measurement or set of measurements and a model of the interactions of the state variables, as estimate could be made of the vector of state variables at any point in the stream, and that the variance of the estimate could be specified at

any given point. Hence, at any arbitrary point, given the time series of observations at the specified sample stations, an estimated time series of the state vector can be formed, which may be assessed for trend. The results of this section indicate that the optimal (satisficing) sample network will have a small number of stations (in many cases a single station) when constraint levels are low.

This result suggests the necessity to use a water quality model when constraint levels are low. At present water quality models are virtually unused as a method of augmenting time series of water quality variables. Consequently, the cost of using and updating parameters for a water quality model must be weighed against the cost of increasing the constraint level.

Another important implication of the results presented in this chapter is the relative insensitivity of network design efficiency to sample station location. This result confirms the original decision to attempt to satisfice rather than optimize station locations. The station location algorithm does not attempt to minimize average variance over the river basin, which would be necessary to achieve a strict optimum in average trend detectability. In fact, the relative insensitivity of network trend detection power to station location suggests that a trend network could be designed to fulfill multiple objectives with little loss in efficiency, for instance the same network might be used for trend detection as well as abatement and establishment of a data base. An example might be placing of stations in such a manner as to provide data base as well as trend information upstream and downstream of a major point source discharge which could withstand a legal test.

An example of a stream with significant reach lengths above and below a major urban area is presented in the following chapter, which illustrates application of the design methodology to the Spokane River in the vicinity of Spokane, Washington. Chapter 7 illustrates an application to the Snohomish River basin, Washington, a basin with several substantial tributaries, unlike both the Spokane and the hypothetical stream investigated in this chapter.

CHAPTER 6

MONITORING SYSTEM DESIGN FOR SPOKANE RIVER

The Spokane River, which drains a semiarid basin in the extreme eastern part of Washington and Northern Idaho, was chosen for the first demonstration application of the design methods presented in Chapters 2-4. Only that part of the Spokane located between its source at Lake Couer d'Alene (USGS river mile 110.6) and its confluence with the Little Spokane River (river mile 56.2) were included in the study (see Figure 6.1). The lower boundary was chosen because the river below river mile 56.2 is in the influence of the backwater of Long Lake, hence is not free-flowing as required in this research.

The stretch of interest has only one tributary which is not dry during all but the late winter and early spring months. This tributary is Hangman Creek, which drains an area of 689 square miles south of the Spokane basin. The mean annual flow of Hangman Creek is less than 5% of that of the Spokane. Instream quality measurements provided by the U. S. Army Corps of Engineers and Kennedy-Tudor Consulting Engineers, Inc. (Kennedy-Tudor, 1974) indicated that the quality of Hangman Creek during normal conditions is at least as good as that of the Spokane, hence, based on the relative flow volumes, sampling of Hangman Creek was not included in the design objective, which was to design a trend detection network for the Spokane River main stem.

In general, the soil in the Spokane basin is sandy and percolates very well, making overland flow and interflow negligible in all but extremely large storms. Groundwater inflows to the river are substantial and

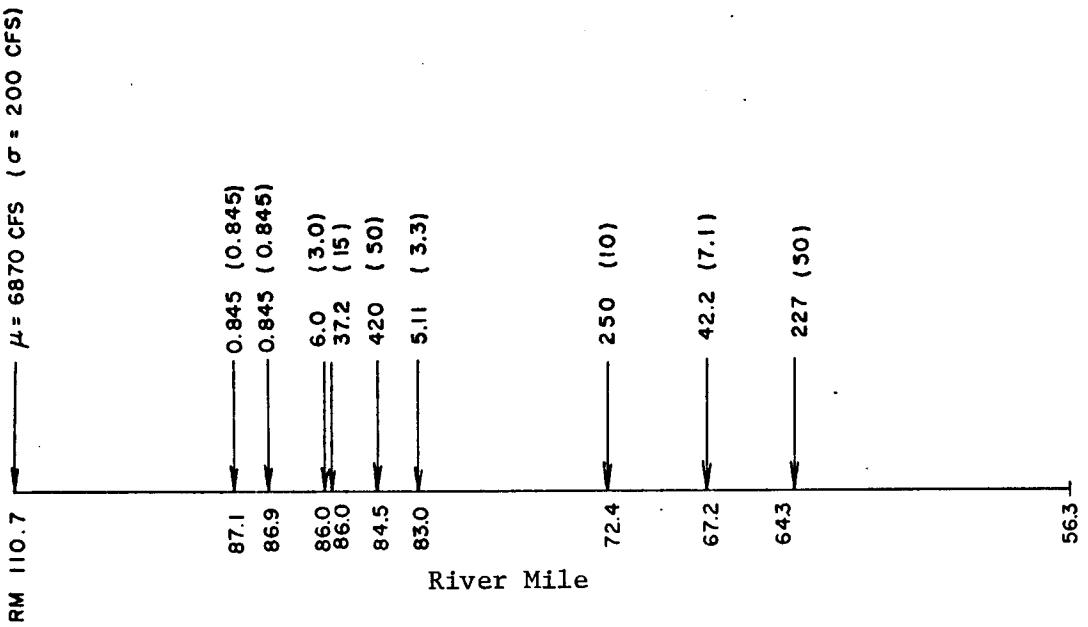

Figure 6.1 Spokane River Study Stretch with Point Source Flow Magnitudes and Standard Deviations

constitute most of the flow during the dry season. Because of the lack of significant tributaries, the influence of nonpoint sources is small except during extreme storm events.

Systems Control, Inc. (Finnemore and Shepherd, 1974) conducted a study of the Spokane River for the Environmental Protection Agency in which several water quality models were tested for applicability. Most of the effort was spent on developing the DOSCI steady state stream model, a deterministic model which formed the basis for the stochastic model developed in Appendix A. The mean parameter values used in this chapter (see Appendix C) were taken from the Systems Control, Inc. study. More recently, Hydrocomp, Inc., and Kennedy-Tudor Consulting Engineers conducted a comprehensive water resource management study of the Spokane basin in which the Hydrocomp Simulation Package (HSP) (Hydrocomp International, 1969)

used. As part of this study, instream quality data were taken at several stations on the Spokane River at four hour intervals for the period September 18-20, 1973 and June 11-12, 1974. The September 1973 data were taken during one of the lowest flow periods on record and included the first substantial rainfall in several months. Consequently, the data, while providing an excellent "worst case" record, are of little use in establishing the "average" trajectory needed for this work. The June, 1974 data were taken during a period which reflected much more nearly average flow and quality conditions. The data collected during this period are reproduced in Appendix C and were used as the linearization trajectory. A straight line fit, rather than a polynomial fit as used in Chapter 5, was used in establishing the linearization trajectory. This choice was made because the polynomial fit often resulted in large peaks and valleys in the trajectory between sample points, rather than a smooth curve (see Figure 6.2)

Data on point source discharges were provided by Kennedy-Tudor, Inc., and are given in Appendix C. Most of the discharges are located in the Spokane Valley upstream of the city proper. Groundwater data provided by Kennedy-Tudor were modelled as two point sources. The discharge volumes and locations are given in Table 6.1. The largest point source discharge is the Spokane Sewage Treatment Plant, and is the only discharge (excluding groundwater) located downstream of the city.

Stream velocity throughout the basin is relatively high. Based on a value of Manning's of 0.038 (Barnes, 1967), a mean stream depth (hydraulic radius) of 8 feet, and a bottom slope of 0.0015, a velocity of about 100 miles/day was calculated. At this velocity, the time of passage through the river basin is only about half a day, hence

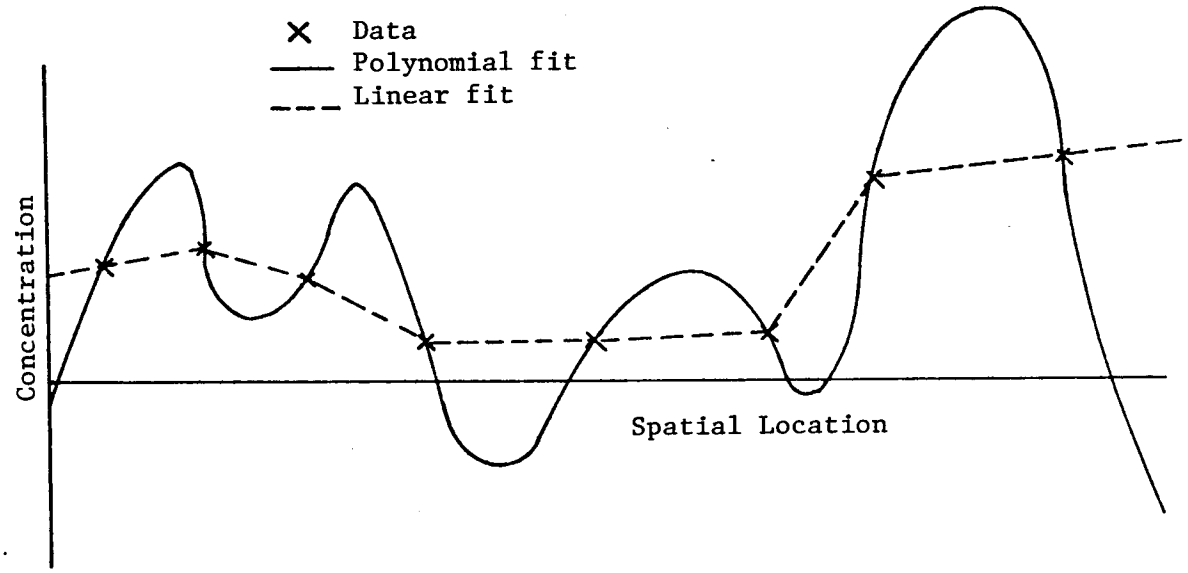

Figure 6.2. Polynomial and Linear Fits to Typical Linearization Trajectory

Table 6.1 Spokane River Discharge Locations and Flows

River Mile	Description	Flow (cfs)
87.1	Hillyard Processing	0.845
86.9	Spokane Industrial Park	0.845
86.0	Kaiser-Mead	6.0
86.0	Kaiser-Trentwood	37.2
84.5	Upper Spokane Groundwater	420
83.6	Inland Empire Paper Co.	5.11
72.4	Hangman Creek	250
67.2	Spokane Sewage Treatment Plant	42
64.3	Lower Spokane Groundwater	227

constituent dynamic interactions are relatively unimportant and may be considered nearly conservative. Consequently, prediction variances do not propagate rapidly, and are affected primarily by advective (point) sources.

Sample station locations were calculated in the same manner as used in Chapter 5 for up to eight stations. The station locations are reported in Table 6.2. Cunningham (1970) suggested that four stations be located on the Spokane. Station placement was to be between major point source discharges, hence station 1 was to be above river mile 87.1, station 2 between RM 83.0 and 86.0, station 3 between RM 67.2 and 83.0, and station 4 below RM 67.2. These station placements are nearly the same as those listed in Table 6.2 for the case of four stations, except that the algorithm used in this work specifies that two stations, rather than one should be located above the principal point sources in the Spokane Valley. The results of Chapter 5 indicate, however, that the

Table 6.2. Candidate Sample Station Locations for Spokane River (river mile)

No. of Stations	Station No. 1	2	3	4	5	6	7	8
1	86.1							
2	95.6	74.3						
3	100.0	85.3	69.2					
4	100.8	87.8	75.9	65.3				
5	102.7	92.2	81.8	72.0	63.9			
6	103.7	94.6	85.1	76.9	68.8	62.5		
7	104.7	96.8	88.5	81.1	73.9	67.1	61.8	
8	105.2	99.0	92.6	85.4	79.0	72.4	66.4	61.4

change in trend detection efficiency is negligible for such a small perturbation in station location, hence the locations proposed by Cunningham could be used if four stations were desired.

The question of how many stations should be specified is much more critical than that of station location. Figures 6.3 and 6.4 show, in the same manner as the results of Chapter 5, the maximum average efficiency as a function of total samples taken over a four year period. Coefficients of variation and lag one correlations for an assumed lag one Markov model are identical to those of Table 5.6. Trend magnitudes are identical to those of Table 5.5.

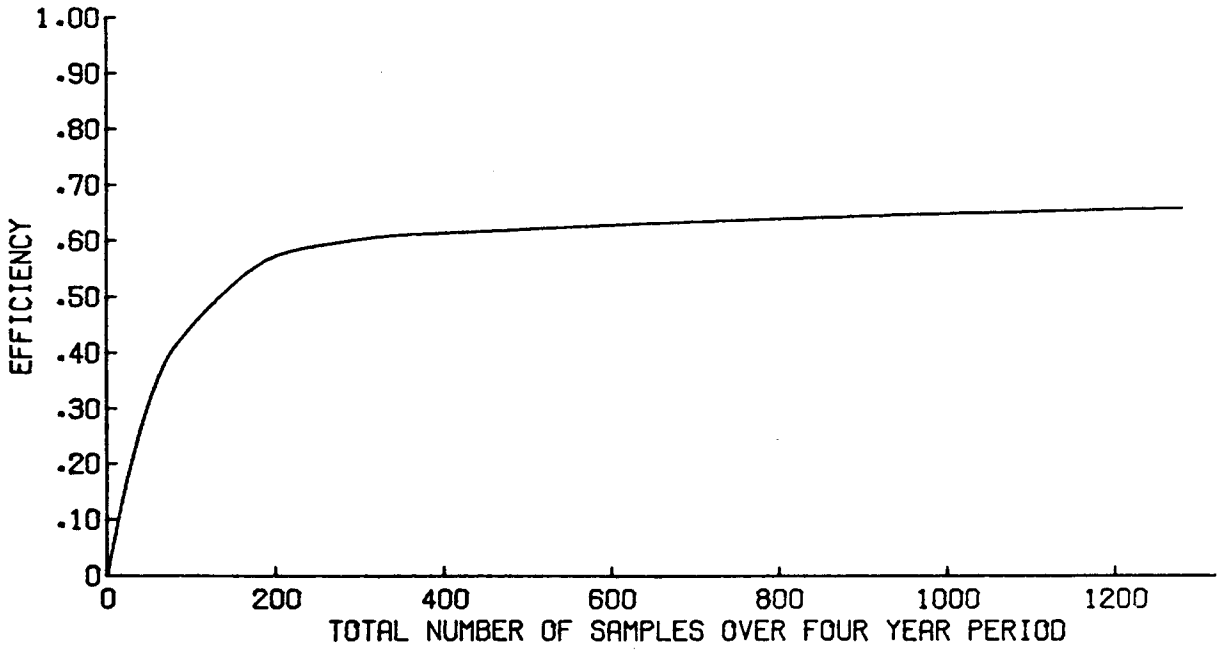

Figure 6.3 Maximum Spatial Average Efficiency vs. Sample Frequency for Spokane River Trend Network

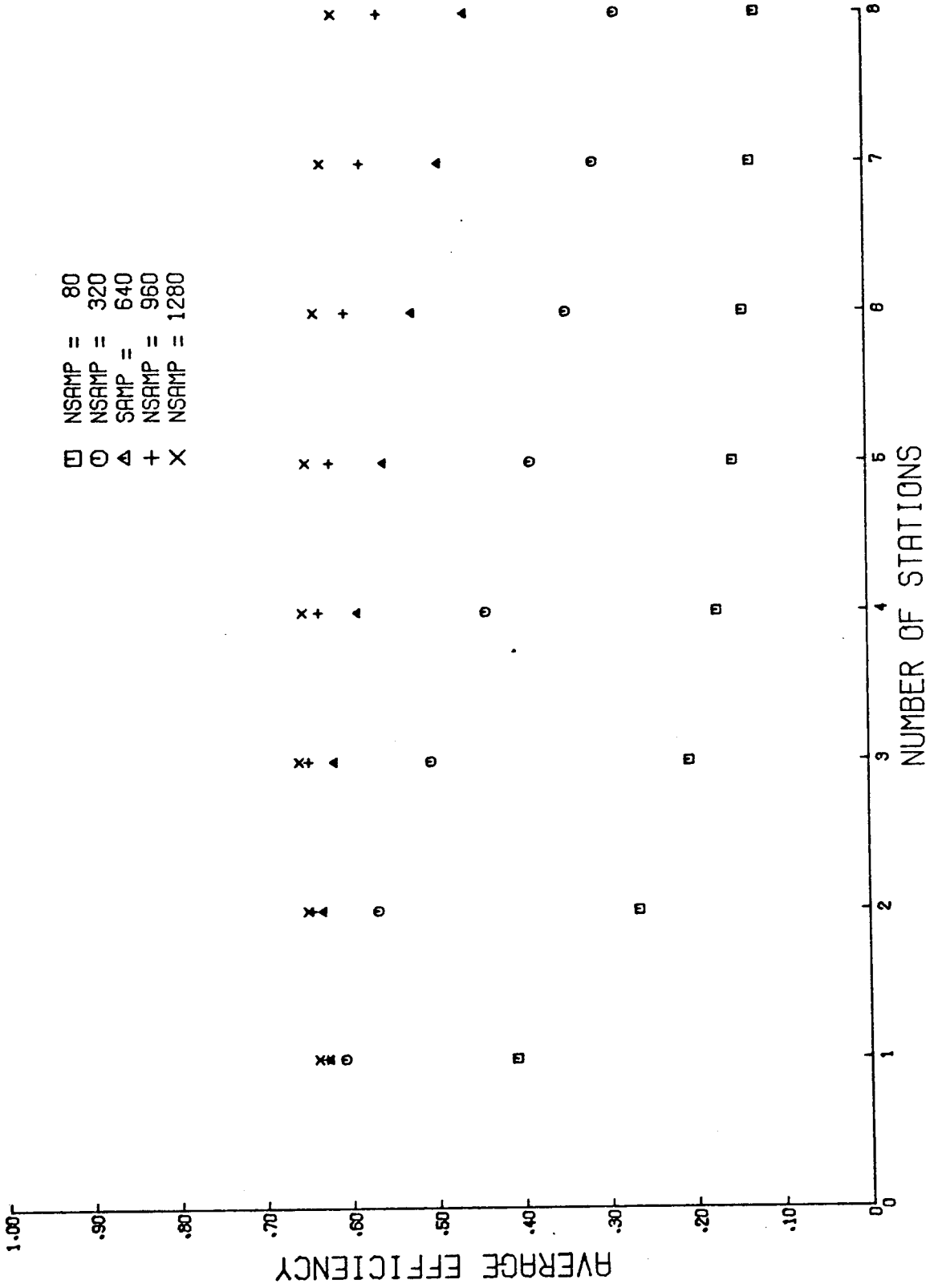

Figure 6.4 Spatial Average Efficiency vs. Number of Stations and Sample Frequency for Spokane River

The results summarized in Figures 6.3 and 6.4 may now be compared with the sampling program proposed for the Spokane River by Cunningham (1970). Cunningham suggested a single ambient water quality monitoring network for three purposes: establishment of water quality standards, implementation and enforcement of water quality standards, and basin planning. The basin planning objective requires trend identification.

The sample program proposed by Cunningham (1970) specified that bi-weekly samples be taken at each of the four stations one year in three. From a trend detection standpoint, a more efficient sample allocation is to take samples at equal intervals over the four year period, because the ratio of equivalent independent samples to actual samples (Figures 4.11 and 4.12) is higher if temporal sample spacing is larger. The equivalent constraint value, then, is NSAMP = 4 x 24 x 4 x 1/3 = 128 samples over the four year period. Interpolating in Figure 6.4, it can be seen that this constraint level is too low to support four stations, in fact efficiency losses will be great if more than one station is used. The present constraint level must be at least tripled to allow efficient operation of two stations, and must be increased by a factor of approximately six to allow efficient operation of four stations.

It should be emphasized that the network proposed by Cunningham has multiple objectives, whereas the network proposed in this chapter has the single objective of trend detection. The additional objectives considered by Cunningham of establishing and implementing water quality standards may be met equally as well, however, by use of a water quality model (calibrated and verified on the basis of an intensive monitoring program separate from the ambient monitoring network) in conjunction with measurements taken at the trend network station(s). Consequently, since

substantial efficiency losses result from utilizing four sample stations rather than one, it is recommended that unless the constraint level (NSAMP) can be increased to about 300, only one sample station be used to characterize the river basin.

CHAPTER 7

MONITORING SYSTEM DESIGN FOR SNOHOMISH RIVER BASIN

The Snohomish River basin was selected for a second demonstration application of the methods developed in this work. In contrast to the Spokane, the Snohomish basin includes two major tributaries (the Snoqualmie and Skykomish Rivers) and several smaller tributaries. The Snohomish basin network is shown schematically in Figure 7.1. Also in

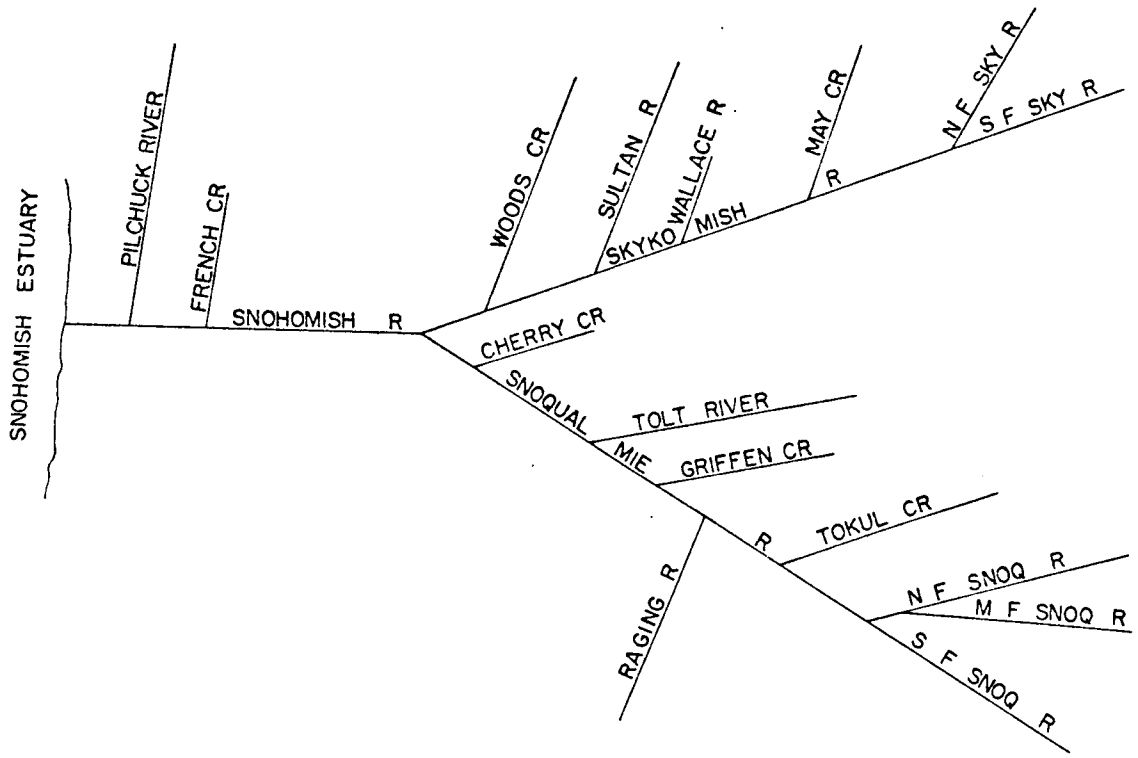

Figure 7.1. Snohomish River Network with Major Tributaries

contrast to the Spokane, the Snohomish basin is in the influence of the marine climate of Western Washington. Annual precipitation in the basin ranges from about 35 inches near the mouth of the Snohomish River to well over 100 inches along the Cascade Crest at the basin headwaters. Unlike the Spokane which has its source in Lake Couer d'Alene, the Snohomish is fed primarily from direct runoff and snowmelt. The basin is mostly heavily forested, with substantial logging operations. Agricultural uses dominate the floodplain in the lower basin.

Nonpoint sources were found, using mass balance techniques, to be the major source of pollutants in the Snohomish basin (Systems Control, Inc., and Snohomish County Planning Department, 1974). The waste discharge data used in the systems control study were provided to the author for use here, and are reported in Appendix D. A comprehensive sampling program was undertaken in the Snohomish basin in November, 1973. The results of this program provided the linearization trajectories and minor tributary constituent concentrations reported in Appendix D. Daily average flow values at several stations in the Snohomish basin for the days during which the sampling program was conducted were obtained from the U.S. Geological Survey and were compared with the historical average flows for the same stations. In general, historic means were about 20% lower than the daily average flows on the sample dates. Relative to the difference between extreme and average conditions, however (usually one or two orders of magnitude) the agreement was close enough to allow characterization of "average" conditions by the sample data.

The design objective was to specify a monitoring system which would maximize trend detection over the Snohomish-Snoqualmie-Skykomish network downstream of river mile 66.7 on the Skykomish River and downstream of

river mile 46.3 on the Snoqualmie River. The weighting function (W_j in eq. 5.1) was taken as 0.42 for the Skykomish and Snoqualmie Rivers above their confluence and 0.16 for the Snohomish River. These relative weights were chosen to approximately reflect the length and flow volumes of the three branches, however any other desired weighting technique might be selected.

The design methods applied in Chapters 5 and 6 are valid for a single river stretch. The Snohomish, with multiple stretches, requires some modification of the design approach. While such optimization methods as linear programming and dynamic programming might be applied to maximizing sample network efficiency, a more informative approach is to simply simulate the several candidate networks. This approach is feasible in a relatively simple network, especially where some of the candidates may be eliminated by inspection. Furthermore, the results of the simulations for this relatively simple network may suggest methods for handling more complex cases, discussed later in this chapter.

None of the smaller tributaries were included in the design network. Consideration of the relative flow volumes and small pollutant loads present in the smaller tributaries indicated that inclusion of sample stations on these streams would be inefficient in terms of the monitoring system objective unless constraint values, NSAMP were extremely high. If sampling objectives other than maximizing trend detection in the main network are to be considered (if, for instance, trends in some or all of the minor tributaries are to be detected) this objective may indicate that the minor tributaries be treated separately.

The candidate sample station allocations are shown in Table 7.1. For each of candidates 2-10, zero and one sample station, respectively,

were postulated on the Snohomish River below the Skykomish-Snoqualmie confluence (candidates 11-19). Table 7.2 lists the station locations for each candidate.

For each fixed number of total stations, the candidate giving the maximum efficiency was chosen. These candidates are given in Table 7.3. The resulting maximum efficiencies for each level of constraint

Table 7.1. Candidate Sample Station Allocations for Snohomish River Basin

Candidate #	Snoqualmie	Skykomish	Snohomish
1	0	0	1
2(11)[a]	1	0	0(1)
3(12)	0	1	0(1)
4(13)	1	1	0(1)
5(14)	1	2	0(1)
6(15)	2	1	0(1)
7(16)	2	2	0(1)
8(17)	3	2	0(1)
9(18)	2	3	0(1)
10(19)	3	3	0(1)

[a]candidates in parentheses include one station on Snohomish River. For instance, candidates 2 and 11 are identical except for the number of stations specified on the Snohomish.

Table 7.2. Candidate Sample Station Locations (River Miles)[a]

Candidate Number	Snoqualmie 1	Snoqualmie 2	Snoqualmie 3	Skykomish 1	Skykomish 2	Skykomish 3	Snohomish
1							16.9
2	21.2						
3				46.0			
4	21.2			46.0			
5	21.2			52.6	35.7		
6	30.0	13.8		46.0			
7	30.0	13.8					
8	34.5	22.0	10.4	52.6	35.7		
9	30.0	13.8		56.4	43.9	31.6	
10	34.5	22.0	10.4	56.4	43.9	31.6	
11	21.2						16.9
12				46.0			17.0
13	21.2			46.0			16.9
14	21.2			52.6	35.7		17.0
15	30.0	13.8		46.0			16.9
16	30.0	13.8		52.6	35.7		16.8
17	34.5	33.0	10.4	52.6	43.9	31.6	16.8
18	30.0	13.8		56.4	43.9	31.6	16.8
19	34.5	22.0	10.4	56.4	43.9	31.6	16.7

[a]candidates are same as listed in Table 7.1, which gives numbers of stations on each tributary for each candidate.

Table 7.3. Preferred Sample Station Allocations

Total Stations	Candidate #
1	2
2	4
3	6
4	7
5	8
6	9
7	19

NSAMP and for each number of total stations are plotted in Figures 7.2 and 7.3, respectively. The results are seen to be very similar to

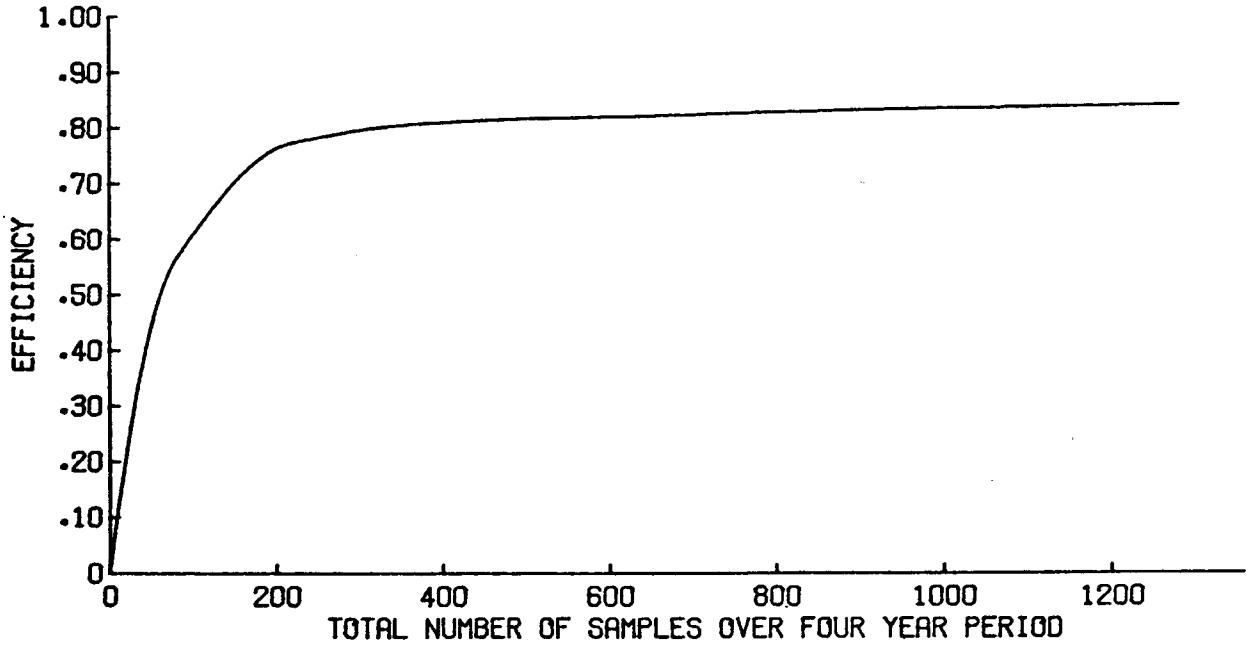

Figure 7.2 Maximum Spatial Average Efficiency vs. Sample Frequency for Snohomish River Trend Network

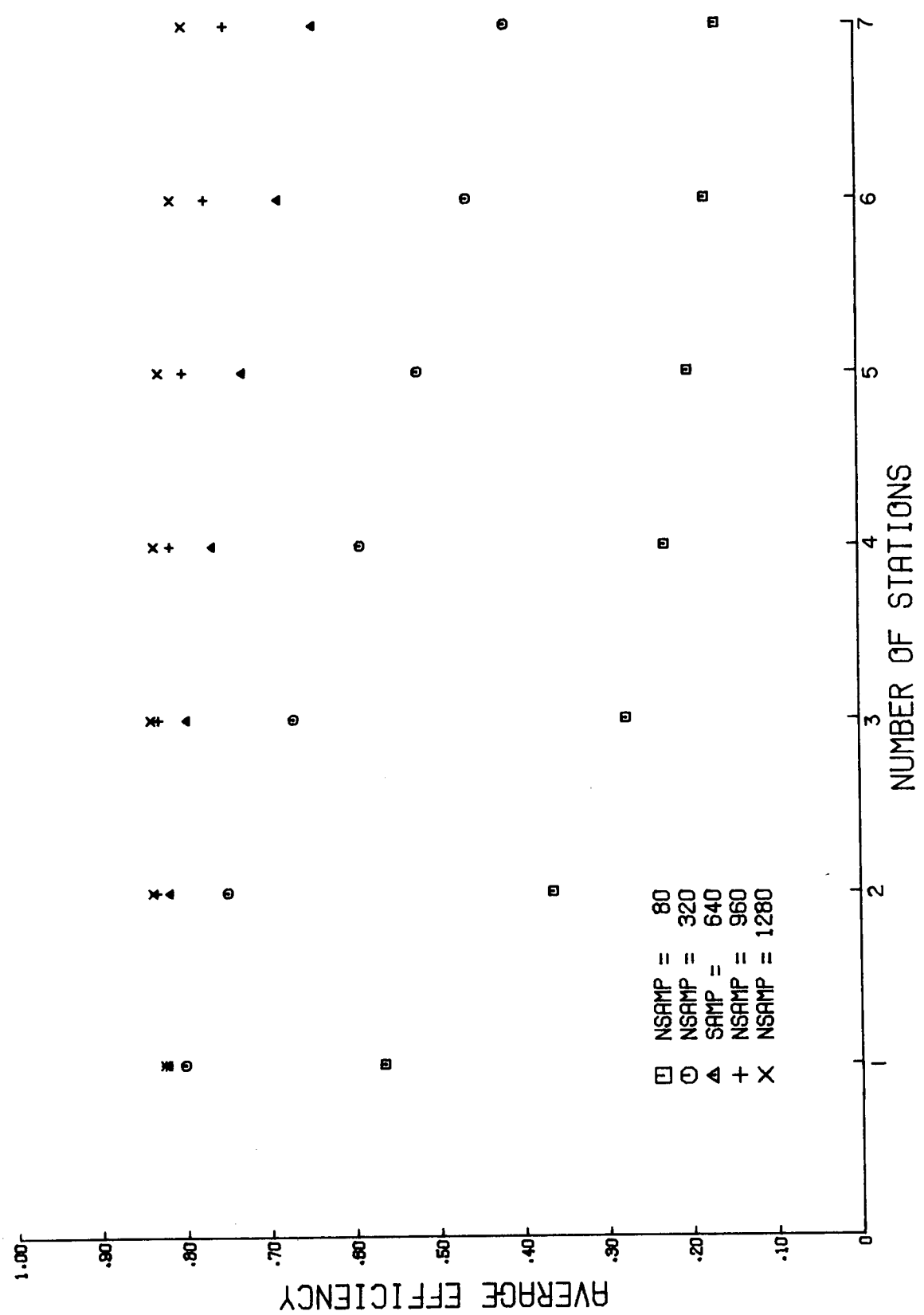

Figure 7.3 Spatial Average Efficiency vs. Number of Stations and Sample Frequency for Snohomish River Basin

those presented in Chapters 5 and 6, specifically choosing the correct number of stations (usually one) is very important when constraint levels are low. Again, station location was found to have a second order effect on efficiency. For instance, for the total number of stations set at three, the resulting efficiencies for the three candidate configurations are given in Table 7.4. The differences are small, suggesting again that station location is not nearly so critical as proper selection of the total number of stations.

Table 7.4. Efficiencies for Three Candidate Station Allocations Specifying Three Stations Total

NSAMP	Candidate # 5	6	13
80	.275	.276	.273
200	.523	.525	.519
320	.668	.670	.663
480	.756	.758	.750
640	.794	.796	.788
800	.814	.816	.808
960	.825	.830	.819
1120	.832	.835	.826
1280	.836	.839	.831

The secondary effect of station location implies that a sophisticated optimization technique for allocating sample stations among river network branches is not merited. The small differences in efficiencies for the various allocations compared in Table 7.4 suggests that a more

straightforward approach might be to allocate stations apriori, perhaps based on a relative comparison of tributaries on the basis of flow value, mean constituent concentrations, and economic importance of water quality in each tributary. Choice between candidates could then be made on the basis of trend detection efficiency as was done here. The satisficing network selected using this method will have almost the same efficiency as would one selected using a sophisticated (and probably costly) global optimization.

Cunningham (1970) proposed that 11 stations be located on the stretches of the Snohomish, Skykomish, and Snoqualmie Rivers included in this study. Additional stations to be located on the minor tributaries are not included in this total. Sampling was to be as proposed for the Spokane basin, semimonthly sampling one year in three. This indicates a constraint level of 4 x 1/3 x 11 x 48 = 704 samples over a four year base period for the entire basin. Interpolating in Figure 7.3, at most three stations can be supported at this constraint level. Two of these stations should be located on the Snoqualmie and one on the Skykomish. The station location algorithm specifies that the stations on the Snoqualmie be located at river miles 30.0 and 13.8 and that the station on the Skykomish be located at river mile 46.0. It is not critical that these station locations be used, however it is important that three stations be specified, rather than the larger number suggested in the earlier work.

It should again be emphasized that the monitoring network proposed by Cunningham is based on multiple objectives (see Chapter 6), rather than the single trend detection objective considered here. However, it appears that the additional objectives considered by Cunningham

can be accommodated equally as well by a small number of stations, and it is recommended that a maximum of three stations be included in the proposed network for the Snohomish River basin.

CHAPTER 8

SUMMARY

The purpose of this research has been to develop a method for the design of stream quality monitoring networks for trend detection. Alternate objectives, such as abatement, were investigated and were found to be either unfeasible or best handled through intensive monitoring programs, for which design methods are presently available. An approach is provided here which yields both spatial sample station locations and temporal sample frequencies for a given constraint, f_c, on the total number of samples which may be taken in a given time period for a specified river basin. In addition, a relative efficiency measure is provided which enables comparison of system performance at different constraint levels f_c. A review of the literature showed that, although most ambient water quality monitoring networks have explicitly or implicitly the primary objective of detecting trends, this objective has not previously been included analytically in a design formulation.

A segmented approach was taken and the problem was partitioned into the two subproblems of spatial station location and temporal frequency specification. Choice of the temporal sample frequency required consideration of the power or probability of detecting a trend (given its existence) for fixed trend magnitude, record length, and sample standard deviation. A complication resulted from dependence which exists in time series of measurements of water quality parameters.

Normalized power curves were derived based on an assumption of independence of the data set for two nonparametric tests (Spearman's

rho and Mann Whitney's tests) for linear and step trends. A method was developed which allowed application of these curves to dependent time series using an equivalent independent sample size. Use of the normalized power curves requires the standard deviation of the time series, in addition to knowledge of the sample size, correlation structure of the time series, and trend magnitude. The theoretical development was based on population values; in practice sample statistics may be used if proper account is taken of persistence in the time series from which the statistics are estimated. Nonparametric tests were used in this development because of their robustness to slight changes in the underlying probability distribution of the data set, nominally assumed to be Gaussian.

State estimation theory provided the link between the two subproblems. The time series variance is composed of two parts, an historical component which may be attributed primarily to meteorological variation, and a measurement and prediction component which results from measurement error and (if detection is desired at points where no sample station is located) errors in predicting water quality based on a measurement at the nearest upstream station. The measurement and prediction variance (standard deviation) is required in both the setting of sample station locations and in determining trend detection power. Measurement and prediction variances were estimated using Kalman filter methods and a knowledge of the dynamics relating water quality constituents in time. An approach combining use of the normalized power curves (modified to admit dependent samples) with the variance propagation trajectory (determined using the Kalman filter approach) allowed comparison of trend detection powers for various sampling strategies for fixed total sample size. The

comparisons were made on the basis of spatial average powers computed for each river reach and weighted to give a basin average power. Demonstration applications were provided for two Washington streams, the Spokane and Snohomish Rivers.

I. Conclusions

Four principal conclusions were suggested by the research reported in this dissertation:

1. It was shown that an earlier theoretical development by Bayley and Hammersley (1946) which allows computation of an equivalent independent sample size from an autocorrelated time series may be extended to allow normalized power curves derived for independent samples to be used in the dependent case, specifically for autocorrelated time series. For time series with a finite span of dependence (i.e., $\sum_{i=1}^{\infty} \rho_i < \infty$) this result was shown to have several striking implications. Since, for such models, there is an upper limit on the equivalent independent sample size over a given time horizon, a limit also exists on the maximum available power in trend detection for a time series of observations collected over this horizon, regardless of how many samples are taken.

Depending on the size of the trend magnitude to time series standard deviation ratio, this maximum power may be substantially less than one. Regardless of the stated objectives of a monitoring system, this result imposes a physical bound which dictates that it will be essentially impossible to detect trends of small magnitude over a short period of time for moderate (i.e., on the order of one) values of the trend to standard deviation ratio, even if an infinite number of samples are taken. This result is quite general and holds for all time series models having at least an exponential decay in the autocorrelation

function, and includes, for instance, the class of autoregressive moving average (ARMA) models frequently used in time series analysis.

2. When maximization of spatial average trend detection power is taken as the objective of a monitoring network, location of the sample stations is relatively unimportant. This insensitivity resulted when state estimation techniques (specifically an optimally driven filter) were used to yield measurement and prediction variances in estimates of water quality constituents based on measurements at upstream stations, and was observed in both demonstration applications. The physical sample station location controls only the measurement and prediction error variance at each point along the stream. This measurement and prediction error variance must be added to the natural (meteorologically driven) variance to yield the total variance in the estimated time series of water quality (state) variables at each point. Since the natural variance at each point is unaffected by station location, the location of the stations, especially in cases where measurement and prediction error is relatively low, may have little effect on trend detectability. The tradeoff in variance reduction between placing a station far upstream as opposed to the resulting downstream growth in variance also tends to reduced the sensitivity of spatial trend detectability to station location (see Figure 2.3).

3. Spatial average trend detection power is highly sensitive to the number of sample stations, when the total sample size is fixed. If the constraint on sample size, f_c, is relatively small (generally less than about 50 samples per year for an entire basin) it is usually much more efficient to use a single station with a relatively high sample frequency than to use multiple stations with correspondingly lower frequencies. Most of the present sampling effort in Washington State,

and in particular the ambient monitoring networks for the two demonstration streams, falls into this category. Only at substantially larger constraint levels can multiple stations be supported. This result comes about because trend detection power increases more rapidly with increased effective independent sample size than with the alternate reduction in standard deviation of the time series (achieved by a lower frequency of measurement at multiple stations) until the maximum effective independent sample size has almost been reached at each station. The best trend detection network, then, is essentially the network containing the maximum number of stations for which the maximum effective independent sample size has been nearly (say $n/n_{max} \sim 0.9$) reached at each station. If the constraint level is too low to reach this level, a single station must be used. As a very rough rule of thumb, it appears that for correlation coefficients in the range of those calculated from the observed data ($\rho \sim 0.75$-0.90) sample frequencies should be approximately weekly at each station.

4. Because constraint levels, f_c, for ambient water quality monitoring are presently quite low (often on the order of magnitude of 50-100 per constituent per year for an entire river basin) the use of water quality models to augment measured data is essential. Modelling becomes less necessary as constraint levels increase, since the number of sample stations increases with constraint level, requiring less sophisticated approaches to extrapolating and interpolating data between measurement stations. The Kalman filter formulation will be extremely helpful in data augmentation, because it allows direct incorporation of measured values and knowledge of the dynamics of parameter interactions. In addition, the same filter model used to describe variance propagation in the design stage may be used to augment data in the collection stage.

Although this research has not examined the question of the level of sophistication required in water quality modelling, it appears that, based on experience with the two demonstration streams, water quality in Washington Streams is governed primarily by advective process and that relatively simple models might suffice for description of water quality variable interactions.

II. Recommendations

This work has served to raise a number of questions not apparent to the author when this research was initiated. The most significant of these are suggested here as recommendations for future research.

A general comment regarding approaches to the utilization of water quality data appears warranted. At present, handling of water quality data is characterized primarily by an apparent quest for quantity rather than utility. Much might be learned from the approaches to data analysis used in the closely related field of water quantity management. In general, the statistical tools developed and/or used by the hydrologic time series analyst have not been brought to bear on water quality data analysis. Several reasons for this are obvious, for instance, water quality assessment requires a multivariate rather than a univariate approach, making data handling problems much more voluminous. In addition, examples of statistical stationarity, the basis for most hydrologic studies, are the exception rather than the rule in water quality time series. Finally, record lengths are, generally, much shorter for water quality parameters as opposed to streamflow measurements. Nevertheless, attempts to build statistical models of water quality time series could prove extremely helpful in gaining insight into the time dependence of water quality variables. For instance, the use of statistical techniques,

particularly for trend analysis of ambient water quality is essential to meaningful action on waste discharge permit renewals; there is no evidence that such analysis is presently used. Beyond the use of statistical techniques for trend detection, regionalization methods could prove extremely helpful in assessing the level and variability of water quality variables in data deficient basins, especially given the severe budget constraints often faced by managing agencies.

The approach suggested by the results of this work of incorporating statistical methods with physical models will probably be necessary before much more progress can be made in assessing changes in the aquatic environment. The necessary changes in approach could probably be included within the framework of existing water quality monitoring programs. The physical modelling required could be based on intensive surveys presently used by most water quality managing agencies. These surveys could provide, periodically, sufficient data to calibrate a water quality model of any given river basin. The model could then be used to augment the data collected in an ambient monitoring program at points of interest where measurements were not taken. Periodic recalibration could be used to correct for nonstationarity in the dynamic interactions. There do not appear to be any conceptual difficulties in implementing such an approach at present, the problem is more one of the volume of work required and the general change in approach to monitoring which is necessary.

Beyond this general recommendation for implementation of the results of this work several specific recommendations for further research are included here.

1. The problem of sample station location merits further investigation. Since basin wide trend detectability is relatively insensitive to station location, the stations may be located to satisfy alternative requirements so long as the required number of stations are used. The method of station location proposed by Sanders (1974) might be used. His approach has the advantage that mixing characteristics are included, which would be an apparent improvement over the one dimensional flow assumption made in this research.

2. A more comprehensive survey of dependence in time series of water quality parameters should be undertaken. For instance, can such time series be adequately described in general by low lag autoregressive models? In addition, some regionalization of parameters would be extremely helpful, for instance coefficients of variation and lag one correlation coefficients might be regionalized to enable design of monitoring systems for data-deficient basins.

3. Extension of the method proposed in this research to multidimensional flow conditions would enable use of the design method for estuaries and impoundments. The principal change required would be to model the variance propagation as a smoothing rather than a filtering problem. This approach would be required since estuaries and impoundments do not have flow regimes which readily enable transformation from temporal to spatial domains. Alternately, the use of multidimensional random field theory (Rodriquez and Mejia, 1974) might be used to describe the multidimensional variance contours associated with different sampling strategies. The statistical part of this work could then be utilized essentially intact to determine optimal sampling strategies.

4. The use of state estimation theory should be investigated for application to area intensive water quality surveys. Station location is far more critical in such surveys than in ambient networks, since no model normally exists to augment such data, or, if one exists, the data collection program is often performed for the purpose of calibrating the model. In such cases measurement sites should be based on the relative information provided by successive measurements. Such a measure is provided by the relative magnitudes of the prediction variances at sample points by the Kalman filter.

5. A comparison should be made of commonly used water quality models based on their predictive capabilities. Such an approach will be essential if increased utility is to be extracted from water quality models in data augmentation. Many operational water quality models presently exist, covering a wide range of complexity. Calibration and operation costs are usually proportional to the level of complexity, making it desirable to select the least complex model which will perform adequately under specified conditions. It is commonly assumed that predictive capability increases with conceptual accuracy. The results shown in Appendix A for the attempted use of Raphael's (1962) model for temperature prediction show that this is not always the case. A comparison of different models based on several extensive data sets would be extremely useful to modellers in determining the complexity necessary in modelling water quality interactions. However, such a comparison should not be made solely on the basis of the ability of the models to "fit" the data, as more complex models, properly calibrated, may always be expected to yield better fits, due to the greater number of adjustable parameters. A more useful comparison would be to examine prediction variances of the different

models using either a number of test traces of stochastic sequences of data sets or theoretically through a Kalman filter adaptation of each of the models.

6. This work has considered allocation of sampling effort within a given river basin for a set constraint, f_c, on the sampling effort for that basin. In practice, a managing agency must allocate its sampling budget on, for instance, a statewide basis to arrive at f_c values for each river basin. This allocation problem is probably not amenable to a purely technical solution as provided for the intra-basin allocation problem studied here. A multiple objective optimization will most likely be required.

7. The constraint level, f_c, on basin-wide sample frequency has been taken as fixed in this research, although efficiency response of trend detection to the constraint level has been provided. The choice of a fixed constraint level is compatible with budget constraints experienced by managing agencies. However, given the opportunity to allocate more funds to monitoring efforts, it may be useful to examine the possible existence of an optimal level of f_c. The optimal level would require assessment of the relative costs of modelling as opposed to monitoring for trend assessment, for instance relatively little (or no) modelling effort is required if extensive monitoring is performed while extensive modelling may allow relatively low monitoring effort.

8. This research has demonstrated an approach to design of trend detection networks for streams. The approach is relatively straightforward, and with some modifications (for instance regional summarization of results might avoid the necessity for computing variance trajectories for each river reach) is capable of direct implementation. Unfortunately,

long time lags have often been observed between development and implementation of applied research as a result of lack of adequate technology transfer. The time lag could best be reduced by a demonstration application to a regional or statewide ambient water quality monitoring program. Such a demonstration application is strongly recommended.

References Cited

Arnold, J. C., "A Markovian Sampling Policy Applied to Water Quality Monitoring of Streams," Biometrics, Vol. 26, No. 6, Dec., 1970, pp. 739-747.

Atkinson, A. C., and Hunter W. G., "The Design of Experiments for Parameter Estimation," Technometrics, Vol. 10, No. 2, May, 1968, pp. 271-289.

Barnes, H. H., "Roughness Characteristics of Natural Channels," Water Supply Paper No. 1949, U.S. Geological Survey, Washington, D.C., 1967.

Bayley, G. U., and Hammersley, J. M., "The Effective Number of Independent Observations in an Autocorrelated Time Series," Journal of the Royal Statistical Society, Vol. 8(1-B), 1946, pp. 184-197.

Berthouex, P. M., and Hunter, W. G., "Problems Associated with Planning BOD Experiments," Journal of the Sanitary Engineering Division, ASCE, Vol. 97, No. SA3, June, 1971a, pp. 333-344.

Berthouex, P. M., and Hunter, W. G., "Statistical Experimental Design: BOD Tests," Journal of the Sanitary Engineering Division, ASCE, Vol. 97, No. SA4, Aug., 1971b, pp. 393-407.

Box, G. E. P. and Jenkins, G. M., Time Series Analysis Forecasting and Control, Holden-Day, San Francisco, 1970, pp. 46-82.

Box, G. E. P., and Lucas, H. L., "Design of Experiments in Non-Linear Situations," Biometrika, Vol. 46, No. 3, June, 1959, pp. 77-90.

Breiman, L., Statistics with a View towards Applications, Ch. 8: "Nonparametric One Sample Tests," Houghton Mifflin, Boston, 1973.

Burges, S. J., and Lettenmaier, D. P., "Probabilistic Methods in Stream Quality Management," Water Resources Bulletin, Vol. 11, No. 1, Feb., 1975, pp. 115-130.

Chamberlain, S. G., et al., "Quantitative Methods for Preliminary Design of Water Quality Surveillance Systems," Water Resources Bulletin, Vol. 10, No. 2, Apr., 1974, pp. 199-219.

Cleary, R. W., and Adrian, D. D., "New Analytical Solutions for Dye Diffusion Equations," Journal of the Environmental Engineering Division, ASCE, Vol. 99, No. EE3, June, 1973, pp. 213-227.

Cleveland, W. S., and Kleiner, B., "A Graphical Technique for Enhancing Scatterplots with Moving Statistics," Bell Laboratories in-house report, Murray Hill, New Jersey, 1974.

Conover, W. J., Practical Non Parametric Statistics, Wiley, New York, 1971.

Cornell, C. A., "First Order Analysis of Model and Parameter Uncertainty," Proceedings of the International Symposium on Uncertainty in Hydrologic and Water Resource Systems, Vol. 3, 1972, pp. 1245-1272.

Cox, H., "On the Estimation of State Variables and Parameters for Noisy Dynamic Systems," IEEE Transactions, Vol. AC-9, No. 1, pp. 5-13, Jan., 1964.

Crawford, N. H., and Linsley, R. K., "Digital Simulation in Hydrology: Stanford Watershed Model IV," Technical Report No. 39, Department of Civil Engineering, Stanford University.

Cunningham, R. K., "A Preliminary Evaluation of Existing Surface Water Quality Monitoring Systems of the Washington State Water Pollution Control Commission," Washington State Water Pollution Control Commission, June, 1970.

Delleur, J. W., Tao, P. C., and Kavvas, M. L., "Trade-Offs Between Practicality and Complexity of Rainfall and Runoff Time Series Models," paper presented at the Fall Annual Meeting of the American Geophysical Union, San Francisco, December, 1974.

Dixon, W. J., "Power Functions of the Sign Test and Power Efficiency for Normal Alternatives," The Annals of Mathematical Statistics, Vol. 24, 1953, pp. 467-473.

Dixon, W. J., "Power under Normality of Several Nonparametric Tests," The Annals of Mathematical Statistics, Vol. 25, 1954, pp. 610-614.

Dracup, J. A., et al., "An Assessment of Optimization Techniques as Applied to Water Resource Systems," report prepared for U. S. Dept. of the Interior, Office of Water Resources Research, Washington, D.C., Aug., 1970.

Elliot, J. M., "Statistical Analysis of Samples of Benthic Invertebrates," Scientific Publication No. 25, Freshwater Biological Association, Ambleside, Westmorland, U.K., 1971.

Enviro Control, Inc., "National Assessment of Trends in Water Quality," report to the Council on Environmental Quality, Washington, D.C., June 1972, PB 210-669.

Environmental Protection Agency, "National Water Quality Inventory, 1974 Report to the Congress," Office of Water Planning and Standards, Washington, D.C., 1974, EPA-440/9-74-001.

Fiering, M. B., and Jackson, B. B., "Synthetic Streamflows," Water Resources Monograph No. 1, American Geophysical Union, Washington, D.C., 1971.

Finnemore, E. J., and Shepherd, J. L., "Spokane River Basin Model Project," report to the Environmental Protection Agency, Seattle, Wash., 6 Vols., 1974.

Gross, A., "A Robust Confidence Interval for Location for Symmetric Long-Tailed Distributions," Proceedings of the National Academy of Sciences, Vol. 70, No. 7, July, 1973, pp. 1995-1997.

Gunnerson, C. G., "Optimizing Sampling Intervals in Tidal Estuaries," Journal of the Sanitary Engineering Division, ASCE, Vol. 92, No. SA2, Apr., 1966, pp. 103-125.

Gupta, V. L., "Information Content of Time Varying Data," Journal of the Hydraulics Division, ASCE, Vol. 99, No. HY3, Mar., 1973, pp. 383-394.

Harper, M. E., "Development and Application of a Multi-Parametric Mathematical Model of Water Quality," Ph.D. Dissertation, University of Washington, 1972.

Hayman, G. E., and Zakkula, G., "Exact Power of Mann-Whitney Test for Exponential and Rectangular Alternatives," The Annals of Mathematical Statistics, Vol. 39, 1966, pp. 945-953.

HydroComp International, "HydroComp Simulation Programming Operations Manual," Second edition, July, 1969.

Ippen, A. T., Estuary and Coastline Hydro Dynamics, McGraw-Hill, New York, 1966, pp. 576-578.

Jazwinski, A. H., "Adaptive Filtering," Proc. of the IFAC Symposium on Multivariable Control Systems, Oct., 1968, Vol. 2, pp. 1-15.

Jazwinski, A. H., Stochastic Processes and Filtering Theory, Academic Press, New York, 1970.

Kalman, R. E., "A New Approach to Linear Filtering and Prediction Problems," Transactions of the American Society of Mechanical Engineers, Journal of Basic Engineering, Vol. 82, No. 2, Mar., 1960, pp. 35-45.

Kalman, R. E., and Bucy, R. S., "New Results in Linear Filtering Theory," Transactions of the American Society of Mechanical Engineers, Journal of Basic Engineering, Vol. 83, No. 2, Mar., 1961, pp. 95-107.

Kalman, R. E., "New Methods in Wiener Filtering Theory," Proceedings of the First National Symposium on Applications of Random Function Theory and Probability, 1963, pp. 270-389.

Kennedy-Tudor Consulting Engineers, "Sampling of Water Quality for Simulation Model Calibration," Report to U.S. Army Corps of Engineers, Seattle District, Mar., 1974.

Kittrell, F. W., "A Practical Guide to Water Quality Studies of Streams," Report CWR-5, Federal Water Pollution Control Administration, Washington, D.C., 1969.

Lenton, R. L., Rodriguez-Iturbe, I., and Schaake, J. C., "The Estimation of ρ in the First Order Autoregressive Model: A Bayesian Approach," Water Resources Research, Vol. 10, No. 2, Apr., 1974, pp. 227-241.

Mandelbrot, B. B., and Wallis, J. R., "Computer Experiments with Fractional Gaussian Noises Part 2, Rescaled Ranges and Spectra," Water Resources Research, Vol. 5, No. 1, Feb., 1969, pp. 242-259.

Martin, R. D., "Robust Estimation Theory and Algorithms," Technical Report, Electrical Engineering Dept., University of Wash., to appear, 1975.

McGarty, T. P., Stochastic Systems and State Estimation, Wiley, New York, 1974.

Moore, S. F., "The Application of Linear Filter Theory to the Design and Improvement of Measurement Systems for Aquatic Environments," Ph.D. Thesis, University of California at Davis, 1971.

Moore, S. F., "Estimation Theory Applications to Design of Water Quality Monitoring Systems," Journal of the Hydraulics Division, ASCE, Vol. 99, No. HY5, May, 1973, pp. 915-931.

NUS Corporation, Cyrus Wm. Rice Div., "Design of Water Quality Surveillance Systems," Report 16090 DBT, Federal Water Quality Administration, Washington, D. C., Aug., 1970.

Perlis, H. J., and Okunseinde, B., "Multiple Kalman Filters in a Distributed Stream Monitoring System," paper presented at the Annual Conference of the Instrument Society of America, June, 1974.

Pomeroy, R. D., and Orlob, G. T., "Problems of Setting Standards and of Surveillance for Water Quality Control," Publication No. 36, California State Water Quality Control Board, Sacramento, California, May, 1967.

Raphael, J. M., "Prediction of Temperature in Rivers and Reservoirs," Journal of the Power Division, ASCE, Vol. 88, No. PO2, July, 1962, pp. 157-181.

Rodriguez-Iturbe, I., and Mejia, J. M., "The Design of Rainfall Networks in Time and Space," Water Resources Research, Vol. 10, No. 4, Aug., 1974, pp. 713-728.

Sanders, T. G., "Rational Design Criteria for a River Quality Monitoring Network," Ph.D. Dissertation, University of Massachusetts, 1974.

Sayers, W. T., "Water Quality Surveillance: The Federal-State Network," Environmental Science and Technology, Vol. 5, No. 2, Feb., 1971, pp. 114-119.

Schwartz, L., and Stear, E. B., "A Computational Comparison of Several Nonlinear Filters," IEEE Transactions, Vol. AC-13, No. 2, pp. 83-86, Feb., 1968.

Sharp, W. E., "Stream Order as a Measure of Sample Source Uncertainty," Water Resources Research, Vol. 6, No. 3, June, 1970, pp. 919-926.

Sharp, W. E., "A Topologically Optimum Water Sampling Plan for Rivers and Streams," Water Resources Research, Vol. 7, No. 6, Dec., 1971, pp. 1641-1646.

Sen, P. K., "On the Properties of U-Statistics when the Observations Are Not Independent: Part One - Estimation of Non-Serial Parameters in Some Stationary Processes," Calcutta Statistical Association Bulletin, Vol. 12, No. 47, Sept., 1963, pp. 69-92.

Sen, P. K., "Some Nonparametric Tests for m-Dependent Time Series," Journal of the American Statistical Association, Vol. 60, pp. 134-147, 1965.

Slack, K. V., et al., "Methods for Collection and Analysis of Aquatic Biological and Microbiological Samples," Book 5 Chapter A4, Techniques of Water Resources Investigations of the United States Geological Survey, USGS, Washington, D. C., 1973.

Steele, T. D., Gilroy, E. J., and Hawkinson, R. U., "Techniques for the Assessment of Areal and Temporal Variations in Streamflow Quality," U.S. Geological Survey Open File Report, Washington, D. C., 1974.

Stochastics, Inc., "Stochastic Modelling for Water Quality Management," Report 16090 DUH, Environmental Protection Agency, Washington, D.C., 1971.

Systems Control, Inc., "Use of Mathematical Models for Water Quality Planning," Water Resources Information System Technical Bulletin #3, Washington State Dept. of Ecology, 1974.

Systems Control, Inc., and Snohomish County Planning Dept., "Water Quality Management Plan for the Snohomish and Stillaguamish River Basins, Volume III: Methodology," November, 1974.

Tarter, M. E., Holcomb, R. L., and Kronmal, R. A., "After the Histogram What? A Description of New Computer Methods for Estimating the Population Density," Proceedings of the Association of Computing Machinery National Meeting, 1967, pp. 511-519.

Vanderholm, D. H., "Planning Water Quality Surveillance," Ph.D. Thesis, Dept. of Agricultural Engineering, Colorado State University, 1972.

Vanderholm, D. H., and Ward, R. C., "Data Acquisition for Water Quality Management - An analysis of Traditional Grab Sampling Methods," Proceedings of the National Symposium on Watersheds in Transition, American Water Resource Association, 1973, pp. 107-112.

Ward, R. C., "Data Acquisition Systems in Water Quality Management," Report EPA-R5-73-014, Environmental Protection Agency, Washington, D.C., May, 1973.

Ward, R. C., and Russel, L., "Data Requirements of a Water Quality Management Program," Water Resources Bulletin, Vol. 9, No. 6, Dec., 1973, pp. 1234-1248.

Ward, R. C., Nichols, S. R., and Skogerboe, G. V., "Surveillance in Water Quality Management," Journal of the Water Pollution Control Federation, Vol. 45, No. 10, Oct., 1973, pp. 2081-2087.

Ward, R. C., and Vanderholm, D. H., "Cost-Effectiveness Methodologies for Data Acquisition in Water Quality Management," Water Resources Research, Vol. 9, No. 3, June, 1973, pp. 536-545.

Wastler, T. A., "Application of Spectral Analysis to Stream and Estuary Field Surveys: I. Individual Power Spectra," Publication No. 999-WP-7, U.S. Public Health Service, Columbus, Ohio, 1963.

Watts, D. G., Discussion of "Evaluation of Seasonal Time Series Models Application to Midwest River Flow Data," by A. T. McKerchar and J. Delleur, Proc. Int. Symp. Uncertainties in Hyd. and Water Res. Systems, Vol. III, pp. 1407-1409, Dec., 1972.

Wilk, M. B., and Gnanadesikan, R., "Probability Plotting Methods for the Analysis of Data," Biometrika, Vol. 55, No. 1, pp. 1-17, 1968.

Wolman, M. G., "The Nation's Rivers," Science, Vol. 174, No. 4012, Nov. 26, 1971, pp. 905-918.

Young, K. and Pissano, W. C., "Operational Hydrology Using Residuals," Journal of the Hydraulics Division, ASCE, Vol. 94, No. HY7, pp. 909-923, July, 1968.

APPENDIX A FILTER MODELS OF A STREAM SYSTEM

The dynamics of the stream system are handled by three independent models. Nutrients, DO, and BOD are modelled by a filter adaptation of EPA's DOSCI steady state stream model (Finnemore and Shepherd, 1974). Temperature is modeled by using a simple heat balance approach. The filter model of coliform uses a first order decay approximation with a distributed source term to account for non-point sources. A transformation of variables is made to model the logarithm of coliform counts rather than the numbers themselves. This transformation makes use of the assumption of normality inherent in the filter model more reasonable, as raw coliform data are usually highly skewed.

Stream velocity is included in all three models as a state variable. This allows modelling of the effect of uncertainty in stream velocity on uncertainty in the state variables. Using the steady state assumption a simple transformation of the standard time dependence in the filter model is made to one of spatial dependence:

$$\frac{d\bar{X}}{ds} = \frac{1}{U}\frac{d\bar{X}}{dt} \qquad (A.1)$$

where $\bar{X}$ = vector of state variables

s = spatial coordinate

U = stream velocity

Hence state estimates and state covariance estimates are for a specified spatial, rather than time coordinate. The interactions within the three models are explained in detail below. No link is provided between the

temperature and nutrient and coliform models, although some of the parameters in the two latter models are temperature dependent. This exclusion is justified by the results provided in Burges and Lettenmaier (1975) which show that uncertainty in BOD and DO estimates due to uncertainty in temperature contributes negligibly to overall parameter uncertainty in BOD and DO models.

Nutrients, DO, and BOD

The dynamics of the filter model for this segment of the stream system follow closely the BOD-DO-nutrient interactions of the DOSCI model. Two classes of state variables are included in the filter model. The first class is referred to as primary variables, and includes those water quality parameters which are of direct interest. The primary variables are:

symbol	state variable designation	
PO_4	X_1	inorganic soluble reactive phosphate (orthophosphate)
BOD	X_2	biochemical oxygen demand
DO	X_3	dissolved oxygen
NH_3	X_4	ammonia
NO_2	X_5	reactive inorganic nitrite
NO_3	X_6	reactive inorganic nitrate

The second class of state variables are referred to as secondary state variables, and are the constants used in linking the primary variables. The secondary vairables for this segment of the stream model are:

symbol	state variable designation	
K_s	X_7	BOD settling constant
K_n	X_8	BOD nitrogen decay coefficient
K_p	X_9	BOD phosphorus decay coefficient
K_c	X_{10}	BOD carbonaceaous decay coefficient
K_{bb}	X_{11}	benthal-non-point source BOD supply constant
K_a	X_{12}	reaeration constant
K_2	X_{13}	NO_2 decay coefficient
K_1	X_{14}	NH_3 decay coefficient
K_v	X_{15}	NH_3 volatization constant
K_{bn}	X_{16}	benthal NH_3 supply constant
K_3	X_{17}	NO_3 settling coefficient
K_{bp}	X_{18}	benthal-non-point source PO_4 supply constant
K_{ps}	X_{19}	PO_4 settling constant
K_{bd}	X_{20}	benthal DO demand constant
R_{bb}	X_{21}	benthal BOD supply rate
R_{bd}	X_{22}	benthal DO demand rate
R_{bn}	X_{23}	benthal NH_3 supply rate
R_{bp}	X_{24}	benthal PO_4 supply rate
U	X_{25}	Cross-section mean stream velocity

The interactions of the primary variables are explained below:

BOD: BOD is lost to ammonia, phosphate, bottom sediments, and directly as carbonaceous dissolved oxygen demand. All losses are modelled as first order reactions. BOD is supplied by non-point sources and benthal esuspension, which is modelled as the product of a supply rate and

a constant. Hence the balance is:

$$\frac{dX_2}{dt} = -(K_s + K_n + K_p + K_c)\ X_2 + K_{bb}R_{bb} \qquad (A.2)$$

Figure A.1 shows this balance schematically.

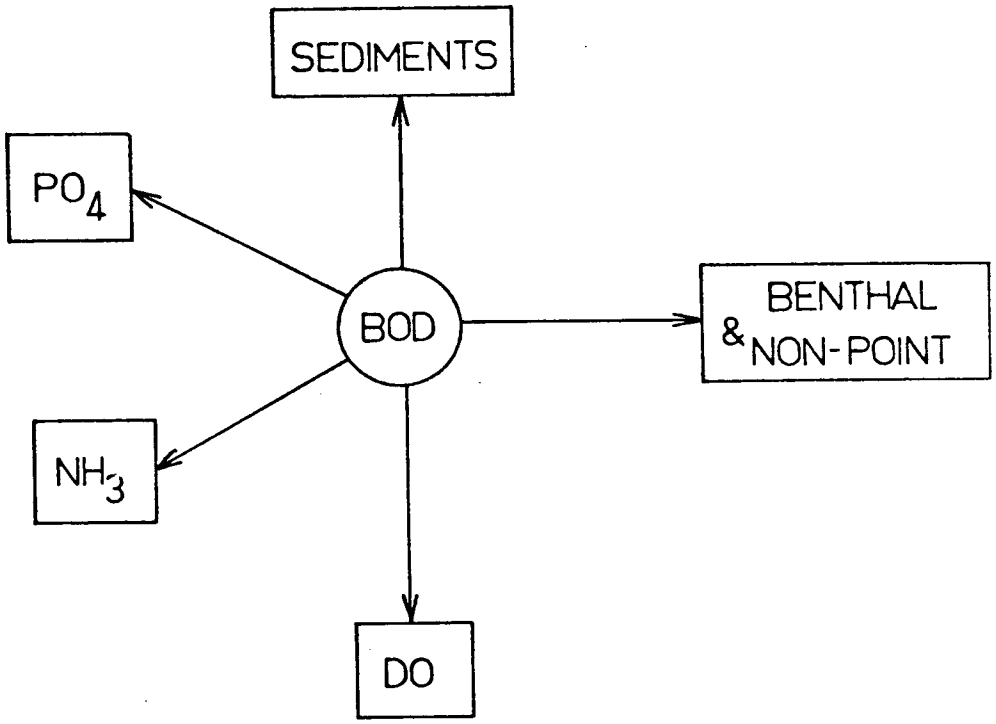

Figure A.1. BOD Mass Balance

DO: Dissolved oxygen is supplied by reaeration if the DO concentration is less than saturation and is lost if the DO value exceeds saturation. Oxygen is given up in the nitrification reactions of NH_3 and NO_2. In addition, DO is lost directly to BOD (carbonaceous BOD) and through direct demand of bottom sediments. Hence the balance is:

$$\frac{dX_3}{dt} = K_a(C_s - X_3) - 1.11\ K_2X_5 - 3.22\ K_1X_4 - K_cX_2 - K_{bd}R_{bd} \qquad (A.3)$$

The factors 1.11 and 3.22 are stoichiometric coefficients from the nitrification reactions of NO_2 and NH_3, respectively. C_s is dissolved oxygen saturation concentration, and is taken as constant. The DO balance is shown schematically in Figure A.2.

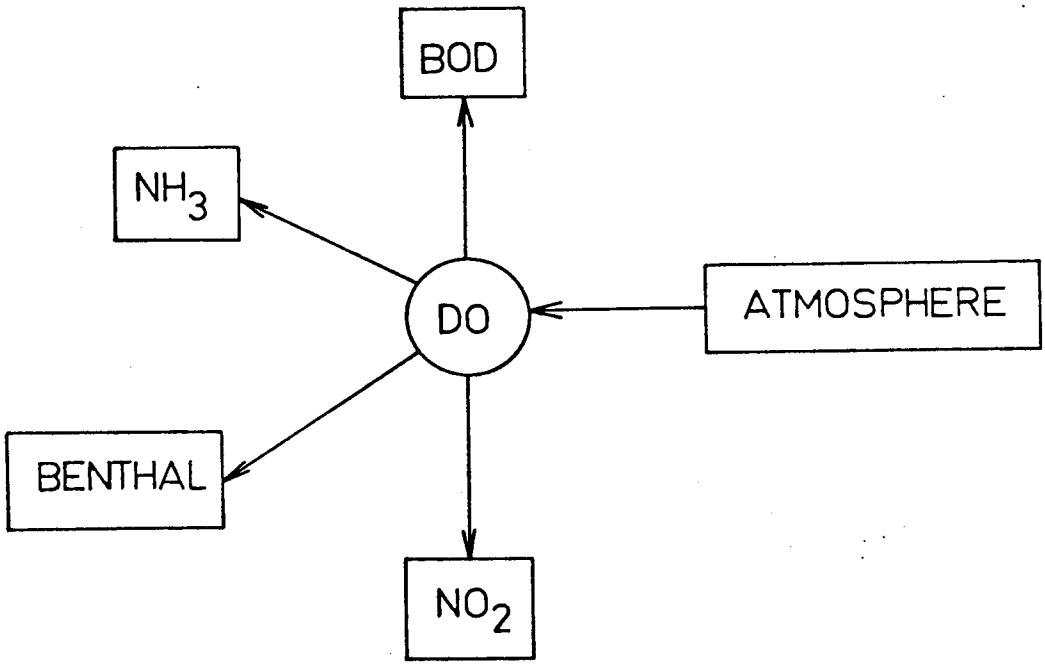

Figure A.2. Dissolved Oxygen Mass Balance

$\underline{PO_4}$: Phosphate is supplied by BOD and bottom sediments and is lost to settling. The bottom sediment supply term also accounts for non-point source supply. The balance is:

$$\frac{dX_1}{dt} = K_{bp}R_{bp} - K_{ps}X_1^2 + K_pX_2 \qquad (A.4)$$

Here, following Finnemore and Shepherd (1974) the decay reaction is modelled as second order. Figure A.3 shows this balance schematically.

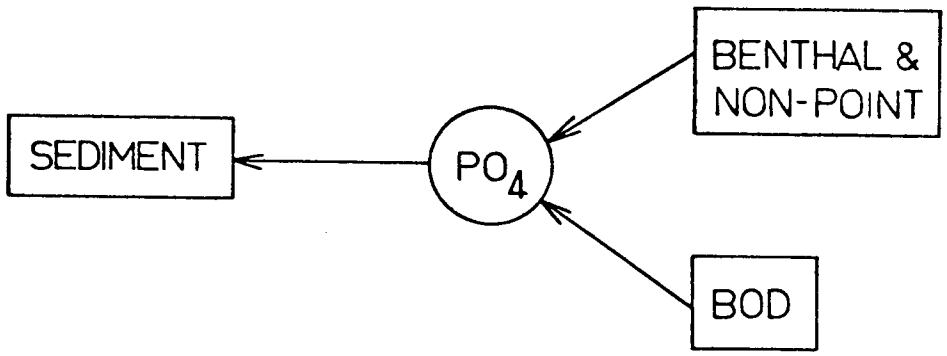

Figure A.3. Orthophosphate Mass Balance

NH_3: Ammonia is supplied by bottom sediments and BOD decay and is lost through volatization and through the nitrification reaction to NO_2. At sufficiently low DO values this reaction may proceed in the reverse direction. This possibility is allowed in the original DOSCI model but not in the filter version since DO levels in the streams of interest were always near saturation.

The balance is:

$$\frac{dX_4}{dt} = -K_v X_4 + K_n X_2 + K_{bn} R_{bn} - K_1 X_4 \qquad (A.5)$$

Figure A.4 shows this balance schematically.

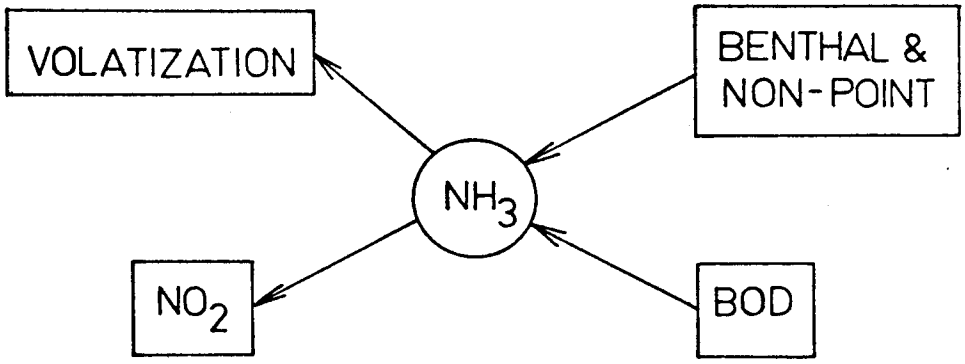

Figure A.4. Ammonia Mass Balance

NO_2: Nitrite is modelled entirely as part of the nitrification reaction. Supply is from ammonia, loss is to nitrate:

$$\frac{dX_5}{dt} = K_1X_4 - K_2X_5 \qquad (A.6)$$

Figure A.5 shows this balance schematically.

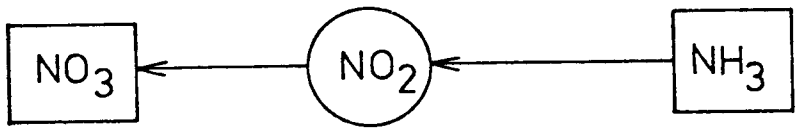

Figure A.5. Nitrite Mass Balance

NO_3: NO_3 is supplied by NO_2 in the nitrification reaction and is lost to sediments through settling:

$$\frac{dX_6}{dt} = K_2X_5 - K_3X_6 \qquad (A.7)$$

Figure A.6 shows this balance schematically.

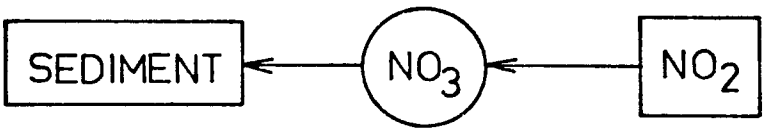

Figure A.6. Nitrate Mass Balance

Advection is included in the model by treating local inflows and withdrawals as occurring at the beginning of each spatial increment, or subreach. Non-point sources of the state variables are included in eqs. A.2-A.7; associated distributed inflows and outflows, e.g., contributions directly from interflow and overland flow or from small channels and groundwater inflow/outflow are treated as point inflows or withdrawals at the head of a subreach. For large inflows, subreaches are set to begin at the intersection point.

The actual filter implementation of the nutrient-DO-BOD model is by means of the optimally driven filter discussed in Appendix B. The total mass balance of the nutrient-DO-BOD model is shown in Figure A.7.

Temperature

The temperature dynamics are derived from a simple heat balance,

$$\frac{dT}{dt} = \frac{Q_t A}{62.4V} \qquad (A.8)$$

where $V/A = \bar{h}$, the mean depth. Transformation to spatial dependence yields

$$\frac{dT}{dx} = \frac{Q_t}{62.4\bar{h}U} \qquad (A.9)$$

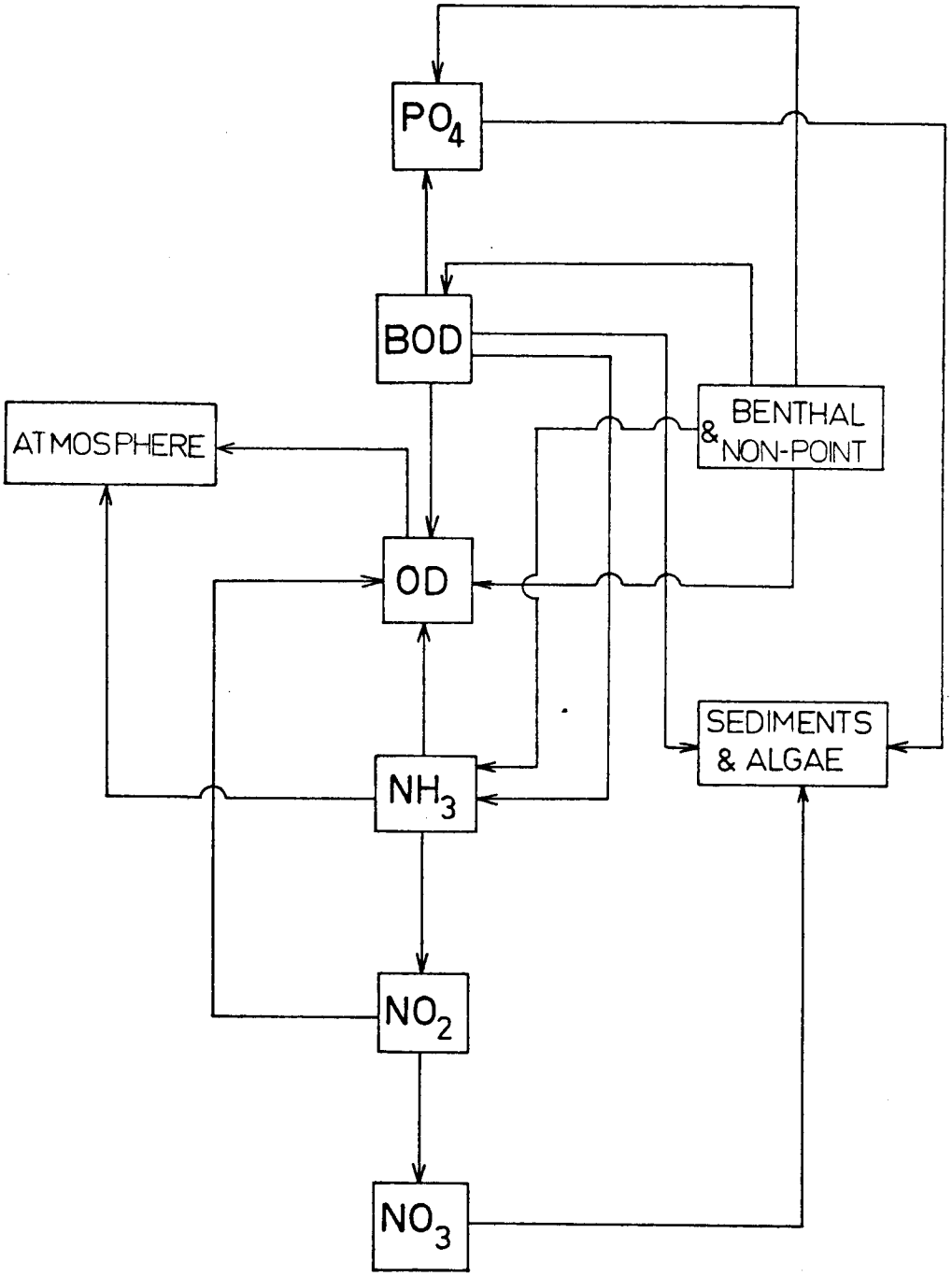

Figure A.7. Mass Balance for Nutrient-DO-BOD Model. OD is oxygen deficit, defined as saturation minus actual dissolved oxygen concentration.

Q_t and $\bar{h}$ are assumed to change linearly with distance downstream, hence

$$\frac{dQ_t}{dx} = C_1, \quad \frac{dC_1}{dt} = 0$$

$$\frac{d\bar{h}}{dx} = C_2, \quad \frac{dC_2}{dt} = 0$$

and velocity is assumed constant, $\frac{dU}{dx} = 0$.

The filter formulation is

$$\frac{d\underline{Y}}{dx} = \begin{vmatrix} Y_2/62.4Y_4Y_6 \\ Y_3 \\ 0 \\ Y_4 \\ 0 \\ 0 \end{vmatrix} \qquad \text{(A.10)}$$

where $Y_1 = T$

$Y_2 = Q_t$

$Y_3 = C_1$

$Y_4 = \bar{h}$

$Y_5 = C_2$

$Y_6 = U$

Following the earlier convention, Y_1 is a primary state variable while Y_j, j=2,..6 are secondary state variables.

An earlier approach attempted a filter adaptation of Raphael's method (Raphael, 1962). This approach uses eq. A.8, where Q_t is taken to be the sum of net short wave solar insolation, net long wave back radiation, conductive heat transfer to the atmosphere, and evaporative

heat transfer:

$$Q_t = kQ_i - 1.663x10^{-7}(T^4 - K\,T_a^4) - .00543U_w P(T_a - T) - 16U_w K_{ev} \qquad (A.11)$$

Here Q_i is net short wave solar insolation to the water body and k is an adjustment for cloud cover. The second term is net long wave radiation from the water body where K is a constant allowing for the "gray body" nature of long wave radiation from the atmosphere. The third term accounts for net energy convection to the atmosphere, which is assumed directly proportional to wind velocity, atmospheric vapor pressure, and air-water temperature differential. The final term is net heat lost to the atmosphere through evaporation, which is assumed directly proportional to wind velocity and the difference in vapor pressure between saturated air at air temperature and actual vapor pressure at air temperature.

The attempted use of Raphael's method was abandoned after investigation of the derived variance trajectories. The long wave radiation term, involving the fourth power of the absolute temperature dominates the characteristics of the variance trajectory, and causes rapid growth of the conditional variance. In addition, relatively small step sizes are required to yield accurate results. Step sizes which are too large cause negative solutions to the variance equation. A typical variance trajectory derived using Raphael's method is shown in Figure A.8 Here the assumed initial values $T_a = 65$, $T_w = 50$, $\bar{h} = 10$, and $U = 50$ mile/day were used with measurements at 5 and 50 miles downstream from the upstream boundary and a tributary located at 42.2 miles downstream. The initial variance in stream temperature was taken as $4°F^2$, with the source flow 1000 cfs. The tributary flow was 100 cfs, with temperature 90° and variance $100°F^2$. The measurement error standard deviation was taken as

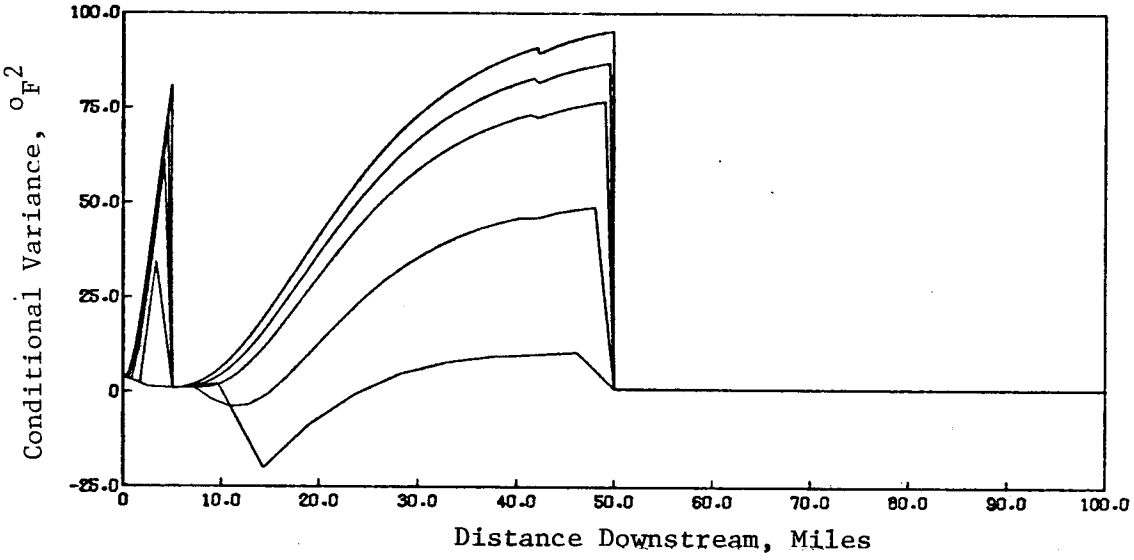

Figure A.8. Variance Propagation for Test Case Using Raphael's Temperature Model

1°F. After two measurements the conditional variance becomes essentially the measurement error variance, however conditional standard deviations of nearly 10°F are predicted between stations 1 and 2. Errors of this size are not physically reasonable, as investigation of historical records shows that variations in mean daily stream temperatures are much smaller. Even with no measurements, standard deviations on the order of 5°F would be expected. Consequently, Raphael's method, while conceptually realistic, was not incorporated as a predictive tool, and a lumped net heat influx term Q_i was used in the temperature modelling.

The actual filter implementation is by means of the optimally driven filter discussed in Appendix B. As in the nutrient-DO-BOD model, advective terms are included at the beginning of each subreach, where complete mixing is assumed.

Coliform

Coliform is modelled as a first order decay reaction with a source term to account for non-point supply:

$$\frac{dC}{dt} = -K_c C + R_c \qquad (A.12)$$

where C = coliform count (numbers-unit volume)

K_c = coliform decay coefficient

R_c = coliform distributed source magnitude

Since coliform levels commonly fluctuate by several orders of magnitude, a transformation is made to allow modelling of log coliform counts, rather than coliform counts themselves. This transformation also will substantially reduce the skew usually present in coliform time series, making the assumption of normality made in use of the filter model more reasonable. The transformation is:

$$Z_c = \ln C, \quad \text{hence } C = \exp(Z_c)$$

and
$$\frac{d}{dt}(\exp(Z_c)) = -K_c \exp(Z_c) + R_c,$$

$$\exp(Z_c)\frac{dZ_c}{dt} = -K_c \exp(Z_c) + R_c,$$

$$\frac{dZ_c}{dt} = -K_c + R_c \exp(-Z_c) \qquad (A.13)$$

Transforming to spatial dependence,

$$\frac{dZ_c}{ds} = \frac{-K_c}{U} + \frac{R_c}{U}\exp(-Z_c) \qquad (A.14)$$

In state variable form, the only primary variable is Z_c, the log coliform count, which is denoted Z_1. The secondary variables are:

symbol	state variable designation	
K_c	Z_2	coliform decay constant
R_c	Z_3	non-point coliform supply rate
U	Z_4	stream mean velocity

Use of the logarithmic model requires that coliform counts be non-zero. The most practical approach to this requirement is to simply replace measured counts of zero with a small number, for instance, if a culture revealed no colonies per 100 ml., this might be arbitrarily replaced by a count of one.

As in the other filter models, advection is included at the beginning of a subreach. The actual filter implementation uses the optimally driven filter of Appendix B.

APPENDIX B OPTIMALLY DRIVEN FILTER

An outline of the derivation of the optimally driven filter is given below. The derivation presented here is not rigorous, but is rather an approach which will give insight into the mechanics of the filter algorithm with some sacrifice in mathematical rigor.

The numerical implementation of the filter is discussed in some detail, and the actual equations used in the coliform model are derived. For a more complete treatment, McGarty (1974, pp. 281-90) should be consulted.

Derivation

Throughout this section the notation $\bar{C}$ denotes a vector, and $\underline{C}$ denotes a matrix. Vectors in standard form are column vectors, hence $\bar{C}$ is a column vector. $\bar{C}^T$ is the row vector transpose of $\bar{C}$. The notation "tr" denotes the trace of a matrix.

We model the system dynamics as

$$\frac{d\bar{X}}{dt} = \bar{f}(\bar{X},t) + \bar{n}(t) \qquad (B.1)$$

where $\bar{X}$ is a vector of state variables and $\bar{n}(t)$ is a Gaussian white noise process. The measurement system is modelled as

$$\bar{Y}(t) = \underline{C}(t)\bar{X}(t) + \bar{w}(t) \qquad (B.2)$$

where $\bar{Y}$ is a vector of measurements, $\underline{C}$ is a coefficient matrix, and $\bar{w}(t)$ is a Gaussian white noise process. The system noise covariance matrix $\underline{Q}$ and the measurement noise covariance matrix $\underline{R}$ are defined as

$$\underline{Q}(t) = E(\bar{n}(t)\bar{n}^T(t)) \tag{B.3}$$

$$\underline{R}(t) = E(\bar{w}(t)\bar{w}^T(t)) \tag{B.4}$$

The forcing function $\bar{f}$ is expanded (to second order) in a Taylor series about an operating point $\bar{X}^*$:

$$\bar{f}(\bar{X}) = \bar{f}(\bar{X}^*) + \underline{A}(\bar{X}^*)(\bar{X}-\bar{X}^*) + 1/2 \sum_{i=1}^{n} \bar{\gamma}_i (\bar{X}-\bar{X}^*)^T \underline{B}_i(\bar{X}^*)(\bar{X}-\bar{X}^*) \tag{B.5}$$

where n is the dimension of the state vector $\bar{X}$ and the $\underline{A}$ matrix is:

$$A(\bar{X}^*) = \left[\begin{array}{ccc} \frac{\partial f_1}{\partial x_1} & \cdots & \frac{\partial f_1}{\partial x_n} \\ \vdots & & \vdots \\ \frac{\partial f_n}{\partial x_1} & \cdots & \frac{\partial f_n}{\partial x_n} \end{array}\right]_{\bar{X}=\bar{X}^*} \tag{B.6}$$

$$\underline{B}_i(\bar{X}^*) = \left[\begin{array}{ccc} \frac{\partial f_i}{\partial X_1 \partial X_1} & \cdots & \frac{\partial f_i}{\partial X_1 \partial X_n} \\ \vdots & & \vdots \\ \frac{\partial f_i}{\partial X_n \partial X_1} & \cdots & \frac{\partial f_i}{\partial X_n \partial X_n} \end{array}\right]_{\bar{X}=\bar{X}^*} \tag{B.7}$$

and $\bar{\gamma}_i = \begin{bmatrix} 0 \\ 0 \\ \cdot \\ \cdot \\ 1 \\ \cdot \\ \cdot \\ 0 \\ 0 \end{bmatrix}$ i i.e., an n x 1 column vector of zeros except for a one in the i'th position.

We note that if $\underline{Q}(t) \equiv 0$, $\frac{d\hat{\bar{X}}}{dt}(t) = f(\hat{\bar{X}}(t))$, where the notation $\hat{\bar{X}}$ indicates a prediction based on given initial conditions. The real system, however, is perturbed by noise. Hence we define an additional forcing function which we hope will in some way compensate for the noise, i.e.,

$$\frac{d\hat{\bar{X}}}{dt}(t) = \bar{f}(\hat{\bar{X}}(t)) + \bar{\psi}(t) \tag{B.8}$$

$\bar{\psi}(t)$ is now chosen so that the expected error $E(\hat{\bar{X}}(t)-\bar{X}(t))$ is zero. Setting the expected error equal to zero and substituting B.5 in B.8 ultimately yields

$$\bar{\psi}(t) = 1/2 \sum_{i=1}^{n} \gamma_i tr(\underline{B}_i(X^*)\underline{M}(t)) \tag{B.9}$$

$$\text{where } \underline{M}(t) = E(\tilde{\bar{X}} \tilde{\bar{X}}^T) \tag{B.10}$$

and $\tilde{\bar{X}}$ is the error in the estimate $\hat{\bar{X}}$ of $\bar{X}$ (i.e., $\tilde{\bar{X}} = \hat{\bar{X}} - \bar{X}$).

The next step is to derive an equation for $\underline{M}(t)$, the state covariance matrix conditioned on a prior measurement. The derivation is based on an assumption of Gaussianness. This assumption yields two simplifications:

(1) Since the apriori distribution of the state vector is assumed Gaussian, any linear combination of the apriori values (including combinations of differentials, which are linear operations) will be Gaussian. Hence, the estimate $\hat{\bar{X}}$ of $\bar{X}$ will be Gaussian.

(2) Since $\bar{X}$ is Gaussian, all the odd moments of $\bar{X}$ will be zero. The assumption of Gaussianness and resulting simplifications combined with the definition of $\underline{M}(t)$ (B.10) and the Taylor series expansion of $\bar{f}$(B.5) yield:

$$\frac{d\underline{M}(t)}{dt} = \underline{A}(\bar{X}^*)\underline{M}(t) + \underline{M}(t)\underline{A}^T(\bar{X}^*) + \underline{Q}(t) \qquad \text{(B.11)}$$

where $\underline{M}(k-1) = \underline{P}(k-1)$ is the initial condition, and $\underline{P}(k-1)$ is the state covariance matrix at discrete time k-1 conditioned on a measurement at time k-1,

$$\underline{P}(k) = E(\tilde{\bar{X}}(k|k)\tilde{\bar{X}}^T(k|k)) \qquad \text{(B.12)}$$

Here, and in the subsequent development, the notation $\cdot(k|j)$ indicates the estimate of a quantity at time k conditioned on a measurement at time j. Also, for simplicity the notation $\cdot(k)$ implies $\cdot(k|k)$.

The filtered estimate of state is <u>defined</u> as

$$\hat{\bar{X}}(k|k) = \hat{\bar{X}}(k|k-1) + \underline{K}(k)\{\bar{Z}(k) - \underline{C}(k)\hat{\bar{X}}(k|k-1)\} \qquad \text{(B.13)}$$

Hence, substituting B.13 in B.12,

$$\underline{P}(k) = (\underline{I} - \underline{K}(k)\underline{C}(k))\underline{M}(k)(\underline{I} - \underline{K}(k)C(k))^T + \underline{K}(k)\underline{R}(k)\underline{K}^T(k) \qquad \text{(B.14)}$$

Here $\underline{C}$, $\underline{M}$, and $\underline{K}$ are matrices defined in eqs. B.2, B.10 and B.13,

respectively and k denotes discrete time.

The solution for $\underline{K}(k)$ requires choice of a statistical cost function. The cost function commonly used is quadratic, i.e., for $\underline{S}(k)$ any arbitrary symmetric n x n positive-definite matrix, the cost, J(k) is

$$J(k) = E(\tilde{\overline{X}}^T(k|k)\underline{S}(k)\tilde{\overline{X}}(k|k)) \qquad \text{(B.15a)}$$

Hence, the cost associated with a bad estimate $\hat{\overline{X}}$ of $\overline{X}$ increases quadratically with the error. The implications of this choice of loss function and other possible choices are discussed in section I of Chapter 3. The choice of a quadratic cost function and the minimization with respect to $\underline{K}(k)$, $\frac{\partial J(k)}{\partial \underline{K}(k)} = 0$ leads to

$$\underline{K}(k) = \underline{M}(k)\underline{C}^T(k)(\underline{C}(k)\underline{M}(k)\underline{C}^T(k) + \underline{R}(k))^{-1} \qquad \text{(B.15)}$$

The complete algorithm may be summarized:

1. Choose $\hat{\overline{X}}(0)$, $\underline{P}(0)$
2. Solve eqs. B.6, B.7, B.9, and B.11 simultaneously for $\underline{M}(t)$ and $\overline{\psi}(t)$.
3. Solve B.15 for $\underline{K}(k)$
4. Solve B.14 for $\underline{P}(k)$
5. Solve B.8 for $\hat{\overline{X}}(k|k-1)$
6. Solve B.13 for $\hat{\overline{X}}(k|k)$
7. Return to step 1, using initial estimates $\hat{\overline{X}}(1|1)$, $\underline{P}(1)$

Numerical Solution

The equations necessary for implementation of the optimally driven filter are listed below for convenience of reference:

$$\frac{d\underline{M}}{dt} = \underline{A}(\bar{X}^*)\underline{M} + \underline{M}\underline{A}^T(\bar{X}^*) + \underline{Q}(t) \tag{B.11}$$

$$\bar{\psi}(t) = 1/2 \sum_{i=1}^{n} \bar{\gamma}_i tr(\underline{B}_i(\bar{X}^*)\underline{M}(t)) \tag{B.9}$$

$$\frac{d\hat{\bar{X}}(t|k-1)}{dt} = \bar{f}(\hat{\bar{X}}^*(t)) + \bar{\psi}(t) \tag{B.8}$$

$$\underline{K}(k) = \underline{M}(k)\underline{C}^T(k)(\underline{C}(k)\underline{M}(k)\underline{C}^T(k) + \underline{R}(k))^{-1} \tag{B.15}$$

$$\underline{P}(k) = (\underline{I} - \underline{K}(k)\underline{C}(k))\underline{M}(k)(\underline{I} - \underline{K}(k)\underline{C}(k))^T + \underline{K}(k)\underline{R}(k)\underline{K}^T(k) \tag{B.14}$$

$$\hat{\bar{X}}(k|k) = \hat{\bar{X}}(k|k-1) + \underline{K}(k)(\bar{Z}(k) - \underline{C}(k)\hat{\bar{X}}(k|k-1)) \tag{B.13}$$

The Taylor series expansion of $\bar{f}$ (eq. B.5) requires a nominal trajectory $\bar{X}^*$ about which the expansion is to take place. The nominal trajectory may be selected *apriori*, or may be an estimate derived from the filter model itself. Consider the latter case first.

If the nominal trajectory is to be derived from the filter model, i.e. $\bar{X}^*(t) = \hat{\bar{X}}(t|k-1)$ eqs. B.8, B.9, and B.11 must be solved simultaneously. The numerical approach used is a simple backwards difference equation:

$$\bar{X}^*_i = \hat{\bar{X}}_{i-1}$$

$$1/\Delta t(\underline{M}_i - \underline{M}_{i-1}) = \underline{A}(\bar{X}^*_i)\underline{M}_{i-1} + \underline{M}_{i-1}\underline{A}^T(\bar{X}^*_i) \tag{B.16}$$

$$\bar{\psi}_i = 1/2 \sum_{j=1}^{n} \bar{\gamma}_j tr(\underline{B}_j(\bar{X}^*_i)\underline{M}_j) \tag{B.17}$$

$$1/\Delta t(\hat{\bar{X}}_i - \hat{\bar{X}}_{i-1}) = \bar{f}(\bar{X}^*_i) + \bar{\psi}_i \qquad (B.18)$$

This sequence of equations is iterated N_k times, where N_k denotes the number of integration units per time step k. Ultimately $\hat{\bar{X}}_k$ is derived, and equations B.13-15 are iterated. Then the new estimate $\hat{\bar{X}}(k|k)$ is used in eqs. B.16-18, and the process repeated.

The simple backwards difference scheme of eqs. B.16-18 is only one of many possible numerical solutions. For instance, a multistep predictor-corrector method or a Runge Kutta method might be used. The convergence of the single step backwards difference approach is relatively slow, and might be improved by use of a more sophisticated method. Three considerations lead to retention of the simpler method. First, the single step approach precludes the presence of extraneous (possibly unstable) solutions to the difference equation as the difference equation and the differential equation are of the same order. Second, the equations are matrix, rather than scalar differential equations. Consequently more sophisticated methods of solution will require additional matrix multiplication, and computational requirements increase very rapidly. Finally, the solutions to eqs. B.16-18 are required at a number of intermediate (between time steps k and k+1) locations to identify the trajectories of the variance and state estimates. Consequently, solution methods which reduce the number of increments required for the same accuracy are not particularly useful, as the intermediate solutions are required as well as the solutions at discrete values of k. Consequently, the simple backwards difference approach to numerical solution of eqs. B.16-18 was retained.

If an aprior nominal trajectory is used, only eqs. B.11 and B.9 need be iterated simultaneously. If only the predicted error covariance matrices $\underline{M}$ and $\underline{P}$ are desired, only eqs. B.14 and B.15 need be iterated subsequently.

In practice, the $\underline{B}$ matrices are often very sparse, and the computational load may be greatly reduced. If the secondary state variables are modelled as being constant, their associated $\underline{B}$ matrices will all be zero, hence the summation in B.9 may be taken over n', the number of primary variables. For the n' non zero $\underline{B}$ matrices, the densities, for the models used, never exceed 50 per cent, and in some cases are as low as about 2 percent. Rather than carry out the classical matrix multiplication indicated in eqs. B.9, the sparsity of the matrices makes it practical to store and manipulate the nonzero elements individually. A further computational savings is realized by noting that all of the rows of the $\underline{A}$ matrix below the n'th row are zero. Hence the multiplications required by eq. B.11 may be reduced substantially as well.

Illustration for Coliform Model

The numerical implementation of the filter algorithm for the coliform model is presented here. The implementation of the other segments of the model (DO-BOD-nutrients and temperature) follows exactly the same approach.

The coliform model dynamics are derived using spatial rather than time dependence:

$$\frac{dZ_c}{dx} = -\frac{K_c}{U} + \frac{R_c}{U}\exp(-Z_c) \qquad (B.19)$$

(See Appendix A for the derivative of eq. B.19.)

Using the notation of Appendix A,

$$\frac{dZ_1}{dx} = \frac{Z_3}{Z_4} \exp(-Z_1) - \frac{Z_2}{Z_4} \tag{B.20}$$

$$\frac{dZ_2}{dx} = \frac{dZ_3}{dx} - \frac{dZ_4}{dx} = 0 \tag{B.21}$$

hence,

$$\bar{f}(\bar{Z},x) = \begin{bmatrix} Z_3/Z_4 \exp(-Z_1) - Z_2/Z_4 \\ 0 \\ 0 \\ 0 \end{bmatrix} \tag{B.22}$$

$$\text{and } \underline{A} = \frac{\partial f_i}{\partial x_j} = \begin{bmatrix} -Z_3/Z_4\exp(-A_1) & -1/Z_4 & \exp(-Z_1)/Z_4 & 1/Z_4^2(Z_2-Z_3\exp(-Z_1)) \\ 0 & 0 & 0 & 0 \\ 0 & 0 & 0 & 0 \\ 0 & 0 & 0 & 0 \end{bmatrix}$$

The $\underline{B}$ matrices are determined using eq. B.7.

Clearly, $\underline{B}_2 = \underline{B}_3 = \underline{B}_4 = 0$, and, for example,

$$B_{1_{11}} = \frac{\partial}{\partial Z_1} (-Z_3/Z_4\exp(-Z_1)) = Z_3/Z_4 \exp(-Z_1)$$

$$\vdots$$

$$B_{1_{44}} = Z_3/Z_4(Z_3\exp(-Z_1) - Z_2)$$

$$\text{hence } \underline{B}_1 = \begin{bmatrix} Z_3/Z_4\exp(-Z_1) & 0 & -1/Z_4\exp(-Z_1) & Z_3/Z_4^2\exp(-Z_1) \\ 0 & 0 & 0 & 1/Z_4^2 \\ -\exp(-Z_1)/Z_4 & 0 & 0 & -\exp(-Z_1)/Z_4^2 \\ Z_3/Z_4^2\exp(-Z_1) & 1/Z_4^2 & -\exp(-Z_1)/Z_4^2 & 2(Z_3\exp(-Z_1)-Z_2)/Z_4^2 \end{bmatrix}$$

The four non-zero elements in $\underline{A}$ and the 10 non-zero elements in $\underline{B}_1$ are stored and eqs. B.8-9, B.11, and B.13-15 are discretized using eqs. B.16-18. In this manner the filter estimates of state and the state covariance matrix may be derived.

APPENDIX C DESIGN DATA FOR SPOKANE RIVER

Data used in the Spokane River demonstration design are given in this appendix. For convenience, the location of the various data in tables are given below.

Table	Contents
C.1	Effluent flow and concentration means
C.2	Effluent flow and concentration variances
C.3	Headwater flow and concentration means and variances
C.4	Secondary state variable means and variances
C.5	Linearization trajectory (instream concentrations)

Effluent flows and mean concentrations were obtained from Kennedy-Tudor Inc. (1974). Effluent flow and concentration variances were established by the author apriori, for most constituents the variances were based on coefficients of variation of approximately one. The linearization trajectory was derived from instream measurements taken by Kennedy-Tudor, Inc., in June, 1974. Headwater conditions were also provided by Kennedy-Tudor. Secondary state variable mean values were obtained from Finnemore and Shepherd (1974), variances were selected by the author and, in most cases, are based on coefficients of variation of about one.

Table C.1. Effluent/Tributary Mean Concentrations

River Mile	Identification	Flow cfs	PO_4 mg/1	BOD mg/1	DO mg/1	NH_3 mg/1	NO_2 mg/1	NO_3 mg/1	Temp. °F	FCX[a] mpn/100 ml
87.1	Hillyard Processing	.845	0	.25	8.0	8.0	0	.8	70	0
86.9	Spokane Ind. Park	.845	4.8	5.3	8.9	3.4	.2	1.42	70	0
86.0	Kaiser-Mead	6.0	.17	.74	8.0	.48	0	1.1	75.2	1.09
86.0	Kaiser-Trentwood	37.2	.15	3.5	5.0	1.8	0	.04	70	2.94
84.5	Upper Spokane Gdwtr.	420	.011	0	8.0	.015	.002	1.123	51.1	0
83.0	Inland Empire Paper	5.11	.56	47.3	5.0	0	0	.1	70	3.0
72.4	Hangman Creek	250	.06	1.0	7.4	.08	.005	.65	55	6.5
67.2	Spokane S.T.P.	42	4.1	121	5.0	13.97	0	.854	61.3	8.02
64.3	Lower Spokane Gdwtr.	227	.011	0	8.0	.015	.002	1.123	51.3	0

[a]Fecal coliform data are listed in natural logarithmic units throughout Appendices C and D.

Table C.2. Discharge Concentration Variances

River Mile	Identification	Flow cfs^2	PO_4 mg/l^2	BOD mg/l^2	DO mg/l^2	NH_3 mg/l^2	NO_2 mg/l^2	NO_3 mg/l^2	Temp. $°F^2$	FCX mpn/100 ml^2
87.1	Hillyard Processing	.714	10^{-4}	.06	1	64	10^{-2}	.64	100	0
86.9	Spokane Ind. Park	.714	25	25	1	9	.04	3	100	.5
86.0	Kaiser-Mead	9.0	.03	.5	1	.25	10^{-2}	1.21	4	1
86.0	Kaiser-Trentwood	225	.02	4	10	3	10^{-2}	.01	100	9
84.5	Upper Spokane Gdwtr.	2500	10^{-4}	1	1	10^{-4}	10^{-6}	1	5	2
83.0	Inland Empire Paper	10	.25	400	9	10^{-2}	10^{-2}	.01	100	9
72.4	Hangman Creek	100	.004	1	1	10^{-4}	10^{-6}	.36	16	4
67.2	Spokane S.T.P.	50	4	10^4	9	25	.5	.64	5	9
64.3	Lower Spokane Gdwtr.	2500	10^{-4}	1	1	10^{-4}	10^{-6}	1	5	2

Table C.3. Spokane River Headwater Data

	Flow cfs	PO_4 mg/l	BOD mg/l	DO mg/l	NH_3 mg/l	NO_2 mg/l	NO_3 mg/l	Temp °F	FCX mpn/100 ml
mean	6870	.018	1.21	9.0	.05	0	.08	55	4
variance	10^4	.0004	1	1	.0025	10^{-4}	10^{-2}	4	2

Table C.4. Secondary State Variable Means and Variances

Parameter	Units	Description	Mean	Variance
K_s	day^{-1}	BOD settling coefficient	.03	$9x10^{-4}$
K_n	day^{-1}	BOD nitrogen decay coefficient	.00333	$2.5x10^{-5}$
K_p	day^{-1}	BOD phosphorus decay coefficient	.0004	$9x10^{-6}$
K_c	day^{-1}	BOD carbonaceous decay constant	.3	.09
K_{bb}	$\frac{m^2}{1}$	benthal-non point source BOD upply constant	.008	$6.4x10^{-5}$
K_a	day^{-1}	reaeration coefficient	.7	.5
K_1	day^{-1}	NH_3 decay coefficient	.096	.015
K_2	day^{-1}	NO_2 decay coefficient	.36	.36
K_v	day^{-1}	NH_3 volatization constant	.3	.04
K_{bn}	$\frac{m^2}{1}$	benthal NH_3 supply constant	.008	$6.4x10^{-5}$
K_3	day^{-1}	NO_3 settling coefficient	.036	10^{-3}
K_{bp}	$\frac{m^2}{1}$	benthal-non point PO_4 supply	.005	$6.4x10^{-5}$
K_{ps}	day^{-1}	PO_4 settling constant	.022	$5x10^{-4}$
K_{bd}	$\frac{m^2}{1}$	benthal DO demand constant	.017	$6.4x10^{-5}$
R_{bb}	$\frac{mg}{m^2 hr}$	benthal BOD supply rate	61	3600
R_{bd}	$\frac{mg}{m^2 hr}$	benthal DO demand rate	15	225
R_{bn}	$\frac{mg}{m^2 hr}$	benthal NH_3 supply rate	.11	.01
R_{bp}	$\frac{mg}{m^2 hr}$	benthal PO_4 supply rate	.065	.015
U	mile/day	cross-section mean stream velocity	75	50
Q_t	$\frac{Btu}{ft^2 hr}$	net heat influx	7	25
C_1	$\frac{Btu}{ft^2 hr\ mile}$	net heat influx change rate	.2	.01

Table C.4 (cont.)

H	ft	upstream boundary depth	2	1
C_2	ft/mile	depth change rate	.05	4×10^{-4}
K_c	day^{-1}	fecal coliform die-off coeff coefficient	.4	.01
R_c	$\frac{mpn}{1000\ ml\text{-}day}$	fecal coliform supply rate	0	0

Table C.5. Linearization Trajectory for Spokane River

River Mile	PO_4 mg/l	BOD mg/l	DO mg/l	NH_3 mg/l	NO_2 mg/l	NO_3 mg/l	Temp. °F	FCX mpn/100 ml
77.9	.002	.4	9.0	.02	.003	.02	57.7	1.6
69.7	.002	.5	10.0	.015	.003	.02	57.6	5.7
66.6	.006	.7	9.5	.025	.003	.035	57.6	5.7

APPENDIX D DESIGN DATA FOR SNOHOMISH RIVER SYSTEM

Design data for each of the three major tributaries in the Snohomish River system are given below. For each tributary, the first table lists the effluent and tributary mean flows and concentrations, the second table lists effluent and tributary flow and concentration variances, and the third table gives the linearization trajectory. For the Snoqualmie and Skykomish Rivers, a fourth table gives headwater conditions.

Effluent and tributary concentrations were provided by the Snohomish County Planning Department (Systems Control, Inc., and Snohomish County Planning Dept., 1974). Variances were estimated apriori, as for the Spokane (Appendix C). Headwater data and the linearization trajectory were based on instream data collected by the Snohomish County Planning Department in November, 1973. Units are identical to those used in Appendix C.

Table D.1.1. Effluent/Tributary Mean Concentrations for Snoqualmie River

River Mile	Identification	Flow	PO_4	BOD	DO	NH_3	NO_2	NO_3	Temp.	FCX
46.3	North Bend Outfall	.3	.08	34	7.1	4.35	.02	.39	55	13
44.5	NF & MF Snoqualmie R.	2930	0	1.4	12.3	0	.005	.31	42	3
41.6	Weyerhauser Outfall	1	.09	21	7.5	.06	.01	.4	55	8
41.0	Snoqualmie Outfull	.2	.53	18	7	2.25	.029	.53	55	8
39.7	Tokul Cr.	441	0	1.4	12	.05	.005	.92	42	8
36.3	Raging R.	420	0	1.6	12	.06	.005	1.31	42	8
36.3	Nonpoint Source	.5	5	30	6	3	0	1.2	55	8.5
35.8	Fall City Outfall	.5	10	30	7	9.8	0	10	55	6.7
35.7	Nonpoint Source	6.67	5	30	6	3	0	1.2	55	8.5
27.3	Griffen Cr.	250	0	2.1	11.9	.06	.003	9	42	3
25.0	Nonpoint Source	2.5	3.5	45	6	1.5	0	.6	55	6.5
24.9	" "	1.25	3.5	45	6	1.5	0	.6	55	6.5
24.0	" "	1.25	3.5	45	6	1.5	0	.6	55	6
23.5	" "	2.5	3.5	45	6	1.5	0	.5	55	6.5
23.0	" "	3.75	3.5	45	6	1.5	0	.6	55	6.5
21.9	Cherry Cr.	70	0	2	11.4	.05	.005	1.13	55	5.6
6.8	Nonpoint Source	3.33	3.5	45	6	1.5	0	.6	55	12
4.9	Dairy Farm Outfall	.1	0	0	5	0	0	0	55	5
2.9	French Cr.	780	0	1.8	12.5	.03	.005	.26	42	3

Table D.1.2. Effluent/Tributary Variances for Snoqualmie River

River Mile	Identification	Flow	PO_4	BOD	DO	NH_3	NO_2	NO_3	Temp.	FCX
46.3	North Bend Outfall	.09	.0025	100	4	4	10^{-4}	.01	4	2
44.5	NF & MF Snoqualmie R.	$25x10^{-5}$	10^{-4}	1	1	10^{-4}	10^{-6}	.01	4	2
41.6	Weyerhauser Outfall	1	.0025	50	4	.0025	10^{-4}	.01	4	2
41.0	Snoqualmie Outfall	.04	.04	16	4	1	10^{-4}	.01	4	2
39.7	Tokul Cr.	2500	10^{-4}	1	1	10^{-4}	10^{-6}	.04	4	2
36.3	Raging R.	2500	10^{-4}	1	1	10^{-4}	10^{-6}	1	4	2
36.3	Nonpoint Source	.25	4	25	4	4	10^{-6}	1	4	2
35.8	Fall City Outfall	.25	25	25	4	4	10^{-6}	4	4	2
35.7	Nonpoint Source	4	4	25	1	1	10^{-6}	1	4	2
27.3	Griffen Cr.	625	10^{-4}	1	1	.0025	10^{-6}	1	4	2
25.0	Nonpoint Source	1	4	100	4	1	10^{-6}	.5	4	2
24.9	" "	1	4	100	4	1	10^{-6}	.5	4	2
24.0	" "	1	4	100	4	1	10^{-6}	.5	4	2
23.5	" "	4	4	100	4	1	10^{-6}	.5	4	2
23.0	" "	16	4	100	4	1	10^{-4}	.5	4	2
21.9	Cherry Cr.	100	10^{-4}	1	1	.0025	10^{-6}	1	4	2
6.9	Nonpoint Source	2	4	100	4	1	10^{-6}	.04	4	2
4.9	Dairy Farm Outfall	.01	10^{-4}	1	4	10^{-4}	10^{-6}	10^{-4}	4	2
2.9	French Cr.	10^{-4}	10^{-4}	1	1	10^{-4}	10^{-6}	.04	4	2

Table D.1.3. Snoqualmie River Linearization Trajectory

River Mile	PO_4	BOD	DO	NH_3	NO_2	NO_3	Temp.	FCX
39.7	.08	3.15	12.3	.005	.005	.54	42.62	1.6
27.2	.06	2.04	12.3	.005	.005	.06	42.8	3.93
24.9	.001	3.9	12.4	.005	.005	.05	42.8	5.1
6.6	.001	4.92	12.1	.005	.005	.52	43.34	3.78

Table D.1.4. Snoqualmie River Headwater Data

	Flow	PO_4	BOD	DO	NH_3	NO_2	NO_3	Temp.	FCX
mean	3460	.08	.901	12.3	.008	.005	.08	42.24	2
variance	$4x10^4$	10^{-4}	1	1	10^{-4}	10^{-6}	10^{-4}	4	2

Table D.2.1. Effluent/Tributary Mean Concentrations for Skykomish River

River Mile	Identification	Flow	PO_4	BOD	DO	NH_3	NO_2	NO_3	Temp.	FCX
62.2	Ideal Cement Co.	.5	0	0	5	0	0	0	55	0
49.6	N.F. Skykomish R.	1870	0	1.1	12.08	.01	.005	.49	42.7	0
40.6	May Cr.	240	.007	1.68	12.68	.011	.005	.248	42.7	2.8
40.6	Nonpoint Source	4	3.5	30	6	1	0	.4	55	2
38.6	Nonpoint Source	12	2.5	30	6	1	0	.4	55	2
35.7	Wallace R.	450	.007	1.7	12.65	.011	.005	.289	42.7	2.8
35.7	Nonpoint Source	24	2.8	30	6	1	0	.4	55	2
34.4	Sultan R.	160	.005	1.96	12.65	.010	.005	.26	42.7	2.8
34.0	Sultan Outfall	.1	7.18	6	7.1	8.5	.02	5.8	55	8
34.0	Nonpoint Source	16	2.5	30	6	1	0	.4	55	4
30.5	Nonpoint Source	65	0	0	12	0	0	0	55	0
25	Woods Cr.	80	.006	1.86	12.5	.012	.005	.275	42.7	2.8
24.9	Nonpoint Source	8	2.5	30	6	1	0	.4	55	2
24.8	Monroe Outfall	.6	4.11	127	7.4	8.1	.27	4.3	55	14
24.8	Nonpoint Source	20	2.5	30	6	1	0	.4	55	2
23.4	St. Reform. Outfall	.4	3	120	5	10	.1	1	55	18
23.4	Nonpoint Source	44	2.5	30	6	1	0	.4	55	2

Table D.2.2. Effluent/Tributary Variances for Skykomish River

River Mile	Identification	Flow	PO_4	BOD	DO	NH_3	NO_2	NO_3	Temp.	FCX
62.2	Ideal Cement Co.	.25	10^{-4}	0	9	10^{-4}	10^{-6}	.01	4	2
49.6	N.F. Skykomish R.	10^4	10^{-6}	1	.25	$2.5x10^{-5}$	10^{-6}	.01	4	2
40.6	May Cr.	2500	10^{-6}	1	1	10^{-4}	10^{-6}	.01	4	2
40.6	Nonpoint Source	4	6	100	9	.25	10^{-6}	.01	4	2
38.6	Nonpoint Source	10	6	100	9	.25	10^{-6}	.01	4	2
35.7	Wallace R.	2500	10^{-6}	1	1	10^{-4}	10^{-6}	.01	4	2
35.7	Nonpoint Source	25	6	100	9	.25	10^{-6}	.01	4	2
34.4	Sultan R.	1000	10^{-6}	1	1	10^{-4}	10^{-6}	.01	4	2
34.0	Sultan Outfall	.01	50	36	4	4	10^{-4}	4	4	2
34.0	Nonpoint Source	4	6	100	9	.25	10^{-6}	.01	4	2
30.5	Nonpoint Source	100	10^{-4}	1	1	10^{-4}	10^{-6}	.01	4	2
25	Woods Cr.	100	10^{-6}	1	1	$2.5x10^{-6}$	10^{-6}	.01	4	2
24.9	Nonpoint Source	16	6	1	9	.25	10^{-6}	.01	4	2
24.8	Monroe Outfall	.36	16	2500	.4	4	.01	1	4	2
24.8	Nonpoint Source	4	6	100	9	.25	10^{-6}	.01	4	2
23.4	St. Reform. Outfall	.16	9	400	9	4	10^{-4}	.25	4	2
23.4	Nonpoint Source	100	6	100	9	.25	10^{-6}	.01	4	2

Table D.2.3. Skykomish River Linearization Trajectory

River Mile	PO_4	BOD	DO	NH_3	NO_2	NO_3	Temp.	FCX
41.0	.001	3.71	13.0	.001	.005	.12	41.72	2.99
34.4	.001	.73	10.8	.001	.005	.19	41.9	2.99
25.5	.001	2.18	12.4	.001	.003	.32	42.8	2.99
24.0	.001	2.66	12.48	.001	.005	.23	42.7	2.99
20.5	.001	2.73	12.45	.001	.005	.22	43.98	4.68

Table D.2.4. Skykomish River Headwater Data

	Flow	PO_4	BOD	DO	NH_3	NO_2	NO_3	Temp.	FCX
mean	3460	.001	1.76	11.9	.001	.005	.49	39.2	2
variance	$4x10^4$	10^{-4}	1	1	10^{-4}	10^{-6}	10^{-4}	4	2

Table D.3.1. Effluent/Tributary Mean Concentrations Snohomish River

River Mile	Identification	Flow	PO_4	BOD	DO	NH_3	NO_2	NO_3	Temp.	FCX
20.5	Nonpoint Source	2.67	2.5	30	6.0	1.0	0	.4	55	9.3
14.7	French Cr.	110	0	2.0	11.0	0	.005	0	42	3.0
13.4	Pilchuck R.	1100	.08	2.21	11.90	0	.005	.04	44.6	4.02

Table D.3.2. Effluent/Tributary Variances for Snohomish River

River Mile	Identification	Flow	PO_4	BOD	DO	NH_3	NO_2	NO_3	Temp.	FCX
20.5	Nonpoint Source	40000	.0025	1	1	10^{-4}	10^{-6}	.0025	4	2
14.7	French Cr.	400	.0025	1	1	10^{-4}	10^{-6}	.0025	4	2
13.4	Pilchuck R.	4	4	100	9	1	10^{-6}	.04	4	2

Table D.3.3. Snohomish River Linearization Trajectory

River Mile	PO_4	BOD	DO	NH_3	NO_2	NO_3	Temp.	FCX
19.5	.08	2.18	12.30	.018	.005	.52	42.8	4.17